PREPARATION AND DETERMINATION OF CATALYTIC ACTIVITIES OF GROUP 8 AND GROUP 9 METAL ION-EXCHANGED ZEOLITE Y CATALYSTS IN DECOMPOSITION OF NITROUS OXIDE TO SOLE NITROGEN AND OXYGEN

A THESIS SUBMITTED TO
THE GRADUATE SCHOOL OF NATURAL AND APPLIED SCIENCES
OF
MIDDLE EAST TECHNICAL UNIVERSITY

BY

PELİN EDİNÇ CÜRDANELİ

IN PARTIAL FULFILLMENT OF THE REQUIREMENTS
FOR
THE DEGREE OF DOCTOR OF PHILOSOPHY
IN
CHEMISTRY

JUNE 2014

Approval of the thesis:

PREPARATION AND DETERMINATION OF CATALYTIC ACTIVITIES OF GROUP 8 AND GROUP 9 METAL ION-EXCHANGED ZEOLITE Y CATALYSTS IN DECOMPOSITION OF NITROUS OXIDE TO SOLE NITROGEN AND OXYGEN

submitted by **PELİN EDİNÇ CÜRDANELİ** in partial fulfillment of the requirements for the degree of **Doctor of Philosophy in Chemistry Department, Middle East Technical University** by,

Prof. Dr. Canan ÖZGEN
Dean, Graduate School of **Natural and Applied Sciences**

Prof. Dr. İlker ÖZKAN
Head of Department, **Chemistry**

Prof. Dr. Saim ÖZKAR
Supervisor, **Department of Chemistry, METU**

Examining Committee Members:

Prof. Dr. Ceyhan KAYRAN
Chemistry Department, METU

Prof. Dr. Saim ÖZKAR
Chemistry Department, METU

Prof. Dr. Ahmet ÖNAL
Chemistry Department, METU

Assoc. Prof. Dr. Ayşen YILMAZ
Chemistry Department, METU

Assist. Prof. Dr. Emrah ÖZENSOY
Chemistry Department, Bilkent University

Date:

I hereby declare that all information in this document has been obtained and presented in accordance with academic rules and ethical conduct. I also declare that, as required by these rules and conduct, I have fully cited and referenced all material and results that are not original to this work.

Name, Last Name: PELİN EDİNÇ CÜRDANELİ

Signature :

ABSTRACT

PREPARATION AND DETERMINATION OF CATALYTIC ACTIVITIES OF GROUP 8 AND GROUP 9 METAL ION-EXCHANGED ZEOLITE Y CATALYSTS IN DECOMPOSITION OF NITROUS OXIDE TO SOLE NITROGEN AND OXYGEN

EDİNÇ CÜRDANELİ, Pelin
Ph. D., Department of Chemistry
Supervisor: Prof. Dr. Saim ÖZKAR

June 2014, 118 pages

The Group 8 and 9 metal(III) ion-exchanged zeolite were prepared from the ion exchange of metal(III) ions with the extra framework Na^+ cations of zeolite Y with a Si/Al ratio of 2.5. They were characterized by using inductively coupled plasma optical emission spectroscopy (ICP-OES), X-ray diffraction (XRD) and X-ray photoelectron spectroscopy (XPS). The Group 8 and 9 metal(III) ion-exchanged zeolite materials prepared were tested as catalysts in decomposition of nitrous oxide to oxygen and nitrogen. The catalytic decomposition of nitrous oxide in the presence of metal(III) ion-exchanged zeolite catalyst was carried out in a continuous flow vertical reactor at flow rate of 100 mL/min of 1000 ppm nitrous oxide helium mixture. The catalytic reaction was followed by monitoring the change in concentration of reactant nitrous oxide as well as the products nitrogen and oxygen by gas chromatography. Side products were followed by NOx analyzer.

Catalytic activity of ruthenium(III) ion-exchanged zeolite Y is studied depending on the ruthenium loading of zeolite and flow rate of nitrous oxide helium mixture. The results collected reveal that ruthenium(III) ion-exchange zeolite with a ruthenium loading of 3.98wt.% is highly active, long-lived, and reusable catalyst providing 100% conversion of nitrous oxide to sole nitrogen and oxygen at 350 °C without any side reaction. This catalyst can be bottled under ambient conditions and repeatedly used in successive runs of nitrous oxide decomposition for up to five months without significant loss in activity. The other two metals of Group 8, iron(III) and osmium(III) ion-exchanged zeolite Y do not show activity as high as that of ruthenium(III) ion-exchanged zeolite Y in the same reaction. Rhodium(III) ion-exchanged zeolite Y (2.12wt.%) gives the highest activity among Group 9 metal ion-exchanged zeolite Y catalysts in decomposition of nitrous oxide.

Keywords: Nitrous oxide; Decomposition; Zeolite; Ruthenium; Osmium; Iron; Rhodium; Cobalt; Iridium

ÖZ

GRUP 8 VE GRUP 9 METAL İYON DEĞİŞİMLİ ZEOLİT Y KATALİZÖRLERİNİN HAZIRLANMASI VE NİTRÖZ OKSİTİN NİTROJEN VE OKSİJENE BOZUNMASI REAKSİYONU İÇİN KATALİK AKTİVİTELERİNİN BELİRLENMESİ

EDİNÇ CÜRDANELİ, Pelin
Doktora, Kimya Bölümü
Tez Yöneticisi: Prof. Dr. Saim ÖZKAR

Haziran 2014, 118 sayfa

Grup 8 ve Grup 9 metal(III) iyon-değişimli zeolite Y, metal(III) iyonları ile zeolite Y (Si/Al =2.5) yapısında bulunan Na^+ katyonlanın yer değiştirmesi yöntemiyle elde edildi ve çiftleşmiş plazma-optik emisyon spektroskopisi (ICP-OES), X-ışınları kırınımı (XRD), X-ışını fotoelektron spektroskopisi (XPS) teknikleri kullanılarak tanımlandı. Elde edilen Grup 8 ve 9 metal(III) iyon-değişimli zeolitler nitröz oksitin oksijene ve nitrojene bozunma reaksiyonunda katalizör olarak kullanıldı. Katalizörler dikey bir reaktöre yüklendikten sonra 1000 ppm nitröz oksit-helyum karışımı 100 mL/dk akışla reaktörden geçirilerek nitröz oksitin katalik bozunması çalışıldı. Katalitik reaksiyon sonucunda nitröz oksit ve oluşan oksijen ve nitrojen ürünlerinin derişimleri gaz kromatografi ile izlendi. Yan ürünler NOx analiz cihazı ile takip edildi.

Rutenyum(III) iyon-değişimli zeolite Y katalizörünün katalitik aktivitesi, zeolitin rutenyum yüklemesi ve reaktörden geçirilen nitröz oksit-helyum karışımının akış hızı esas alınarak çalışıldı. Ağırlıkça %3.98 rutenyum içeren rutenyum(III) iyon-değişimli zeolite Y katalizörünün oldukça etkin, uzun ömürlü ve tekrar kullanılabilir bir katalizör olduğu görüldü. Bu katalizör, 350 °C'de, nitröz oksiti yan ürün vermeksizin %100 oranda oksijen ve nitrojene dönüştürdü. Ortam koşullarında tutulan katalizör, nitröz oksitin bozunmasında beş ay süresince defalarca kullanılmasına rağmen aktivitesinde belirgin bir düşüş gözlenmedi. Diğer Grup 8 metalleri, demir(III) ve osmiyum(III) iyon-değişimli zeolite Y katalizörleri, nitröz oksitin bozunmasında rutenyum(III) iyon-değişimli zeolite Y kadar yüksek aktivite göstermediler. Ağırlıkça %2.12 rodyum içeren rodyum(III) iyon-değişimli zeolit Y, nitröz oksiti 475 °C'de tamamıyla oksijen ve nitrojene dönüştürerek Grup 9 metalleri arasında en yüksek aktiviteyi gösterdi.

Anahtar Kelimeler: Nitröz oksit; Bozunma; Zeolit ; Rutenyum; Osmiyum; Demir; Rodyum; Kobalt; İridyum

To My Husband & Family

ACKNOWLEDGMENTS

I would like to express my deepest thanks and appreciation to my supervisor, Prof. Dr. Saim ÖZKAR, for his supervision and continuous support during all stages of this thesis.

I would like to acknowledge the fervent support of TUBITAK SAGE for the generous use of their facilities and personnel to complete this study.

I would like to express my sincere appreciation to my husband Sertaç CÜRDANELI for his crucial advices and invaluable efforts during the preparation of this thesis.

I would like to express my special thanks to my father A. Bülent EDİNÇ for his endless help. He was always ready, day and night, for my every single request.

Finally, the greatest thanks go to my family who supported and encouraged me throughout my whole life. It would be impossible without their patience and understanding.

TABLE OF CONTENTS

CHAPTERS

LIST OF TABLES

TABLES

LIST OF FIGURES

FIGURES

CHAPTER 1

INTRODUCTION

1.1 The Importance of Nitrous Oxide:

Nitrous oxide (N_2O) is a crucial and interesting chemical to study for many aspects. It is a very well-known greenhouse gas and many scientists have been researching for decreasing its concentration in atmosphere since its contribution to global warming arises as a potential threat. On the other hand, nitrous oxide is a precious source in defense industry for being a multipurpose chemical because it can be used as both oxidizer and monopropellant in propulsion systems.

1.1.1 The Place of Nitrous Oxide in Global Warming

Nitrous oxide is one of the major greenhouse gases which cause global warming and depletion of stratospheric ozone [1]. Actually, nitrous oxide is naturally present in the atmosphere as a product of Earth's nitrogen cycle however its concentration has increased due to extensive use of fossil fuels, synthetic and organic N fertilizers and through the burning of biomass [2]. According to the report of EPA (United States Environmental Protection Agency), 40% of total emission come from human activities (Figure 1) [3], and 4.7-7 million ton nitrous oxide is given to the atmosphere by these activities per year [4,5]. Nitrous oxide is a long lived gas and its impact on global warming is 310 times greater than that of carbon dioxide. In addition it has a residence time of 120 years in the atmosphere [6,7]. The Intergovernmental Panel on Climate Change (IPCC) has reported that concentration of nitrous oxide in the atmosphere has increased from ~270 ppb to 319 ppb by the year 2005 [8].

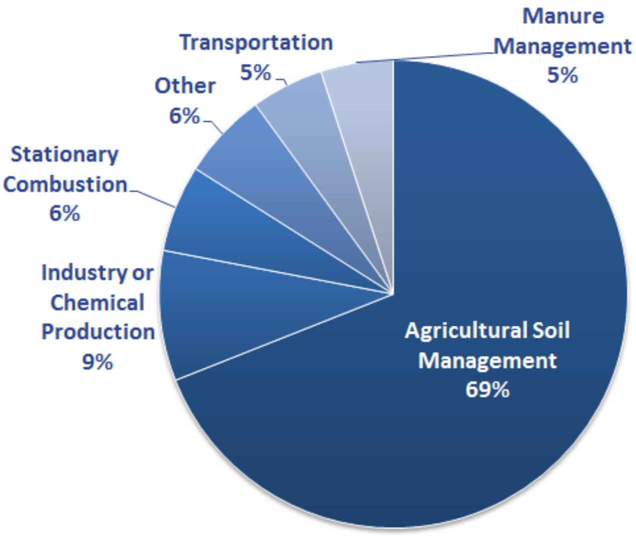

Figure 1. Nitrous Oxide Emission Estimates reported by United States Environmental Protection Agency (EPA) [3]

With this data, nitrous oxide contributes about 5% of global warming potential [9] which results in global climate changes such as increasing temperature and changes in precipitation patterns. Thus, this increase arises as a serious threat to the world's managed and natural ecosystems and could greatly affect the global agricultural economy [10]. By Kyoto protocol signed in 1997 and Gothenburg Protocol signed in 1999, many countries started to follow and reduce emissions of greenhouse gases including nitric oxides [11]. Therefore many studies have been carried out on decomposing nitrous oxide to its elements, nitrogen and oxygen in order to reduce its concentration in atmosphere.

1.1.2 The Usage of Nitrous Oxide in Defense and Space Industries

While such efforts have been carried out because of environmental concerns, defense and aerospace industry have been considering the application areas of nitrous oxide for its physical and chemical properties. Nitrous oxide is non-flammable, non-corrosive, non-toxic chemical and it is stable at ambient conditions.

This chemical can be stored safely since it is compatible with common structural materials such as ozone, halogens and alkali metals. Liquid or compressed gas of nitrous oxide can be stored practically from -34 ºC to 60 ºC. It decomposes exothermically at ~1640 ºC yielding free oxygen which can be used for combusting with variety of fuels. The application areas of Nitrous Oxide in Space and Defense Industries can be summarized as follows [12]:

- Cold-gas thrusters for attitude control of a spacecraft
- Monopropellant thrusters for spacecraft station-keeping and small orbit maneuvers
- Resistojet thrusters
- Bipropellant thrusters for large orbital maneuvering
- Gas generators
- Turbine drives
- Source of breathing oxygen for spacecraft
- Emergency life-support
- Hot gas source for Ramjet Engine ground tests

Considering the application areas of nitrous oxide are evaluated, it is clearly seen that it has three main roles in Defense and Space Industries: i) Monopropellant as a member of propulsion systems, ii) Decomposed Nitrous Oxide as an oxidizer in bipropellant propulsion systems, and iii) Decomposed Nitrous Oxide as a member of hot gas source in ramjet engine test setups.

1.1.2.1 Nitrous Oxide as a Monopropellant

There are three main monopropellant propulsion systems in the application; Nitrous Oxide (N_2O), Hydrogen Peroxide (H_2O_2) and Hydrazine (N_2H_4) [12]. Although the nitrous oxide is a new and promising monopropellant which can be directly used in the propulsion systems (Surrey Space Centre’s Mark-IV resistojet thruster uses this gas for orbit connection on the UoSAT-12 mini-satellite [13]), hydrogen peroxide monopropellant thrusters were employed on the number of missions [14,15,16] and hydrazine monopropellant thrusters are extensively used space technology [17,18]. Zakirov and Sweeting have compared those three monopropellants in a thruster and revealed that specific impulse of nitrous oxide is 15% higher than H_2O_2 while it is 16% lower than N_2H_4. However, considering the storage density, it is seen that nitrous oxide requires 45% lower space than N_2H_4 and 26% lower space than H_2O_2 [12].

In addition to the area of performance, it is known that hydrazine is a very toxic, carcinogenic, and flammable material while nitrous oxide is non-toxic and non-flammable.

1.1.2.2 Nitrous Oxide as a Bipropellant

Since the late 1990's, N_2O has been used as an oxidizer in hybrid rocket motors [19]. Thicksten et al. have reported a study in 2008, showing comparable performance of nitrous oxide with liquid oxygen (LOX) in a hybrid thruster testing (Figure 2) [20].

Nitrous oxide can also be used in amateur rocketry in combination with solid and liquid fuels. Hydroxyl terminated poly butadiene (HTPB), polypropylene, asphalt can be given as examples of solid fuel whereas alcohols are the examples of liquid fuels [21,22,23,24].

(a) (b)

Figure 2. (a) The 250,000 lb thrust motor, utilizing LOX and HTPB (b) Test Firing of Streaker SLV Hybrid Upper Stage Using Nitrous Oxide and HTPB [20]

Nitrous oxide decomposition results in hot nitrogen-oxygen mixture that can be used to oxidize a fuel. Theoretical performance of several nitrous oxide bipropellant combinations has been evaluated to determine their feasibility for future applications [12], and it is identified that HTPB, polyethylene and RP-1 are the three most practical fuels for nitrous oxide bipropellants on small satellites and upper stages [25].

1.1.2.3 Nitrous Oxide as a Hot Gas Source

Although the application of nitrous oxide as a propellant dates back to 1990's [12,13,16,17,19,21,25], the use of decomposed nitrous oxide as a hot gas source due to its exothermic decomposition reaction is a new phenomenon.

The decomposed nitrous oxide is intended to be used in ramjet engine ground test facilities. The main idea behind ground testing of the ramjet engine is simulating the air conditions similar to the conditions at the entrance of an engine at high altitudes, and velocities.

The most important point in the establishment of the ramjet engine test facilities is the requirement for the hot gas (air) in order to simulate the stagnation temperature at the air inlet of the combustion chamber.

Nitrous oxide decomposes into nitrogen and oxygen by an exothermic reaction occurring approximately at 1600 ºC. This exothermic reaction generates ~82 kJ of heat per mole of nitrous oxide at ambient conditions [26].

Usage of the heat evolved from the decomposition of nitrous oxide as a hot gas source is thought to be a new and an efficient way to compensate this requirement.

1.2 Motivation of the Thesis

TÜBİTAK SAGE is the Defense Industries Research and Development Institute of Turkey and its main research and development area is the missiles. TÜBİTAK SAGE designs and installs test setups in order to compensate its requirements for the development of missile systems.

Propulsion Systems Division of TÜBİTAK SAGE is involved in the development of solid propellant rocket motors, liquid propellant rocket engines, and air breathing engines including supersonic and hypersonic systems.

Developing a supersonic and a hypersonic air breathing engine for the missile requires first successive development phases, then detailed design improvements and demonstrations on ground, and finally acceptance tests on the flight vehicle in the flight envelope.

Performing a flight test, including captive-carry tests is a complicated and an expensive phenomenon due to its nature, which includes the usage of military ground facilities, requirement for the fighters and the soldiers, and ~10.000 liters of fuel per flight. Therefore, it is very important to qualify the system on the ground, in the most realistic environment possible.

Air breathing engine combustion chamber needs to be tested alone, before the testing of full propulsion system, and the missile. Ramjet Engines are tested in ground test facilities, which may be classified as connected pipe test facilities, semi-free jet test facilities, and free jet test facilities [27]. The main idea behind ground testing of the engine is simulating the air conditions similar to the conditions at the entrance of an engine at high altitudes, and velocities.

Connected Pipe Test Facility is such as basic facility that, hot air is ducted directly into the combustion chamber as shown in Figure 3.

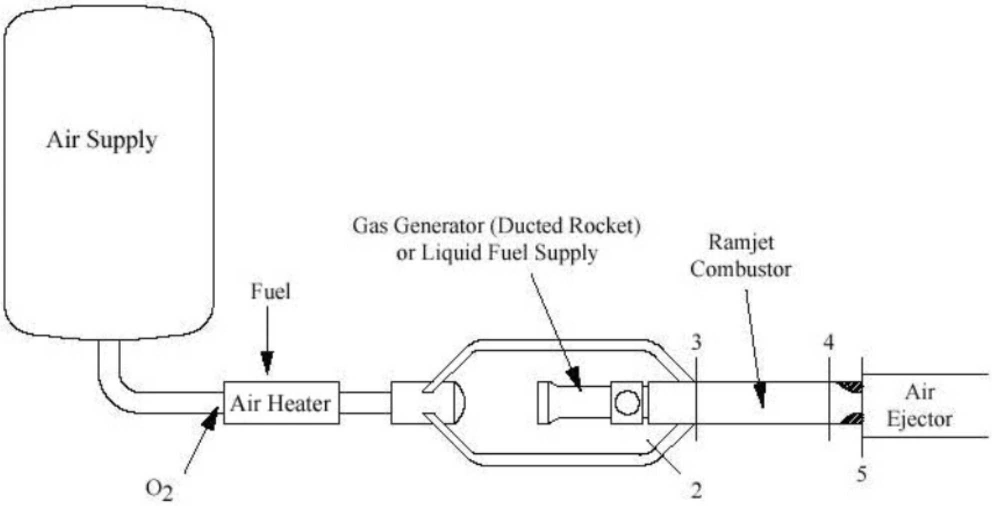

Figure 3. Schematic of a Connected-Pipe Test [27]

Semi-free jet facility and free-jet facility are similar systems, and these setups allow the researchers to test not only the combustion chamber but also the air intakes of the system. Free jet facility also serves to test the whole propulsion system, and these tests are primarily conducted to verify the functional operation and performance of the whole propulsion system.

Stagnation (total) temperature is the temperature at a stagnation point in a fluid flow and the stagnation point is defined as the point where the speed of the fluid (air) is zero and all of the kinetic energy has been converted to an internal energy (temperature). Total temperature is calculated by the Equation 1 [28].

$$T_t = T_s\left(1 + \frac{\gamma - 1}{2} M^2\right) \qquad (1)$$

where;

T_t : Total Temperature (K)

T_s : Static (free-stream) Temperature (K)

γ : Ratio of specific heats (1.4 for dry air)[29]

M : Mach number (flight speed, 1M=331.29 m/s @ standard dry air at 0 °C and at a barometric pressure of 101,325 kPa) [30]

Once the flight velocity increases, total temperature increases by the square of the Mach number. Table 1 represents the change of Total Temperature with respect to Mach number for a sea level flight at 27 °C (300K).

Table 1. Change of Total Temperature with Velocity

Velocity (M)	**Total Temperature (K)**
0.0	300.0
0.1	300.6
0.2	302.4
0.3	305.4
0.4	309.6
0.5	315.0
0.6	321.6
0.7	329.4
0.8	338.4
0.9	348.6
1.0	360.0
1.1	372.6
1.2	386.4
1.3	401.4
1.4	417.6
1.5	435.0
2.0	540.0
2.5	675.0
3.0	840.0
3.5	1035.0
4.0	1260.0
4.5	1515.0
5.0	1800.0

It is clearly seen from the Table 1 that the total temperature reaches to very high values (>800 °C) for supersonic and hypersonic missiles and simulating such conditions become harder for the simple ground test systems (electrical heating systems, heat exchangers, etc.) [27].

Usage of the heat evolved from the decomposition of nitrous oxide as a hot gas source is thought to be a new and efficient way to compensate this requirement. Nitrous oxide decomposes into nitrogen and oxygen by an exothermic reaction (Equation 2) occurring approximately at 1600 ºC.

$$N_2O(g) \rightarrow N_2(g) + \frac{1}{2} O_2(g) + \text{Heat} \quad (2)$$

However, a heat input is required in order to initiate the reaction since the energy barrier of nitrous oxide decomposition is 250 kJ/mole [31]. Therefore, the gas must be heated to above 1000 °C to attain the required reaction rates.

Ground test systems are fed by high capacity tanks and heating up the gases while flowing through these pipelines requires incredibly high energy which results in extreme increase in cost of tests.

Figure 4 shows the Ramjet Engine test facility hot gas supply system intended to be established by TUBITAK SAGE in the Internal Ballistics Laboratory.

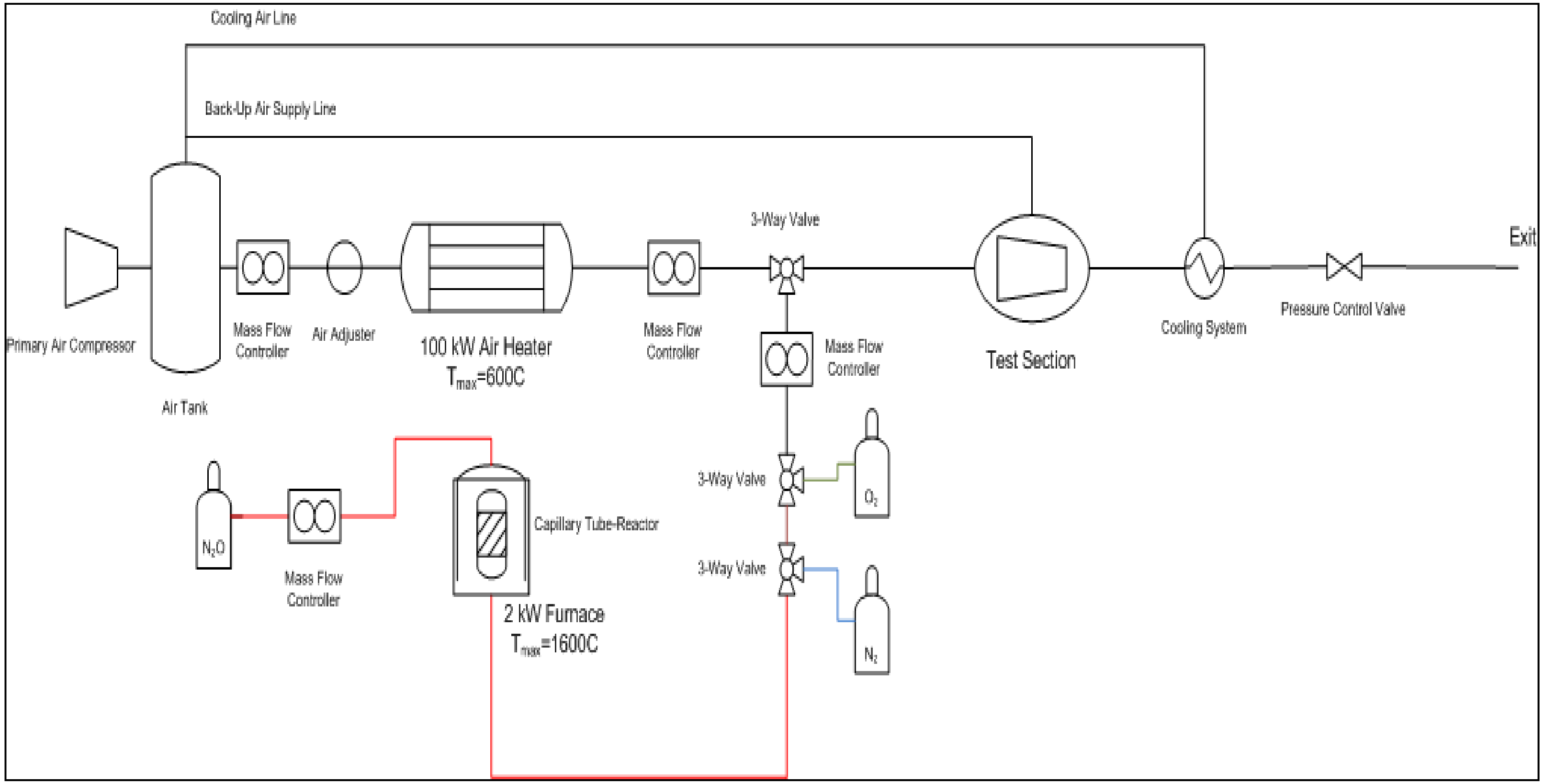

Figure 4. Flow-Diagram of All-Up Round Test Facility

On the other hand, the energy barrier of the reaction and thus the reaction temperature can be drastically lowered by using an appropriate catalyst.

1.3 Catalysts used for the Decomposition of Nitrous Oxide

As mentioned before, catalysis has a great importance in nitrous oxide removal technologies and defense industry. Catalysis reaction is based on the catalytic decomposition of nitrous oxide to nitrogen and oxygen at much lower temperatures than its natural decomposition temperature of 1670 ºC. The catalytic decomposition reaction can be described simply in four steps [32,33].

$$N_2O \rightarrow N_2 + O_{ad} \qquad (k_1) \qquad (3)$$

$$O_2 \rightarrow 2O_{ad} \qquad (k_2) \qquad (4)$$

$$N_2O + O_{ad} \rightarrow N_2 + O_2 \qquad (k_3) \qquad (5)$$

$$2O_{ad} \leftrightarrow O_2 \qquad (k'_2) \qquad (6)$$

The surface of the catalyst can be oxidized by a molecule of nitrous oxide as shown in Eq. (3) or this oxidation can be achieved by chemisorptions of molecular oxygen from gaseous phase (Eq.(4)). The type of oxidation of surface depends on the pressure of oxygen. Low oxygen pressure orients the reaction to Eq. (3) whereas the high pressure oxygen orients the Eq. (4). Also, reduction of the catalyst surface has two alternative mechanisms. The path obeys either Eley-Rideal mechanism just shown in Eq. (5) or two adsorbed oxygen atoms can recombine by following the Langmuir-Hinshelwood mechanism (Eq. (6)).

The decomposition of nitrous oxide has been studied over different types of catalysts for a long time. Metals, pure and mixed oxides, supported systems and zeolites generate an inclusive literature for decomposition studies [34]. The documents date back to 1920’s [35, 36, 37].

A literature survey shows that transition metals supported on metal oxides or zeolites come forward by their high activities in decomposition of nitrous oxide. Fe, Co, Ni, Cu, Ru and Rh metals have been commonly suited on different type of zeolites such as ZSM-5, ZSM-11, Beta (BEA), mordenite (MOR), ultra stable zeolite Y (USY), zeolite A and zeolite X [38, 39, 40, 41, 42, 43, 44, 45], and some metal oxides [46].

High activity catalysts are achieved by the combination of appropriate metal ions and zeolites. Thus, the change in any of the subject constituents may affect the activity. For example, platinum loses its activity when it is suited into a zeolite, although it has high activity as pure metal. Cobalt gives different activity depending on the host zeolite. Co exchanged ZSM-5 or ZSM-11 zeolites have higher activity than Co-MOR or Co-Y catalysts.

Wang et al. have studied the effect of zeolite structure on catalytic performance of Fe-zeolites in decomposition of nitrous oxide and determined the activity of solid-state iron exchanged ZSM-5, ZSM-35, mordenite and beta zeolites by using UV-visible diffuse reflectance, in-situ FTIR and in situ visible Raman spectroscopic techniques. These catalysts have exhibited activity above 427 ºC. Fe-ZSM-5, Fe-ZSM-35 and Fe-beta catalysts started the decomposition of nitrous oxide at 427 ºC and reached 100% conversion at 500 ºC. However, in case of Fe-mordenite, the reaction took place at 500 ºC and completed at 580 ºC [47]. The high activity of Fe-ZSM-35 has put down to the presence of highly active binuclear iron sites which can form in framework of ZSM-35. *Liu et al.* have also reported a comparative study on direct decomposition of nitrous oxide by keeping zeolite type as BEA but changing the metal cation as to iron, copper and cobalt [48]. Fe-BEA has shown the highest activity among these three, by giving 100% conversion at 417 ºC whereas Cu-beta could finish the reaction at 577 ºC. Variety in these activities was associated with the formation of an intermediate which decreases the catalytic activity and different energy barriers for oxygen desorption step of nitrous oxide decomposition.

Cobalt is another transition metal which has shown high activity in nitrous oxide decomposition when used with ZSM-5 [49,50,51]. *Armor et al.* have emphasized that the catalytic activity is affected by the preparation method of catalysts [52]. *Crus et al.* have shown the variation with the preparation of Co-ZSM5 catalysts by three different methods: cation exchange, ammonia addition after cation exchange and solid state exchange. *Liu et al.* have studied a series of cobalt exchanged zeolites with ZSM-5, BEA, MOR and USY structures [53]. The first three structures have shown higher activities than that of USY. The formation of active Co^{2+} ions in ZSM-5, BEA and MOR structures resulted in high activity in decomposition of nitrous oxide. However, less active cobalt oxides have formed in case of USY and cause a decrease in the activity of the catalyst. This study has shown that the activity of Co^{2+} ions depends on the location in the zeolite structure, their chemical coordination and distances between Co ions.

Although the wide range of studies for iron, cobalt and copper metals have been carried out for nitrous oxide decomposition reactions, the works for noble metals such as rhodium, ruthenium and iridium can be investigated separately since some of them exhibit higher activity for decomposition of nitrous oxide when compared with the other metals.

K. Yuzaki et al. have studied Rh catalysts on decomposition reaction of nitrous oxide by using $Rh(NO_3)_3$ as precursor and USY, FSM-16 and Al_2O_3 as supports. Rh/NaY has been prepared from the ion exchange reaction of $Rh(H_2O)_6^{3+}$ with NaY [54, 55]. All catalysts have completed the reaction below 350 ºC. Rh-USY and Rh/NaY have exhibited the highest activity by giving 100% conversion at 250 ºC with a 2 wt.% loading of rhodium. *G. Centi et al.* have studied with impregnated Rh-ZSM-5 and alumina samples having rhodium content of 4 wt.%. Rh-ZSM-5 [56]. *Oi et al.* have studied the decomposition of nitrous oxide over supported rhodium catalysts (Rh/ZnO, Rh/CeO_2, Rh/ZSM-5, Cu-ZSM-5 and $Co\text{-}Al\text{-}CO_3$-HT) and found Rh/ZnO as the most active one among them since it gave complete conversion at 300 ºC [46]. *J. Haber et al.* reported rhodium supported alumina in the presence of alkali metal promoters [57]. It has been determined that total conversion was reached at 450 ºC and addition of promoters had a strong influence on the activity of catalysts.

Hussain et al. have studied rhodium supported on a new generation of mesoporous molecular sieves, MCM-41 (mobile composition of matter) and SBA-15 (Santa Barbara Amorphous). In this study, rhodium catalysts supported on MCM-41 or SBA-15 has been prepared by impregnation method and nitrous oxide decomposition has been investigated depending on the dispersion, and particle size of rhodium nanoparticles. They have concluded that materials having three dimensional pore structure such as MCM-41 and SBA-15, exhibit higher activity since they reduce the risk of blockage due to agglomeration of metals at higher temperatures. These structures also enable transportation of reactant and products through the pores easily [33]. In addition, these new generation catalysts have been studied for having higher hydrothermal stability for large scale applications of nitrous oxide decomposition [58].

S. Qun et al. have reported the activity of iridium exchanged USY (Si/Al =11.6) catalysts and compared its activity with the bimetallic Ir/Fe-USY, Ru/Fe-USY, Rh/Fe-USY and Pd/Fe-USY catalysts. Ir-USY has shown activity between 300 -500 ºC. The addition of iridium to Fe-USY has enhanced the activity and decreased the total conversion temperature from 500 ºC to 350 ºC for 2.0 wt.% of iridium loading [59]. *Inoue et al.* have shown iridium catalysts supported on alumina exhibiting an activity between 200 ºC and 500 ºC and conclude that oxygen desorption starts above 350 ºC from catalyst surface and therefore it can be used for decomposition of nitrous oxide with the presence of oxygen above 400 ºC [60].

Li et al. have studied transition metal ions, iron(III), cobalt(II), copper(II), ruthenium(III) and rhodium(III), ion-exchanged into ZSM-5 as catalysts in decomposition of nitrous oxide and the latter two have shown to be the most active ones, providing complete conversion of nitrous oxide to nitrogen and oxygen at 350 °C by using 0.6 % metal loading of zeolite [61]. However, in that study, the durability and reusability of catalysts have not been tested and the effect of metal loading on the catalytic activity has not been reported either. *Mc. Carty et al.* have used US-Y with a relatively high silica–alumina ratio (Si/Al = 29) as support and ruthenium(III) ion exchanged US-Y with different metal loading as catalyst in decomposition of nitrous oxide [62,63]. Although they have shown high activity of the catalyst in decomposition of nitrous oxide at temperature as low as 200 °C, the durability and reusability of the catalyst have not been reported as acid zeolites cannot be stored and used at ambient conditions since they can easily decompose with humidity. Ruthenium(III) ion exchanged Beta, zeolite Y and ZSM-5 prepared by using the $[Ru(NH_3)_6]^{3+}$ complex ion have been tested as catalyst in decomposition of nitrous oxide and only 70% conversion could have been achieved at 450 °C as measured by gas chromatography [64]. $[Ru(NH_3)_6]^{3+}$ may not be an appropriate cation to be ion-exchanged into zeolite Y since its diameter is very large to get into the pores of zeolite Y at room temperature. That may be the reason of not obtaining a complete conversion at 450 °C. Labhsetwar et al. have synthesized Ru + Ag/US-Y and Ru + Co/US-Y catalysts by applying two step ion-exchange reactions [65]. In the first step, $RuCl_3$ has been ion-exchanged into US-Y, while $AgNO_3$ or cobalt acetate solutions were used for the second ion-exchange into Ru-US-Y. However, complete decomposition of nitrous oxide could have been achieved at ~450 °C for Ru+Ag/US-Y, while Ru+Co/US-Y could provide complete decomposition of nitrous oxide at ~350 °C.

Kaptajein et al. have reported the results of a study on the decomposition of nitrous oxide over various types of catalysts in 1996 [34]. Table 2 shows the extended summary on the decomposition of nitrous oxide over various types of catalysts.

Table 2. Summary of the studies on the decomposition of nitrous oxide over various types of catalysts

Zeolite Type	Temperature Range, °C	Reactor System	Gases Investigated with N_2O	Ref.
Fe-Mor	300-550	Flow	-	[40]
Fe-Y, Ca, La, Eu, Cr, Mn, exchanged Fe-Y	400-530	Flow	-	[44], [45]
Fe-ZSM-5	330-630	Batch	-	[38], [43]
Fe-ZSM-5, Fe-ZSM-35, Fe-beta, Fe-Mor	300-500	Flow	-	[47]
Ru-NaZSM-5	330-630	Flow (TPR)	-	[62]
Ir/Fe-USY	200-600	Flow	NO	[59]
Fe, Ru in ZSM-5	180-530	Flow	-	[41]
Co, Cu in ZSM-5, ZSM-11, Y, L, Ferrierite, Beta, Mor, Erionite	330-530	Flow	-	[61],[49] [53],[56]
M-BEA(beta) M: Fe,Co,Cu	300-650	Flow, N_2O-TPD	-	[48]
Co-ZSM-5, Cu- ZSM-5	330-430	Flow	NO, H_2O	[61]
Co-ZSM-5	300-550	Flow	CO,NO, CH_4,O_2	[51]
Ni-ZSM-5, Mn- ZSM-5, Fe- ZSM-5	330-530	Flow	-	[61]
Ru in ZSM-5 and USY	130-530	Flow	-	[63]
Ru-BEA, Ru-Y, Ru-ZSM-5	180-580	Flow	-	[64]
Ru+Ag/US-Y, Ru+Co/US-Y	130-530	Flow	-	[65]
Cu, Co, Ni, Mn in Na-A	430-630	Batch	-	[40]
Rh/ZnO, CeO_2, ZSM-5, Cu-ZSM-5, Co-Al-CO_3-HT(hydrotalcite)	150-500	Flow	O_2,NO_2, H_2O	[46]
Rh/S (support) S: USY, Na-Y, Al_2O_3, ZrO_2, FSM-16, CeO_2, La_2O_3,	200-400	Flow	-	[54], [55]
Rh/S(support) S:Al_2O_3, ZSM-5, TiO_2, ZrO_2, Mg-Al oxide	200-500	Flow	O_2,NO, H_2O, SO_2	[56]
Rh+ Na_2O/Al_2O_3 Promoters: Li, Na, K, Cs	200-450	Flow	-	[57]
Rh/S(support) S: MCM-41, SBA-15-S, SBA-15-C, KIT-6	100-620	Flow, TPR	O_2	[33]
Metal: Rh-Ru-Pd-Fe Support: SBA-15, KIT-6	100-600	Flow	H_2O	[58]
Ir/Al_2O_3	200-500	Flow	O_2	[60]

1.4 Scope of Thesis

Development of catalysts for nitrous oxide decomposition is a very critical issue for chemical and defense industries. Firstly, in Chemical Industry, the nitric acid and adipic acid plants are liable for the generation of nitrous oxide which is a greenhouse gas and damages the ozone layer. Thus, decomposition of nitrous oxide is an environmental concern. Secondly, in Defense Industry, nitrous oxide is one of the most important members of the propulsion system as a propellant (as a monopropellant and as an oxidizer in bipropellant systems after its decomposition). In addition, it is also a crucial member of the ramjet engine ground test facilities as a heat source in order to compensate the hot gas requirement after its decomposition.

There are many kinds of catalysts used for decomposition reaction such as metals, metal oxides and metals supported by zeolites.

Transition metals have distinctive properties rather than other metals since they have d subshells partially filled with electrons. This gives them ability to exist in several oxidation states and therefore they provide pathways for catalytic reactions [66]. They have shown activity in the decomposition of nitrous oxide at temperature below 550 °C when introduced into porous structures by various methods such as impregnation, ion exchange or solid state exchange reactions. Especially, ruthenium and rhodium exchanged zeolites have exhibited complete decomposition of nitrous oxide to oxygen and nitrogen at temperatures below 350 °C [61].

In this context, zeolite Y with a silica/alumina ratio of Si/Al = 2.5 was selected as a suitable host material for transition metals for its advantageous properties. First of all, it is stable in aqueous solution as well as solid at high temperatures up to 600 °C. In addition, the structure of zeolite Y gives the opportunity of studying with various materials since it provides large cavities [67].

Framework of zeolite Y consists of sodalite cages (β-cages, 0.7nm) and hexagonal prisms. The connection of these structures (Figure 5) results in a three dimensional pore system with large supercages (α-cages) of 1.3 nm diameter [68,69,70,71].

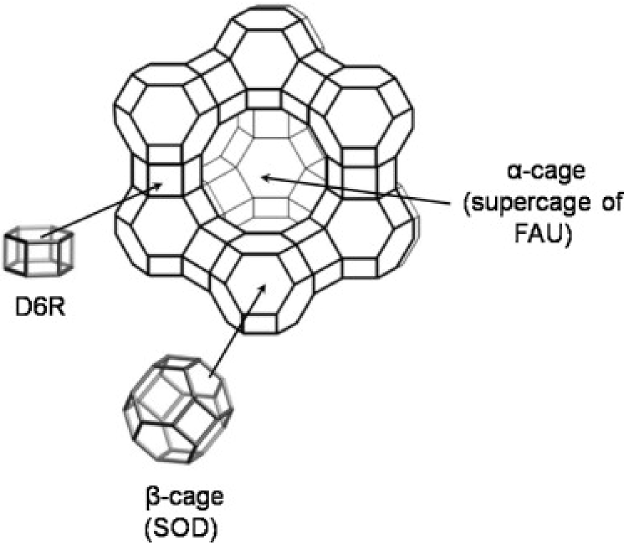

Figure 5. The framework structure of FAU including its cavities [72]

This three dimensional pore structure enables transferring of substrates or products throughout the framework although one of the pores might be blocked (Figure 6).

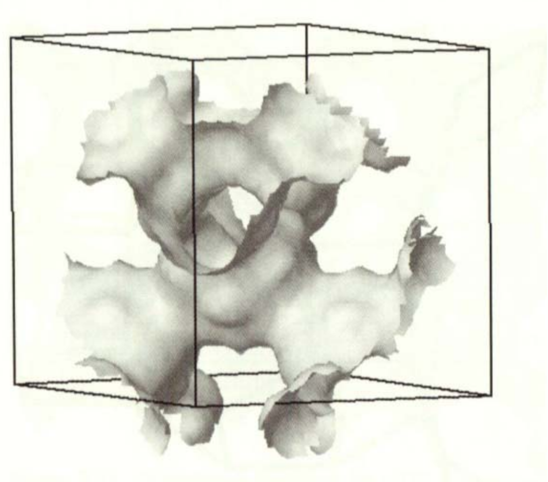

Figure 6. Three dimensional channel system in FAU with 12-ring pores opening in large super cages [73].

The main pore structure has an aperture of 7.4 Å which allows the passage of small molecules. The sodalite and α cages have a void volume of 51% in Zeolite Y. The supercage itself represents the 45% volume of the unit cell volume [74].

Although some efforts have been devoted to use the transition metal ion-exchanged zeolite Y in decomposition of nitrous oxide, a thorough investigation of these catalytic materials has not been reported yet. The catalytic properties such as durability, reusability, activity depending on the metal loading of zeolite need to be studied. Also, the selection of metal ion to be used in ion-exchange is important as well as the zeolite in obtaining the metal ion-exchanged zeolite with the desired amount of metal ions within cages of zeolite. The metal ions remained on the external surface of zeolite are not as active as the ones in the cages. As observed in some of previous studies [72], an incomplete ion-exchange of metal ions into zeolite may cause to a lower conversion rate or high temperature required for an appreciable rate of conversion.

In this study, transition metals of Group 8 (Fe, Ru, Os) and Group 9 (Co, Rh, Ir) were introduced to zeolite Y by ion exchange of metal chlorides which are small enough to enter the cages of zeolite Y through the 7.4 Å aperture [67]. The prepared catalysts were used for catalytic decomposition of nitrous oxide.

By this study, a database could be created for needs of TUBİTAK-SAGE including information about the production, characterization, and activities with respect to metal loadings of Group 8 and Group 9 metal exchanged zeolites. Additionally, the stability, durability and reusability of catalysts will be studied in decomposition of nitrous oxide since these properties are the key factors in selecting appropriate catalysts in practical applications. The ones which show high activities will be candidates for applications in large scale all up round tests for future studies of TUBİTAK-SAGE and tried for the first time for hot gas sources in such experimentation in Turkey. Moreover, a new temperature and flow controlled experimental set-up could be designed in laboratories of TUBİTAK-SAGE, capable of testing catalyst activity and analyze side reactions during catalysis reaction.

The studies carried out in scope of this thesis are given in summary below;

(i) Ru(III), Os(III), Fe(III), Co(II), Ir(III) and Rh(III) exchanged zeolite Y were prepared and characterized by ICP-EOS, ICP-MS, XRD and XPS techniques.

(ii) Catalytic activity of ruthenium(III) ion-exchanged zeolite Y was studied in the decomposition of nitrous oxide to nitrogen and oxygen depending on the ruthenium loading of zeolite and the flow rate of nitrous oxide.

(iii) Activity of ruthenium(III) ion-exchanged zeolite Y was compared with the other two metals of Group 8, Os(III) and Fe(III) .

(iv) The intrazeolite ruthenium(0) nanoclusters were prepared from the reduction of Ru^{+3}-exchanged zeolite-Y with sodium borohydride following the procedure described elsewhere [75] and the nanoclusters were also used for the decomposition of nitrous oxide. The activity of nanoclusters was compared with that of Ru^{+3}-exchanged zeolite-Y.

(v) The stability and reusability tests were performed for ruthenium(III) ion-exchanged zeolite-Y.

(vi) Catalytic activity of rhodium(III) and iridium(III) ion exchanged zeolite Y were studied in the decomposition of nitrous oxide depending on metal loadings of zeolite Y.

(vii) The activities of Group 9 exchanged zeolite Y catalysts were compared with each other.

(viii) The comparison of activities of Group 8 and Group 9 metal exchanged zeolite catalysts were done.

(ix) NOx analyses were performed for Group 8 and Group 9 metal exchanged zeolite catalysts.

CHAPTER 2

GENERAL DEFINITIONS

2.1 Catalysts:

Catalyst is a substance that increases the rate of approach to equilibrium of a chemical reaction without being substantially consumed in the reaction [76]. The phenomenon occurring when a catalyst is involved is named as catalysis. Catalysts have been used for many years in nature, in industry and in scientific applications. The usage of catalysis contributes to one sixth value of all manufactured goods [77].

Catalytic reactions take place in various phases such as in solutions, within the solution like confines of micelles, within polymer gels, within the molecular scale cages of crystalline solids such as molecular sieve zeolites and on the surface of solids in the presence of variety of catalysts. Acid base catalysts, metal, metal oxide or organometallic catalysts, organic and inorganic polymers can be given as examples for catalysts. However, catalysts can be mainly divided into three groups as homogeneous, heterogeneous and biochemical catalysts or enzymes. The first two was classified depending on whether the catalyst exists in the same phase with the substrate or not. Homogeneous catalysts are present in the same phase as the substrates. Proton acids used in esterification of acids or organometallic compounds where transition metals are stabilized by ligands can be given as typical examples of homogeneous catalysts. Heterogeneous catalysts, on the other hand, are in different phase from that of the substrates. Usually, solid catalysts placed in a liquid reaction mixture or placed in a reactor and fed by gas flows. In case of homogeneous catalysts, more effective mixing is possible since catalyst and the substrates are in the same phase. But this fact brings out the disadvantage of recovery. On the other hand, heterogeneous catalysts give the opportunity of recovery which is favorable in manufacturing processes. Today, industry prefers using heterogeneous catalysts for their easy separation from reaction products and for their reusability, stability, low cost and low toxicity properties. Heterogeneous catalysts generally work in a three-step process.

i) One or more reactants are adsorbed on to the exterior surface of catalysts at active sites

ii) Reaction takes place

iii) The products desorb from the catalyst surface and diffuse away.

Two distinct mechanisms are given in the surface-catalyzed transformation of gas phase species A and B to a product C in Figure 7.

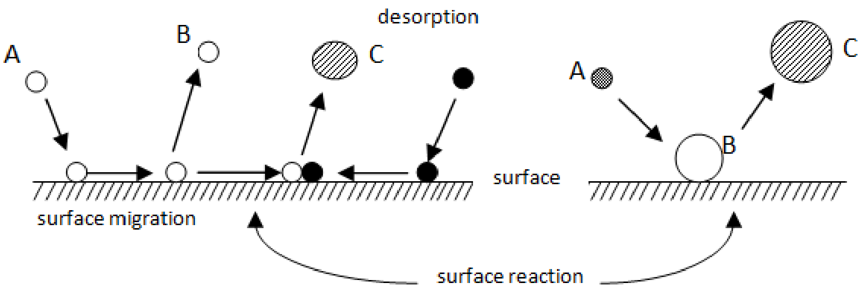

Figure 7. Mechanisms for surface-catalyzed transformation of gas phase species A and B to a product C.

In the first mechanism, either both species can attach to the surface following an atomic reorganization resulting an adsorbed layer or these adsorbed species undergo bimolecular reaction to form products (Langmuir-Hinshelwood Mechanism). In the second case, only one of these species is bound, and is converted to product when the other impinges upon it from the gas phase (Elay –Rideal Mechanism). In most cases, the first mechanism holds good far more than the second one.

The terms adsorption and absorption must be distinguished from each other. Adsorption is a preferential accumulation of material at a surface, absorption is a bulk phenomenon. One must note that, the amount of gas taken up by a solid at a fixed pressure and temperature is proportional to its surface area, not to its volume. In this situation adsorption predominates. This distinction is lost in the case of materials which capable of intercalating guest species or are highly microporous as zeolites having cavities and channels of molecular dimensions so that most of the surface area resides inside the solid.

Biochemical catalysts or enzymes, on the other hand, cannot be categorized according to phase difference. They are gigantic molecules having typical molecular weights in the range of 6,000 to 600,000. Their structures are very complex and specific for only one biological reaction, or sometimes one class of reactions (Figure 8). In other words, they work as lock and key mechanism. All biological reactions in nature have been processed by enzymes [78].

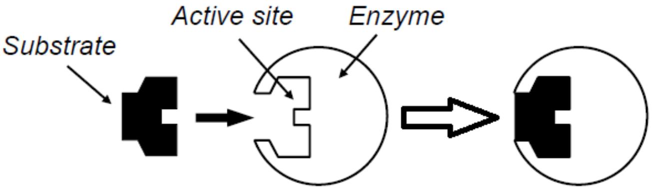

Figure 8. Key and lock mechanism for enzymes

Catalysts increase the rate of processes by introducing new pathways so called *mechanisms* having lower activation energies (E_a) when compared to that of uncatalyzed reaction. A catalyst does not affect the total Gibbs Free Energy (ΔG) of overall reaction. However, it provides new elementary steps having lower entropy and enthalpy of activation thus, decreases Gibbs free energies of activation (ΔG^{++}) (Figure 9).

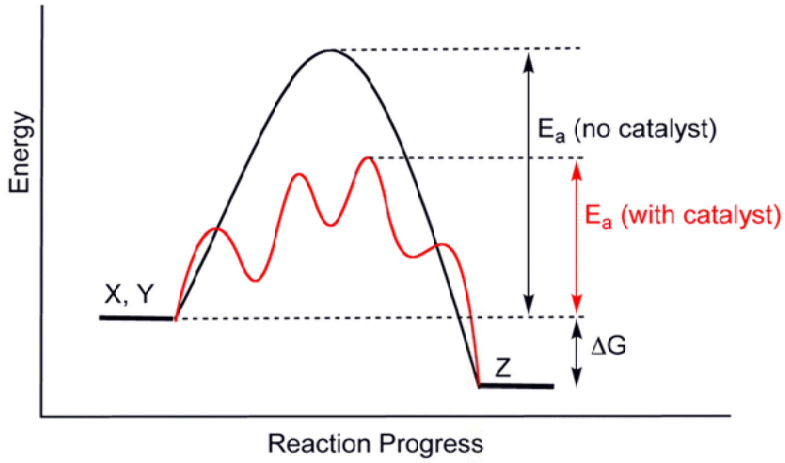

Figure 9. Potential energy diagram for both uncatalyzed and catalyzed conditions of a reaction

Catalysts decrease the activation energy of a reaction in two ways. In the first way, catalyst provides a surface where reactants can come together and change their orientation and thus increase the probability of collisions. The energy of these collisions then becomes high enough to overcome the activation energy. The entropy of the reaction is also reduced by the presence of catalysts since it holds the reactants together in an oriented way. Secondly, catalysts form bonds with reactants and reduced the energy needed by reactants to complete the reaction.

While working with catalysts, some terms are also mentioned such as, *inhibitors*, *promoters* and *poisons*. An inhibitor is a material which slows down a reaction. For example, a competitive inhibitor slows down the reaction by competing with reactants in bonding to the catalyst. A very strong inhibitor will bond to catalyst so strongly that it prevents reactant from reaching to catalysts. These inhibitors are called poisons [78]. Promoters, on the contrary, are not themselves catalysts but improve the catalyst performance when mixed in small amounts with catalysts. These materials can aid the dispersion of catalysts or protect the catalyst surface to prevent unwanted production of materials which will deactivate the catalyst.

The term activity is a quantitative measure of how fast a catalyst works. It is usually defined as reaction rate for conversion of reactants into products. During catalytic reactions, some products may form in addition to desired ones and a catalyst has an activity for each particular reaction. Selectivity is a measure of the catalyst's ability to direct the conversion to the desired products. This phenomenon is more important in large scale applications.

In practice, catalysts are chosen on the basis of stability. The higher the stability, the lower the rate at which the catalyst loses its activity or selectivity, or both. When the catalyst loses its activation; in other words, when it is deactivated, it may be regenerated by applications of some treatments.

The activity of a catalyst can be determined by following the concentration of reactants and products with respect to time. Most of the reactions give rate curves just in shown in Figure 10.

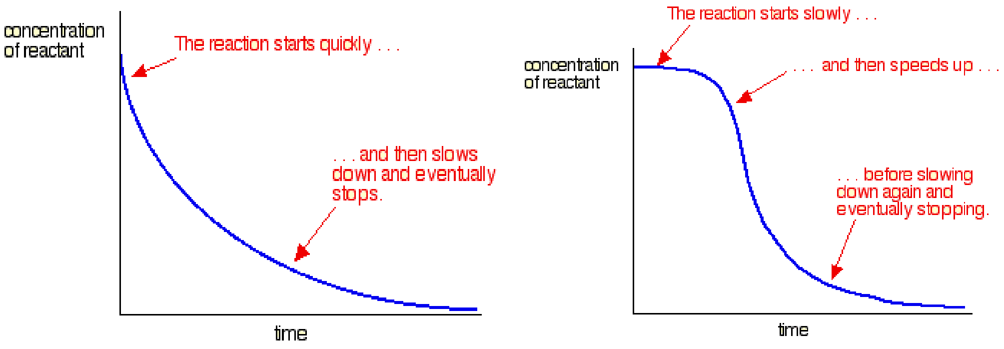

(a) (b)

Figure 10. The diagrams of activity of catalysts: (a) Concentration versus time graph of fast occurring catalytic reaction (b) Concentration versus time graph of autocatalytic or temperature dependent reactions.

At the beginning where reactant concentrations are high, reaction may start quickly and show a rapid fall in the reaction graph. Then, as the reactant concentrations decrease, the reaction slows down and eventually stops by the consumption of reactants.

In the second case, reaction may catalyze by some of its reaction products (autocatalysis) and by the formation of catalyst, reaction rate increases. Or, there might be some sort of surface coating on the catalyst where the reactant has to penetrate before the expected reaction can happen. Also, the reaction rate may be increased by increasing the temperature of reactions. In all these cases, the reaction starts slowly, until the catalyst is activated by penetration or increasing of temperature. Then, by the consumption of reactants, reaction slows down and eventually stops.

2.2 Zeolites:

Zeolites are crystalline aluminosilicates with tetrahedral framework structure enclosing cavities occupied by cations and water molecules, both of which have enough freedom of movement to permit cation exchange and reversible dehydration [79]. Cronstedt, the Swedish mineralogist, discovered the first zeolitic minerals in 1756 [80]. He named this new type of material as zeolites (greek: zeos= boil, lithos=stone) since he observed steam after heating these minerals. Between the years 1777 and 1800s, properties of zeolites were described by several authors including their adsorption properties and reversible cation exchange and dehydration processes. The first hydrothermal synthesis of a zeolite was reported by St. Claire Deville [81]. Friedel have observed that some liquids were occluded by dehydrated zeolites in 1896, and developed an idea that zeolites have open spongy structures [82]. In 1925, the first molecular sieve effect was published by Weigel and Steinhoff [83]. Since the time zeolites first used in petroleum processing in the 1960s, zeolite catalysis has undergone rapid and dynamic advances. By the year 1981, the number of US patents published related to zeolites exceeds 5000 and literature was containing over 25000 articles about zeolites [84]. Currently, 160 different types of zeolites are known. Of this large number of zeolites, many of them are found in nature [85]. However, only a few have found commercial applications. Synthetic zeolites were mostly preferred ones in catalytic applications due to impurities found in natural zeolites.

The annual market of synthetic zeolites and molecular sieves has grown enormously. The major application areas of this market are ion-exchange materials, adsorbents and catalysts. The main application areas of zeolites are shown in the Figure 11.

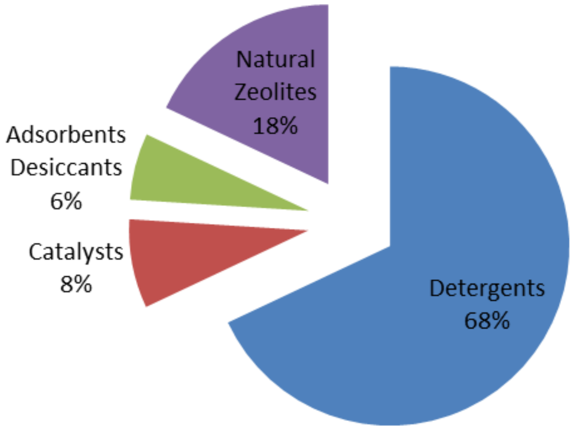

Figure 11. Main Application Areas of Zeolites [86]

Zeolites are formed by hydrothermal synthesis, typically under mild conditions [87]. The nature of zeolite is determined by the synthesis conditions, i.e., reactant concentrations, pH, time, temperature, and the nature and concentration of added promotors. Desired particle sizes and shapes are obtained by controlling the crystallization process. A schematic diagram of synthesis of Faujisite simply shown in Figure 12.

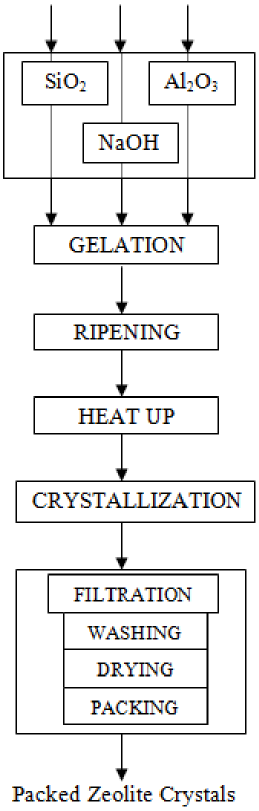

Figure 12. Synthesis of Faujisite

The fundamental building block of all zeolites is tetrahedrons (TO_4, T for tetrahedra) of four oxygen anions surrounding a small silicon or aluminum ion (Figure 13) and each of the four oxygen anions is shared with another silica or alumina tetrahedron (Figure 14).

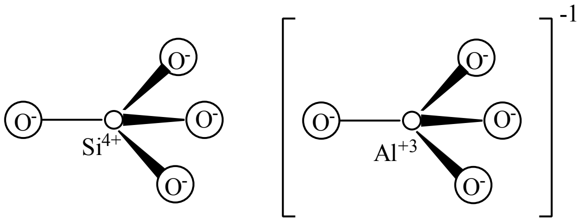

Figure 13.Primary Buildings Blocks of Zeolites

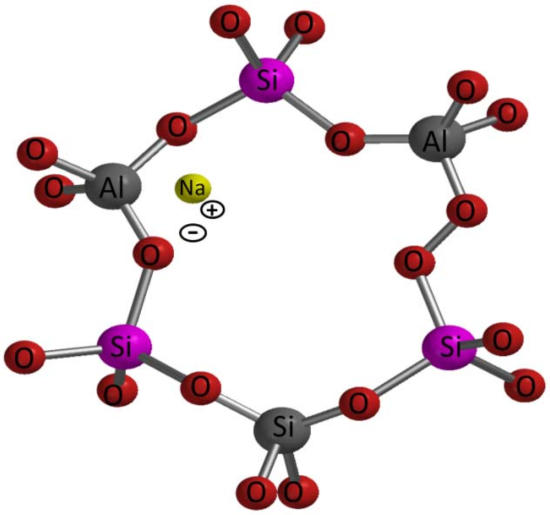

Figure 14. Illustration of charge compensation of negative charge in the framework by extra framework Na^+ cations.

Each silicon ion has its +4 charge balanced by the four tetrahedron oxygens and silica tetrahedra (SiO_4) are therefore electrically neutral. Each alumina tetrahedron (AlO_4) has a residual charge of -1 since trivalent aluminum is bonded to four oxygen anions. Therefore each alumina tetrahedron requires a +1 charge from cation in the structure to maintain electrical neutrality. The most alkaline, earth alkaline and transition metal cations can be used for balancing the negative charge in the framework. Typically, Na^+ cations are the charge compensating cations in the framework of zeolites.

The unit cell formula of zeolites is usually written as:

$$Na_x(AlO_2)_x(SiO_2)_y.nH_2O \text{ or } Na_x[Al_xSi_{y-x}O_{2y}]_nH_2O$$

The primary building units link together to form more *complex building units* (CBUs) in other words *secondary building units*. The simplest examples of these structures are rings. All zeolites are formed by these rings of different sizes. Ring containing n tetrahedra are called n-ring. The most common ones are 4, 5, 6, 8, 10, or 12 tetrahedra rings [88] but rings formed by 14, 18, and up to 20 tetrahedra have also been reported [89, 90, 91, 92].

When a ring defines the polyhedral unit, it is also called a window. Structures of some rings were illustrated in Figure 15.

The construction of larger units from these rings results in structures such as cages [88]. The size of the cages depends on the shape and geometry of the rings. Figure 16 shows different types of cages.

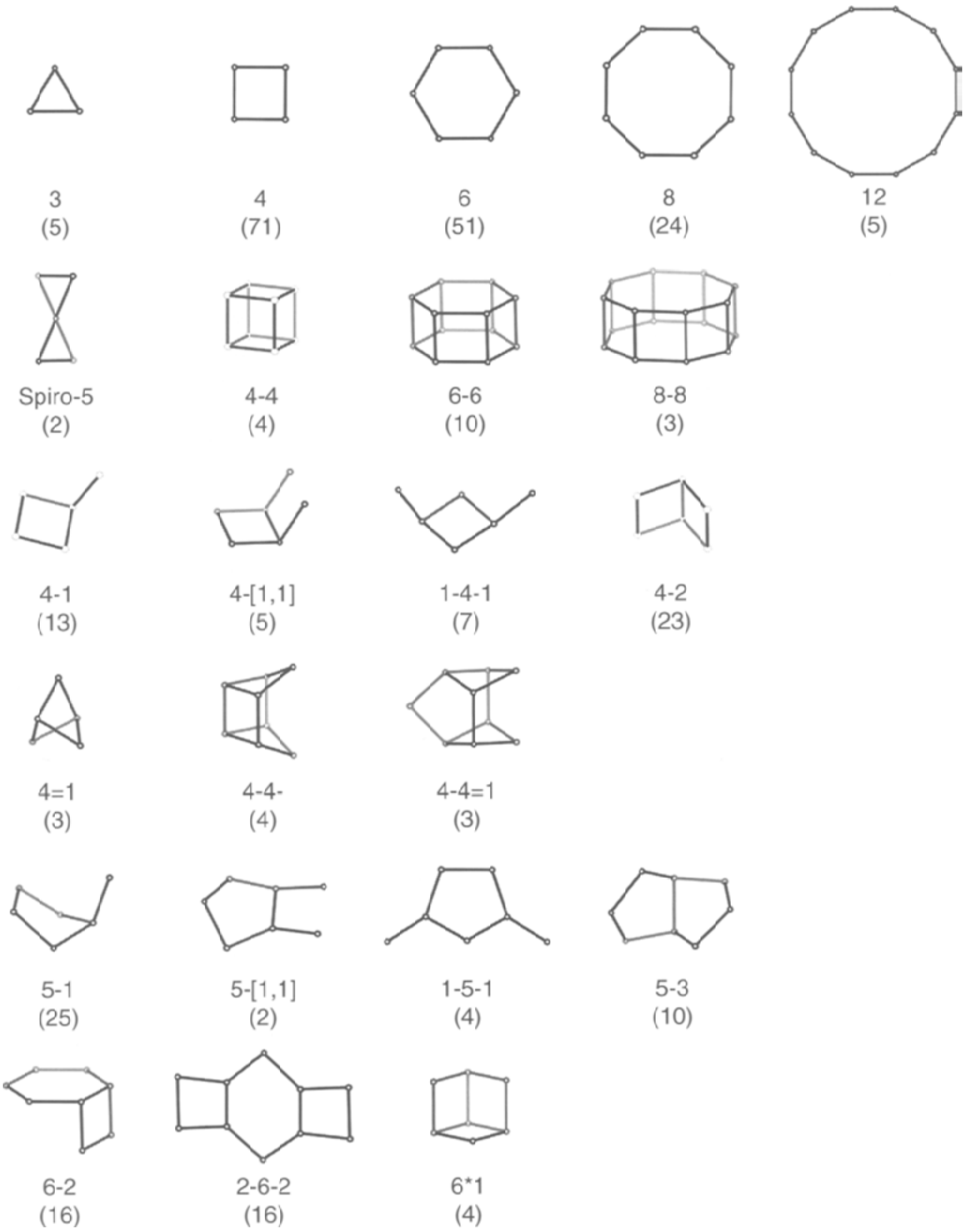

Figure 15. Structures of Some Rings (frequency of occurrence is shown in parenthesis) [73]

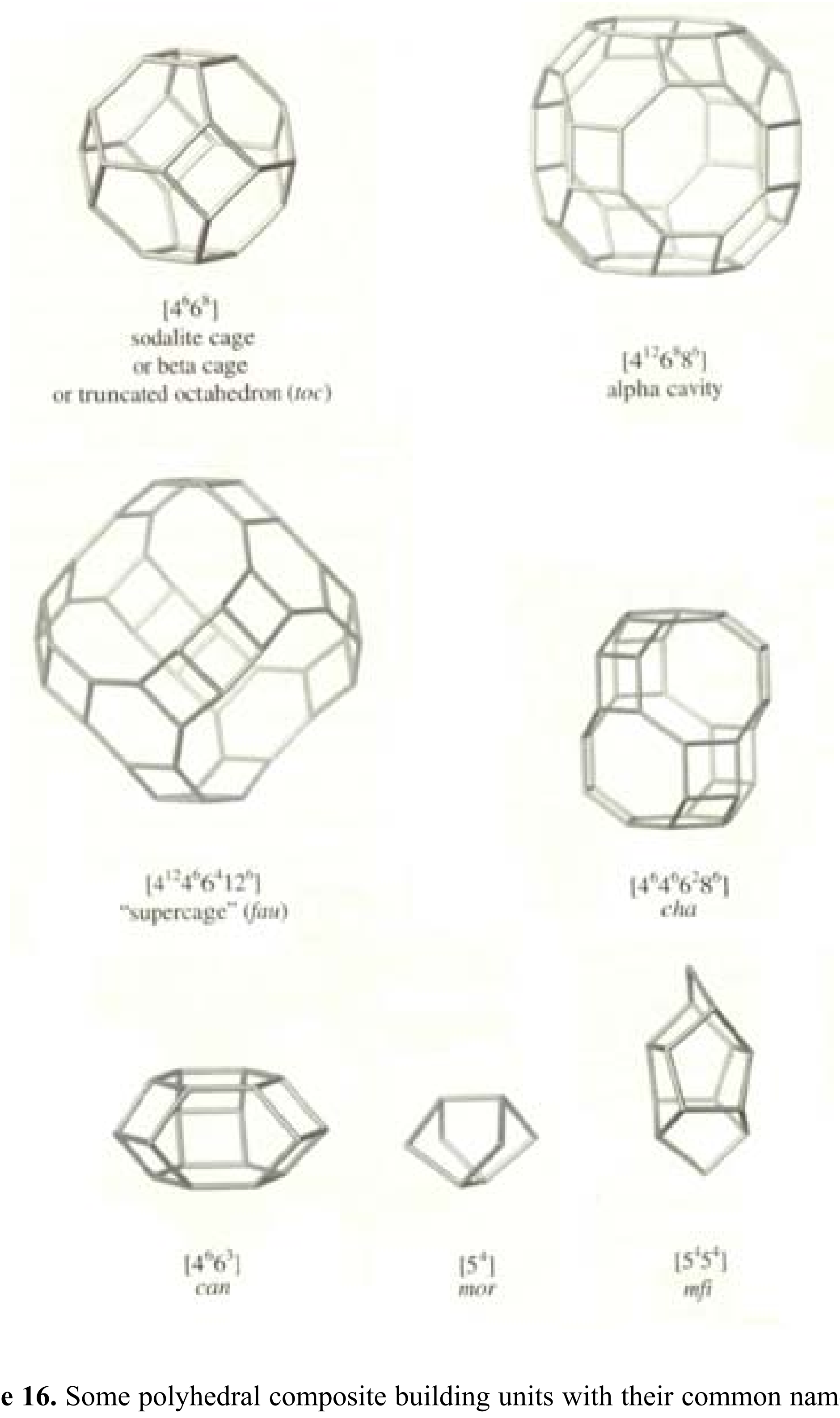

$[4^6 6^8]$
sodalite cage
or beta cage
or truncated octahedron (*toc*)

$[4^{12} 6^8 8^6]$
alpha cavity

$[4^{12} 4^6 6^4 12^4]$
"supercage" (*fau*)

$[4^6 4^6 6^2 8^6]$
cha

$[4^6 6^5]$
can

$[5^4]$
mor

$[5^4 5^4]$
mfi

Figure 16. Some polyhedral composite building units with their common names and symbols indicated. The nodes are Si and Al which are tetrahedrally coordinated to each other. Oxygen atoms have been left out for clearity [73].

Zeolites A, X, and Y are consist of tetrahedra linked to form cubo-octahedra or so called sodalite cage units. When these units are linked through four membered rings zeolite A is formed. The sodalite unit, which contains 24 silica and alumina tetrahedra, is the secondary building block of a number of zeolites including zeolite A, zeolite X, zeolite Y and faujisite. It is usually considered that 6-rings are the limiting ring size to form a cage. Thus, molecules having a free diameter of 2,6Å such as water, helium or hydrogen ions can penetrate into these units through six membered oxygen rings. The complex building units were denoted by a descriptor $[n_i^{mi}]$ where m denotes the number of n rings defining the polyhedron. Sodalite cages can be represented by $[4^6 6^8]$ indicating that it is formed by the connection of six 4-rings and eight 6-rings.

Chains are one dimensional polyhedral secondary units that are frequently found among zeolite structures (Figure 17).

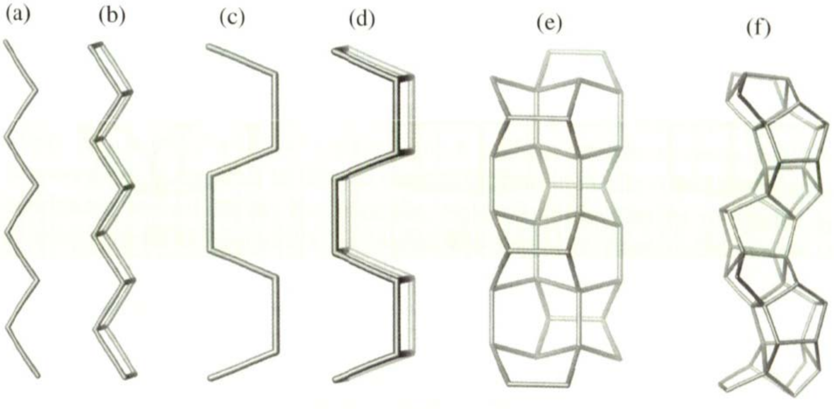

Figure 17. Some examples for chain composite buildings: (a) Single chain, zig zag (b) double chain, double zig zag (c) Single chain, crankshaft (d) double crankshaft (e) Complex chain (f) Complex pentasil chain [73].

ZSM-5 and zeolite L zeolites give good examples for chains. In case of ZSM-5, the chains are formed by connection of 5 membered rings. However, for zeolite Y, chains contain 4-rings, 6- rings and 8-rings. Chain structures vary due to connections of rings just in the case of other secondary building units.

Cavities are polyhedral units which were different from cages since they contain windows allowing the passage of molecules in and out of the cavity [93]. In the case of cavities, water molecules, linear alkanes and small molecules like CO_2 and N_2 can penetrate. In Figure 18 pore sizes of some zeolite frameworks and kinematic diameters of various gases and organic molecules are given. As the pore size of zeolites gets larger, large molecules having high kinetic diameters can pass through these pores.

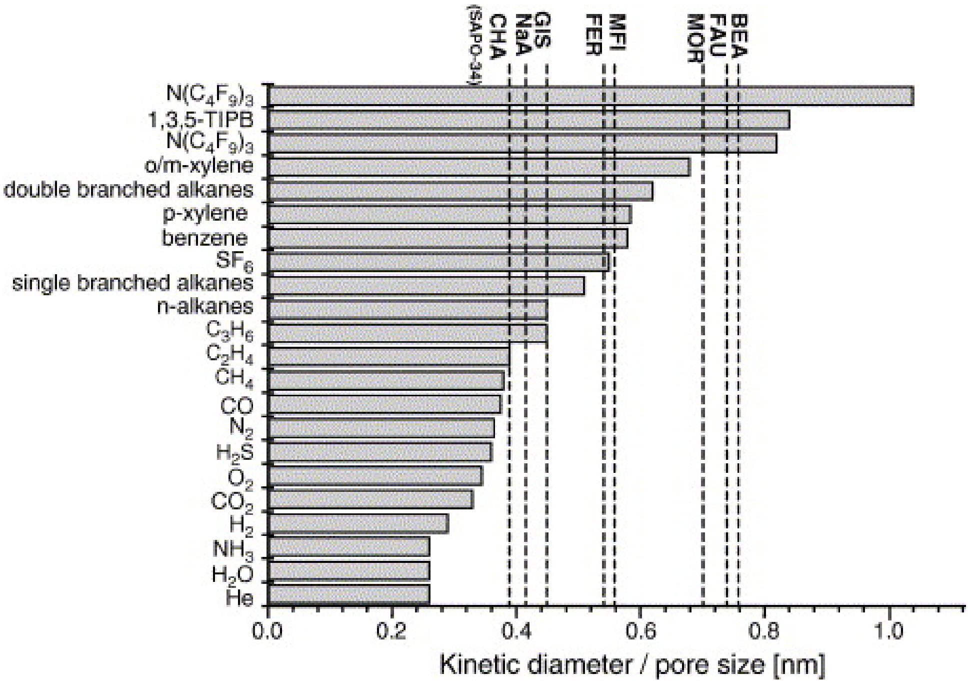

Figure 18. Pore sizes of some zeolite structures and comparative kinetic diameters of common molecules used in various catalytic applications [94]

A channel is a pore that is infinitely extended in at least one dimension with minimum aperture size (n ring) allowing guest molecules to diffuse along the pore. The aperture dimensions of channels are determined by the number of T atoms of the n ring. Structures with 8-ring, 10-ring, or 12-ring channel apertures are the most common ones which are known as small, medium and large pore zeolites respectively. Guest molecules are in van der Waals contact with the oxygen atoms in the framework as they move inside the channels and cavities inside the zeolite [95]. However, T atoms in framework are surrounded by the four oxygen atoms and are sterically shielded by them. Therefore, guest molecules cannot be in direct van der Waals contact with T atoms. In addition we can talk about the interaction between guest molecules and extra framework cations which are coordinated with framework oxygen atoms.

The pore apertures given in previous figures are only approximation based on free diameter values. In fact, the exact dimensions depend on particular structure and composition of zeolite in question. When cations coordinate at channel windows, they reduce the opening size and in some cases they may block the passage of molecules into the crystal [96]. In addition, adsorbed molecules may perturb the position of framework atoms and may change the exact dimensions of the free diameter due to flexibility of zeolite framework caused by plenty of internal void space [97,98,99,100].

Zeolites structure types are denoted by a three letter code [85]. For example, FAU is used for denotion of faujisite structure whereas MOR is used to indicate mordenite. Some structure types, their designations and information about structures are given in Table 3.

Table 3. Constituent Units of Zeolite Types and their designations [101]

Code	Full Name	Secondary Building Units			
FAU	Faujisite	4	6		6-6
LTA	Linde Type A	4	6	8	4-4
RHO	Rho	4	6	8	8-8
CHA	Chabazite	4	6		6-6
KFI	ZK-5	4	6	8	6-6
OFF	Offrite		6		
PHI	Phillipsite	4		8	
ERI	Erionite	4	6		
LTL	Linde Type L		6		
MOR	Mordenite		5-1		
MEL	ZSM-11		5-1		
MFI	ZSM-5		5-1		

The properties of zeolites are determined according to their chemical composition. In other words, composition of framework, the identity of extra framework cations and guest species changes the chemical properties of the zeolite. Framework composition is given as the ratio of silicon to aluminum (Si/Al). Experimentally, the lowest limit of Si/Al ratio is one. Zeolites having a Si/Al ratio lower than 10 are called low silica zeolites whereas the ones having higher Si/Al ratio than ten, named as high silica zeolites. Low silica zeolites contain a large number of aluminum cations(+3) whose negative charge in framework need to be balanced by extra framework cations. Thus, low silica zeolites have high ion exchange capacity. In case of higher aluminum content materials, the bonding is more ionic in character as compared to the siliceous counterparts. The thermal stability without losing the structural integrity decreases as the aluminum content increases [102]. It is also found that maximal number of acid sites (i.e protons) increases with the amount of aluminum in the framework. Also, the strength of acid sites decreases as aluminum fraction increases [103]. Because, $[AlO_{4/2}]^-$ groups increase the effective charge of oxygen atom on acid site and make it less prone to donate proton.

One way of changing the chemical properties of a zeolite is to replace some or all of the tetrahedral framework atoms with other atom types. If the zeolite structure is composed of totally silicon it does not require any counterbalancing cations since the framework is neutral [73]. Substitution of some Si^{+4} cations with Al^{+3} cations creates a negative charge which needs to be balanced by extra framework cations as explained previously. Other cations can incorporate into frameworks such as B, P, Fe, Zn, Ga and Ge in addition to Al and Si. In 1971, P^{+5} cations were substituted in the framework [104] and later aluminophophate materials, $AlPO_4$, were prepared without using any silicon in the framework [105]. These aluminophosphate materials created a new class having over 50 members. This class includes new framework types in addition to some aluminosilicate analogs. It is determined that at least 16 different elements exist in the framework of aluminophosphate. In addition to this class, borosilicates [106], gallosilicates [107], zincosilicates [108], and germanosilicates [109] are the other common examples having different and unusual properties reported in the literature.

2.3 Transition Metal Nanoclusters:

Transition metal nanoclusters can be briefly described as metal particles having diameters between 1-10 nm [110]. These particles have unique chemical and physical properties since their properties lie somewhere between single-particle species and bulky species [111]. Bulk materials have energy bands resulting from the combination of infinite number of energetically similar orbitals. The valence bands of transition metals contain s and d electrons. The valence and conduction bands overlap to some extent and conduction band is partially occupied by mobile electrons. This situation enables electrical conductivity of metals. However, in case of semiconductors, there is a specific energy gap between valence and conduction bands. This energy gap increases in case of insulators and render electron mobility impossible.

When the size of metal particle is reduced continuously, the overlap of valence and conduction bands starts to disappear and an energy gap is created just in case of semiconductors and then these bands turn into discrete energy levels with further reduction of particle size. These materials are called as quantum dots and obey quantum mechanical rules. This development ends up with the formation of typical molecular situation [112] (Figure 19).

Transition metal clusters can be produced by either top down or bottom up methods. Top down method applications are carried out by physical approaches and bulk materials are broken down to obtain nanosized materials [113]. On the other hand, in bottom-up method, nanoclusters are built up by generating individual atoms which group to form a stable nucleus which are then stabilized [114]. Bottom up approach provides convenient ways to control particle size and can be done by (i) chemical reduction of metal salts [115], (ii) thermal, photochemical or sonochemical decomposition [116], (iii) decomposition of organometallics [117], (iv) metal vapor synthesis [118] and (v) electrochemical reduction [119].

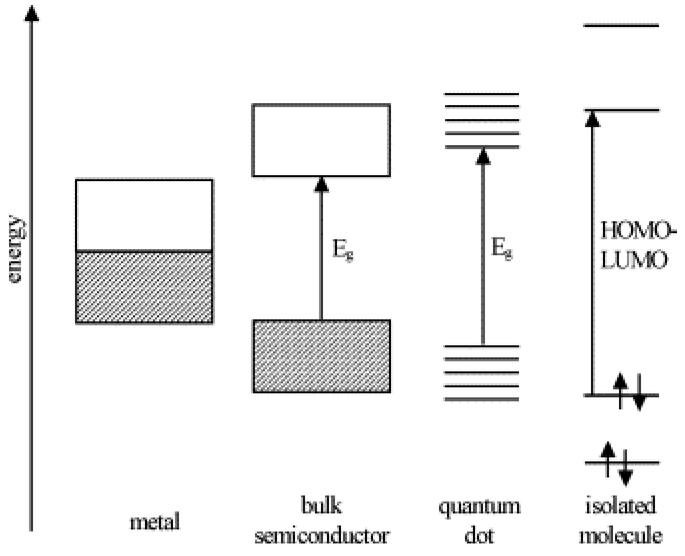

Figure 19. The formation of electronic energy levels for metal, bulk materials, quantum dot and isolated molecules [120]

Stabilization is the key element for production of metal nanoclusters because only stabilization enables these materials to be bottleable and storable. Stabilization is named according to the type of the protecting shell. Thus, stabilization can be achieved sterically (Figure 20), electrostatically (Figure 21), electrostericly (Figure 22) or in the presence of a ligand or solvent.

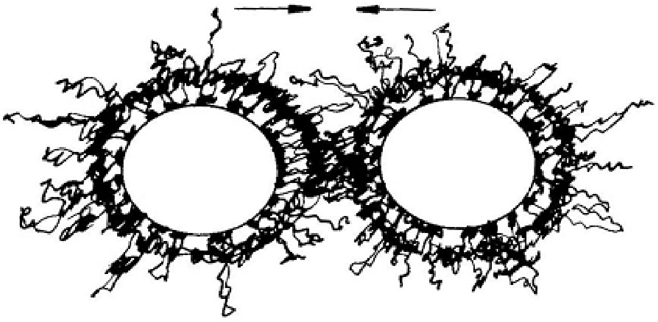

Figure 20. Schematic representation of steric repulsion

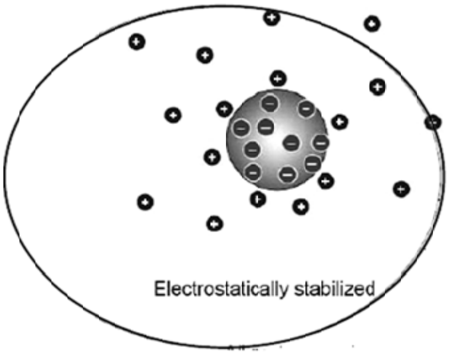

Figure 21. Schematic representation of electrostatic stabilization

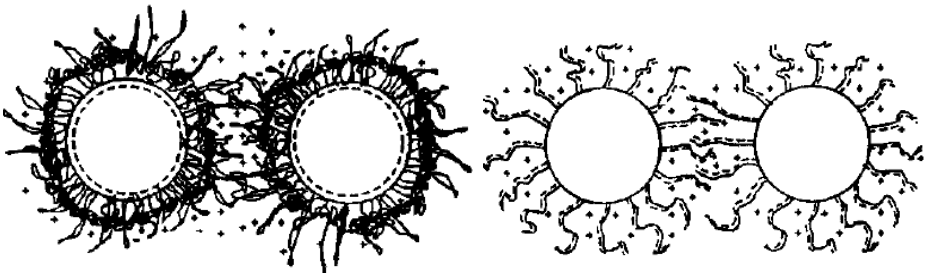

Figure 22. Schematic representation of electrosteric stabilization: (a) Charged particles with nonionic polymers and (b) Polyelectrolytes attached to uncharged particles

Electrostatic stabilization is based on the mutual repulsion of like electrical charges. Anions and cations which interact with the surface of metallic particle form a double layer. This layer forms a coulombic repulsion. Steric stabilization consists in covering the particles in polymers which avoids the particle from getting close in the range of attractive forces. Sometimes, when polymer attached to charged particle, polymer layer forms and in addition an electric potential to the solid surface would preserve. Therefore both electrostatic repulsion and steric restriction prevents agglomeration.

CHAPTER 3

EXPERIMENTAL

3.1 Materials:

Ruthenium(III) chloride trihydrate ($RuCl_3{\cdot}3H_2O$), osmium(III) chloride hydrate ($OsCl_3{\cdot}xH2O$), Iron(III) chloride hexahydrate ($FeCl_3{\cdot}6H_2O$), cobalt(II) chloride hexahydrate ($CoCl_2.6H_2O$), rhodium(III) chloride hydrate ($RhCl_3{\cdot}xH_2O$), iridium(III) chloride hydrate ($IrCl_3{\cdot}xH_2O$), sodium borohydride (98 %) and sodium zeolite-Y ($Na_{56}(AlO_2)_{56}(SiO_2)_{156}{\cdot}xH_2O$) were purchased from Aldrich. Deionized water was obtained by using a two-step water purification system (Elix5/Milli-Q System -18.2 MΩ.cm @ 25 °C, TOC<10 ppb). All glassware and Teflon coated magnetic stir bars were cleaned with acetone, followed by copious rinsing with distilled water before drying in an oven at 150 °C.

3.2 Characterization of Catalysts

The ruthenium, iron, rhodium and cobalt contents of prepared zeolite samples were determined by ICP-OES (Inductively Coupled Plasma Optical Emission Spectroscopy, Perkin Elmer Optima 4300DV Leeman-Direct Reading Echelle). These analyses were performed by dissolving each sample in the mixture of nitric acid and hydrochloric acid in 1/3 ratio. Iridium contents of prepared Ir-Y zeolites were determined by ICP-MS (Perkin Elmer DRC II) since the metal loadings were not high enough to work with ICP-OES. ICP-MS analyses were performed by dissolving fresh aqua regia with hydrofluoric acid and then boric acid was added.

Powder X-ray diffraction (XRD) patterns were recorded with a Rigaku X-ray diffractometer using Cu Kα radiation (40 kV, 30 mA) at room temperature by scanning between 0° and 55° 2θ with 1°/min rate. The X-Ray photoelectron spectroscopy (XPS) analyses were performed with Physical Electronics PHI 5000 VersaProbe using monochromatic Al Kα lines of Al (1486.6eV, 10 mA) as an X-ray source. The FT-IR spectra of zeolite Y and catalysts were taken by Pyris 100 FT-IR spectrometer. The pellets were prepared by mixing the samples with KBr in 1/50 ratio.

3.3 Preparation of metal exchanged zeolite-Y (Ru^{+3}-Y, Fe^{+3}-Y, Os^{+3}-Y, Co^{+2}-Y, Rh^{+3}-Y, Ir^{+3}-Y)

Ruthenium(III) cations were introduced into zeolite Y by ion-exchange [121]. The sodium form of zeolite Y (~500 mg) was added to a solution of $RuCl_3·3H_2O$ (~70 mg) in 100 mL H_2O in a 250 mL round bottom flask. This suspension was stirred at room temperature for three days. The sample was filtered by suction filtration through Whatman 1 filter paper and washed three times with 20 mL deionized water. The filtered solid was dried under vacuum at room temperature.

Fe-Y, Os-Y, Co-Y, Rh-Y and Ir-Y catalysts were prepared by following the same ion exchange procedure [121] and using $FeCl_3·6H_2O$, $OsCl_3·xH_2O$, $CoCl_2.6H_2O$, $RhCl_3·xH_2O$ and $IrCl_3·xH_2O$, respectively.

3.4 Preparation of intrazeolite ruthenium(0) nanoclusters

The intrazeolite ruthenium(0) nanoclusters were prepared from the reduction of Ru^{+3}-exchanged zeolite-Y with sodium borohydride following the procedure described elsewhere [75,114]. Ru-Y sample (3.8 wt.% ruthenium loading, $[Ru^{+3}]$ = 0.02 mM) was added into 100 mL $NaBH_4$ solution (150 mM) at room temperature. Ru^{+3} cations were reduced by $NaBH_4$ and nanoclusters were formed. $[NaBH_4]/[Ru^{3+}]$ ratio was kept over 500 to ensure complete reduction of Ru^{3+} within the cavities of zeolite Y. When the hydrogen evolution finished (less than five minutes), the sample was filtered by suction through Whatman 1 filter paper. The filtered sample was washed three times with 20 mL deionized water to remove metaborate and chloride anions, sample was collected as black powder and transferred into schlenk tube. The tube was placed in a water bath at 70 ºC and dried under vacuum. Dried samples kept in schlenk tube under vacuum at room temperature.

3.5 Method for testing catalytic activity of ion exchanged-zeolite Y catalysts and intrazeolite(0) nanoclusters:

The catalytic activities were determined by monitoring the concentrations of nitrous oxide and its decomposition products, nitrogen and oxygen via gas chromatography (Agilent 7890A with TCD detector). Figure 23 shows the experimental setup designed to perform the experiments.

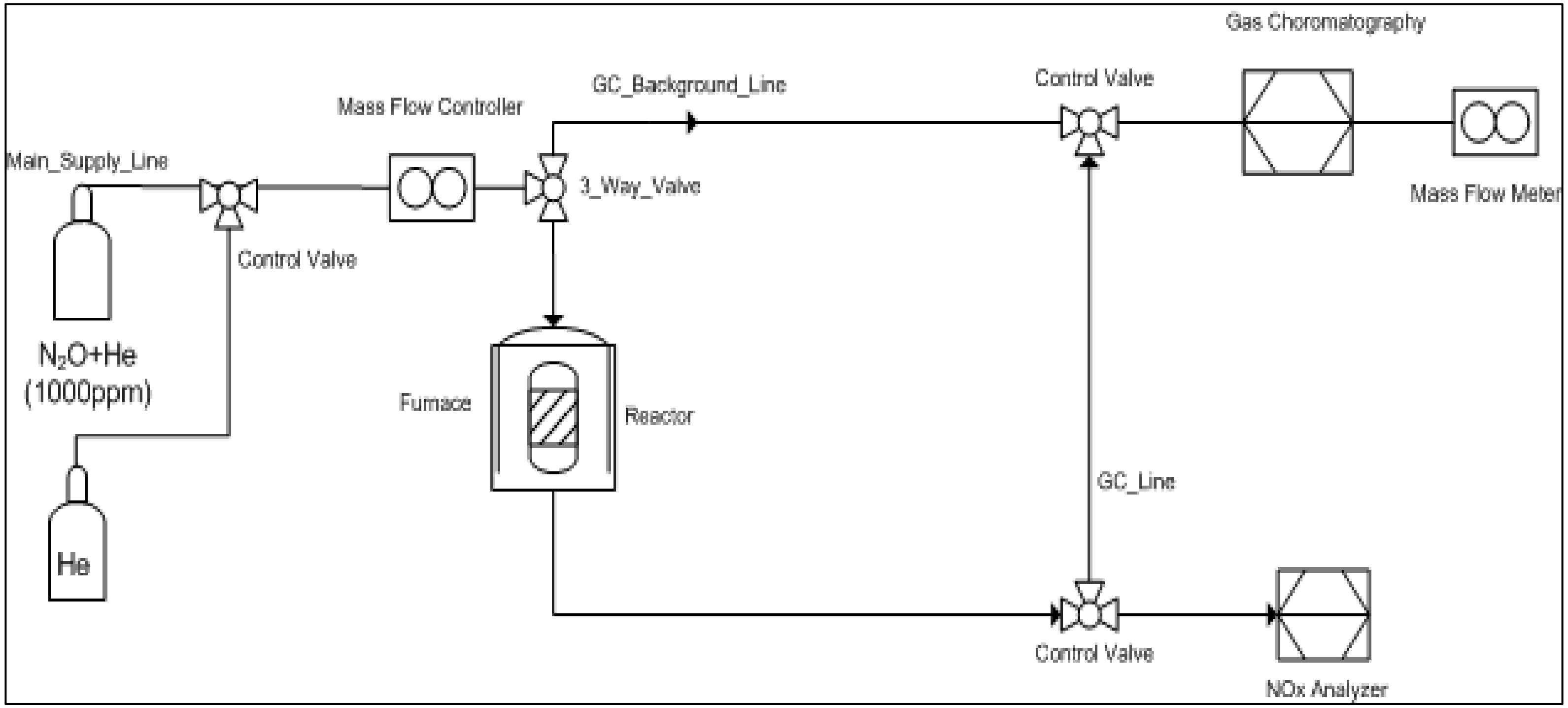

Figure 23. Diagram of experimental set-up designed for the catalytic decomposition of nitrous oxide, showing the tubing, reactor, and instrument connections.

Nitrous Oxide (1000 ppm N_2O in He) was supplied to the system from the pressurized (230 bars) tank and the whole lines (main supply line, GC Background line, hot gas line, and GC line) were assembled by using ¼" copper pipes with the wall thickness of 0.03". All connections were made with Swagelok leak-free fittings. The quartz reactor was connected to the pipeline using Lewvac quartz to metal (SS316) adapters (Figure 24).

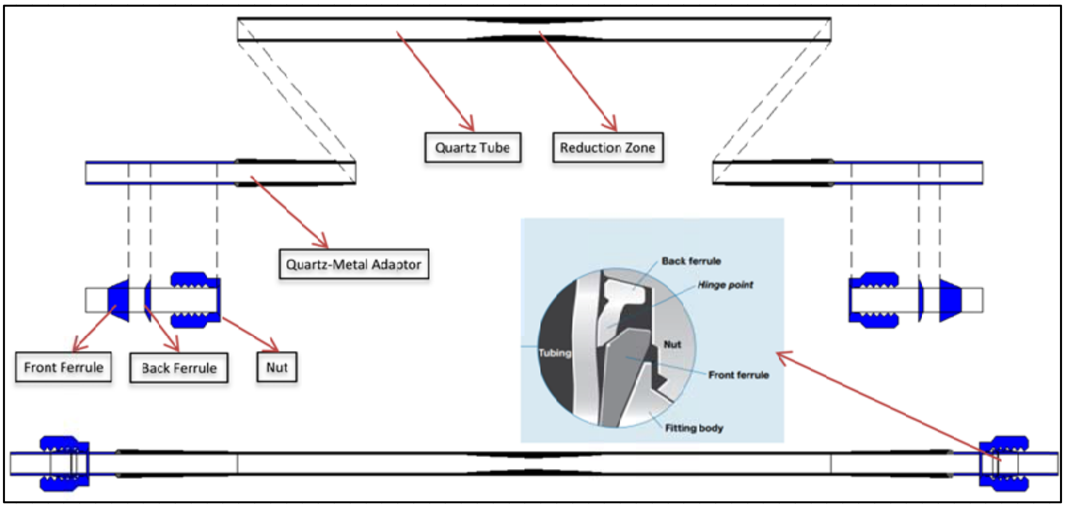

Figure 24. The reactor and its complementary pieces

Swagelok Unions were applied onto the metal sections of the subject adapter and the whole reactor section was installed to the copper pipe by using Swagelok Copper to metal reductions. The reactor was a ¼ "quartz tube with a shrinking section in the middle, to hold the catalyst using glass wool. Reactor was placed vertically to the pipeline and surrounded by a temperature controlled vertical furnace (Protherm). The temperature of reactor was also measured with k-type thermocouple from the outside of the shrinking section (Omega Heavy Duty Transition Probe with Inconel Sheath), and the temperature data were monitored by IOtech Daqbook/2000 data acquisition system. Flow rates of nitrous oxide were adjusted by Aalborg GFC 17 mass flow controller between 50 mL/min to 500 mL/min. Reaction gases were analyzed using gas chromatograph (Agilent 7890A) with a thermal conductivity detector (TCD). Molecular sieve and propaq Q columns were used to separate nitrous oxide, nitrogen and oxygen gases. The reaction was also followed for side products via online chemiluminescence gas analyzer (Ecophysics CLD-60-NOx Analyzer). Outgoing flow from GC was monitored by a flow meter (Agilent ADM 2000) in order to check the presence of any leakage.

GC and NOx analyzers were calibrated before use with standard calibration gases. Three point calibrations were performed for gas chromatograph. The calibration was repeated on every six months. On the other hand, NOx analyzer was calibrated before each run by introducing 40 ppm NO calibration gas.

Before starting the experiments, the system including the capillary tube reactor was cleaned by a flow of Helium at a rate of 100 mL/min for an hour. The oven was heated up to 200 °C. When the system was free of oxygen and nitrogen, the reactant gas (1000 ppm N_2O in He) was supplied to the system at a flow rate of 100 mL/min. The catalytic activity tests were performed by following the concentrations of nitrous oxide, oxygen and nitrogen gases by gas chromatography. Catalytic activities of Ru-Y samples were investigated between 200-425 °C. The reaction temperature was increased to 600 °C for other samples in order to achieve complete conversion. During the measurements, the temperature was increased in 25 °C increments and hold for 30 minutes at each step to reach the steady state. The N_2O conversions were determined by analyzing N_2O and N_2 concentrations evaluated by gas chromatography. The conversion was calculated using the following equation (Eq. 7).

$$Conversion\ (\%) = \frac{[N_2]}{[N_2]+[N_2O]} \times 100 \qquad (7)$$

The existence of any side reactions, thus the side products were followed by an online NOx analyzer. Data were collected at every 30 seconds.

3.5.1 Calibration of Gas Chromatography

Three different gas mixtures were prepared in order to perform three point calibrations for gas chromatography. Each mixture contained different concentrations of oxygen, nitrogen and nitrous oxide. Since the decomposition reaction is giving 1:2 ratio of oxygen and nitrogen and the starting concentration of nitrous oxide is 1000 ppm, the concentration ranges of nitrogen and oxygen were selected as 100 ppm - 400 ppm and 200 ppm - 800 ppm respectively. In order to follow the nitrous oxide concentration in wide range, the nitrous oxide concentration levels were selected between 200 ppm - 800 ppm. The detailed information of calibration gases were given in Table 4.

Table 4. Concentrations of gases (ppm) in helium used for the calibration of gas chromatography

	Oxygen	Nitrogen	Nitrous oxide
Calibration Gas 1	100	200	800
Calibration Gas 2	200	400	600
Calibration Gas 3	400	800	200

All calibrations were done by feeding calibration gases through background line shown in Figure 23. Before starting the experiments, background line was cleaned with 100 mL/min flow of helium gas for thirty minutes. The sign of any leakage, thus the presence of nitrogen or oxygen peaks, was checked by gas chromatography and calibration was started after being sure that the pipeline is totally clean. For each calibration gas, at least three repeatable data were collected and the best value among them was selected. The selected values from these three gases were entered to the software and the calibration curves were drawn automatically. The calibration results were saved as a new method and used for the following measurements. Correlation value of each calibration curve should be above 0.999 for the accuracy of calculations. The examples for calibration curves can be seen in Figure 25.

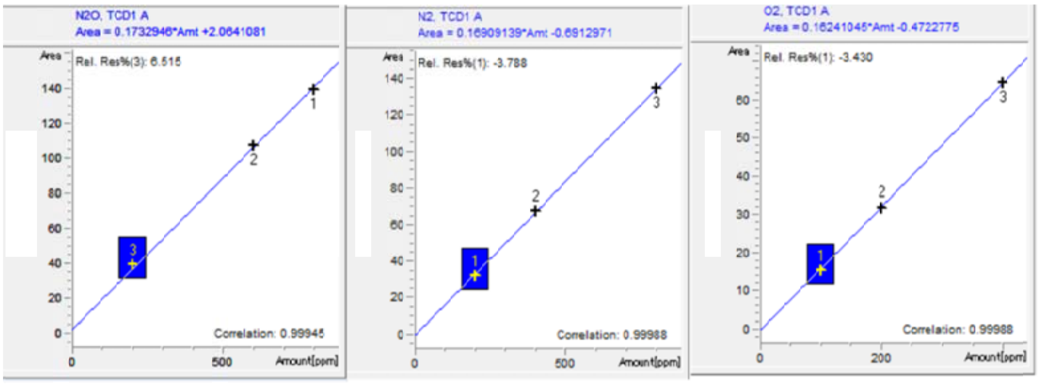

Figure 25. Calibrations curves for N_2O, N_2 and O_2 gases calculated automatically by Gas Chromatography

3.5.2 Validation/Correction of NOx Analyzer

NOx analyzer was validated by using 40 ppm NO calibration gas with the flow rate of 100 ml/min before each run. Before introducing the calibration gas, the instrument was set to zero by giving air from the atmosphere (NOx value in the air was assumed to be zero). Then, the system was fed by 40 ppm NO gas and corrections were done automatically by the NOx analyzer.

3.6 Testing the effect of ruthenium loading on the catalytic activity by keeping catalyst amount constant (100 mg)

A series of experiments were performed with five different ruthenium loading of 3.8, 2.03, 1.00, 0.65 and 0.36 wt.% Ru in order to determine the change in activity when ruthenium content in catalysts was increased. For each run, 100 mg of catalyst was loaded to reactor and 1000 ppm of N_2O was given to pipeline at a flow rate of 100 mL/min. All experiments were carried out in the same way as described in section 3.5. Temperature was set to 200 °C at the beginning of the test and, then, increased in 25 °C steps by holding thirty minutes at each temperature step. Experiments were carried out until the observation of complete decomposition (425 °C).

3.7 Testing the effect of ruthenium loading on the catalytic activity by keeping the ruthenium amount constant (1.6 ± 0.1 mg)

A series of experiments were performed with four different samples with 3.8, 2.03, 1.00 and 0.65 wt.% ruthenium loading by keeping the amount of zeolite constant. Each catalyst amount was adjusted to contain 1.6 ± 0.1 mg ruthenium. The samples weights were arranged as follows: Ru-Y1 : 40 mg, Ru-Y2: 85 mg, Ru-Y3:165 mg, Ru-Y4: 250 mg. However, no experiment could be performed using the lowest loading Ru-Y5 catalyst (0.36 wt.%) since the amount of the catalyst material required exceeded the capacity of the small scale reactor to operate under the same flow rate of 100 mL/min. Tests were performed between 200-400 °C and temperature was increased in 25 °C increments by holding thirty minutes at each step.

3.8 Testing the effect of flow rates on catalytic activities

Catalytic decomposition of nitrous oxide to nitrogen and oxygen was performed at various flow rates in the range of 50-500 mL/min (50, 100, 150, 200, 250, 300, 350, 400, 450, 500 mL/min N_2O, 1000 ppm) at 350 ºC using 100 mg of Ru-Y1 catalyst

(3.98 wt.%). The changes in concentration of the reactant (nitrous oxide) as well as the products nitrogen and oxygen were monitored by gas chromatography.

3.9 Testing the reusability of the Ru-Y catalysts

Ru-Y catalysts were prepared in the form of powder and stored under ambient conditions until the use in catalytic decomposition of nitrous oxide. The reusability of catalyst was tested in subsequent runs of nitrous oxide decomposition performed by using the catalyst recovered after the previous run. The activity of catalyst of Ru-Y1 (3.98 wt.%) was followed by gas chromatograph at ten different runs (2, 4, 7, 8, 9, 10, 15, 23 and 150 days after first run) at 350 ºC. The same catalyst (Ru-Y1 (3.98 wt.%)) was used for each run without application any pretreatment. All tests were performed with 1000 ppm N_2O in He at a flow rate of 100 mL/min.

3.10 Catalytic activity of zeolite confined ruthenium(0) nanoclusters:

Zeolite confined ruthenium(0) nanoclusters were prepared from the reduction of ruthenium(III) ions in the highest loading of Ru-Y1 sample (3.98 wt.%,) with sodium borohydride (150 mM) and tested in the catalytic decomposition of nitrous oxide in the temperature range 200-400 °C under the same conditions described before in section 2.5. (1000 ppm N_2O, Flow rate: 100 mL/min.)

3.11 Comparison of catalytic activity of ruthenium-zeolite Y catalyst with that of other Group-8 metal-zeolite Y.

The catalytic decomposition of nitrous oxide was performed starting with 100 mg of Fe-Y or Os-Y catalyst with a metal loading of 3 wt.% . The metal loading of Os-Y catalyst was given by theoretical calculation since its loading could not be determined by ICP-OES because of formation of toxic OsO_4 gases during experimental procedure. The catalyst samples were directly placed into vertical reactor without any pretreatment and the catalytic decomposition of nitrous oxide was followed in the temperature range of 200-600 °C at a flow rate of 100 mL/min by monitoring the reactant and product gases via gas chromatography. The reaction system was kept for 30 min at each temperature, and then the released gas was analyzed by gas chromatograph.

3.12 Testing the catalytic activity of rhodium(III) exchanged zeolite Y depending on metal loading by keeping the catalyst amount constant (100 mg)

In a series of experiments, the catalytic activity of rhodium(III) ion exchanged zeolite Y samples with various rhodium loadings (0.153, 0.30, 0.42, 0.48, 0.64, 2.12 wt.% Rh) was tested in decomposition of nitrous oxide (1000 ppm N_2O in He, 100 mL/min) by using the same experimental set-up as described in section 3.5. Various experimental procedures were applied for determination of nitrous oxide conversions correctly. First, the reactor was preheated up to 300 ºC and temperature was raised to 550 ºC by an increment of 25 ºC in each step. Thirty minutes waiting time was applied at every heating step in order to achieve steady state. However, activity of the catalyst in nitrous oxide conversion decreased during 30 minutes waiting time. Second procedure was continuous heating of samples from 250 ºC to 550 ºC with a heating rate of 3 ºC/ min (Procedure-1). Lastly, heating-cooling experiments were performed to obtain more reliable results for conversion of nitrous oxide. In this procedure, the temperature of reactor was increased in 25 °C increments between 300 ºC to 600 ºC by holding temperature constant for thirty minutes at each heating step (Procedure-2). After reaching 600 ºC, the reactor was cooled down by holding the temperature constant for 30 minutes at every 25 ºC (Procedure-3).

3.13 Testing the catalytic activities of rhodium(III) exchanged zeolite Y catalysts by keeping the rhodium amount constant (0.15 ± 0.01 mg)

A series of experiments were performed with four different samples (0.15, 0.30, 0.48 and 0.64 wt.% rhodium loadings) by keeping the rhodium content in zeolite constant. Each catalyst amount was adjusted to contain 0.15 ± 0.01 mg rhodium. The samples weights were arranged as follows: Rh-Y2: 24 mg, Rh-Y3: 31 mg, Rh-Y5: 50mg, Rh-Y6: 100 mg. However, no experiment could be performed using the highest loading Rh-Y1 catalyst (2.12 wt.%) since the amount of the catalyst material required was not enough for proper testing. Tests were performed between 250 -550 °C and temperature was increased continuously at a rate of 3 °C/min (Procedure-1). Data were collected at every 25 °C. Then, a second procedure was applied to three catalysts; Rh-Y2: 25 mg, Rh-Y5: 50 mg and Rh-Y6: 100 mg. The temperature of reactors was increased in 25 °C increments between 300 ºC to 600 ºC by holding temperature constant for thirty minutes at each heating step (Procedure-2). After reaching 600 ºC, the reactor was cooled to starting temperature by holding temperature constant for 30 minutes at every 25 ºC (Procedure-3). In all procedures, the flow rate of N_2O (1000 ppm in He) was 100 mL/min.

3.14 Testing the catalytic activities of rhodium(III) exchanged zeolite Y catalysts by keeping the rhodium amount constant (0.15 ± 0.01 mg) at 50 mL/min flow of N_2O

Heating-cooling procedure was applied to three catalysts (Rh-Y2: 24 mg , Rh-Y5: 50 mg and Rh-Y6: 100 mg) under 50 mL/min flow of N_2O (1000 ppm in He). The temperature of reactors was increased in 25 °C increments between 300 ºC to 600 ºC by holding temperature constant for thirty minutes at each heating step. After reaching 600 ºC, the reactor was cooled to starting temperature by holding temperature constant for 30 minutes at every 25 ºC.

3.15 Testing the catalytic activities of iridium (III) exchanged zeolite Y catalysts

Iridium(III) exchanged zeolite Y catalysts were prepared as six different loadings of iridium in the range of 253-675 mg/kg (253, 268, 322,324, 580, 675 mg/kg iridium loadings). Two different procedures were applied for catalytic activity tests of iridium(III) exchanged zeolite Y samples. In the first procedure, catalysts were started to be tested between 350-600 ºC by waiting 30 minutes at each temperature step of 25 ºC without any pretreatment. Due to deactivation a second procedure was applied and the samples were preheated to 500 ºC at the beginning of experiments. After cooling the reactor to 300 ºC, activities were examined by continuous heating between 300-600 ºC at a heating rate of 3 ºC/min. In all procedures, the flow rate of N_2O (1000 ppm in He) was 100 mL/min.

3.16 Determination of catalytic activity of cobalt(II) exchanged zeolite Y catalyst

Cobalt(II) exchanged zeolite (5.17 wt.%) was weighed as 100 mg and placed directly to vertical quartz reactor without any pretreatments. The catalytic activity was examined between 250-600 ºC by taking continuous and consequtive measurements. The heating rate of oven was 3 ºC/min. The presence of any deactivation was controlled by waiting at each temperature step for 30 minutes between 425-550 ºC. Since no deactivation was detected the continuous heating was carried on between 200-600 ºC.

3.17 Determination of side products by NOx analyzer

During gas chromatography analysis, if the ratio of concentrations of nitrogen to oxygen is different from 2:1 or there is a decrease in catalytic activity of any sample, side product determinations were performed with NOx analyzer. The temperature range of measurement was decided by the data taken from GC. Firstly, the pipeline was cleaned by a flow of He at 100 mL/min for an hour and the temperature was arranged as the desired value where the reaction will be performed. NO, NOx and NO_2 concentrations were followed by online NOx analyzer.

CHAPTER 4

RESULTS AND DISCUSSIONS

4.1 Preparation and characterization of ruthenium(III) ion-exchanged zeolite-Y

Ruthenium(III) ion exchanged zeolite Y (Ru-Y) was prepared in five different metal loadings by ion exchange of ruthenium(III) ions with sodium cations of zeolite Y following the procedure described elsewhere [121]. To a suspension of sodium zeolite Y (~500 mg) in 100 mL distilled water was added a solution of $RuCl_3 \cdot 3H_2O$ containing certain amount of ruthenium depending on the metal loading of zeolite desired. After stirring for three days, the zeolite powder was collected on a Whatman 1 filter paper, washed three times with distilled water (3×20 mL) and dried under vacuum all at room temperature. The ruthenium content of zeolite was determined by ICP-OES. The results are listed in Table 5.

Table 5. Ruthenium content of the ruthenium(III) ion-exchanged zeolite Y samples determined by ICP-OES.

Catalyst	wt. % Ru content
Ru-Y1	3.98 ± 0.01
Ru-Y2	2.03 ± 0.01
Ru-Y3	1.00 ± 0.01
Ru-Y4	0.65 ± 0.04
Ru-Y5	0.36 ± 0.01

The comparison of powder XRD patterns of zeolite Y and Ru-Y1 sample with the loading of 3.98 wt.% ruthenium displayed in Figure 26 shows that the zeolite framework lattice remains essentially intact after the ion exchange of its sodium cations with ruthenium(III) ions. Even after Ru-Y1 sample has been reused more than 10 times in catalytic decomposition of nitrous oxide its XRD pattern is the same as the authentic one. Conclusively, XRD patterns clearly show that there is no change in crystal lattices of zeolite Y host due to the incorporation of ruthenium(III) cation into zeolite Y and catalytic reactions. The patterns of RuO_2 and Ru particles lie between the range of 25°-80° [122]. The expected peak positions of ruthenium reflections below 35° are marked in comparative XRD patterns of Ru-Y1. As the concentration of ruthenium is less than 5%, the XRD pattern doesn't show any ruthenium phase. Therefore, the oxidation state of ruthenium and surface composition of catalysts were analyzed by X-ray photoelectron spectroscopy (XPS).

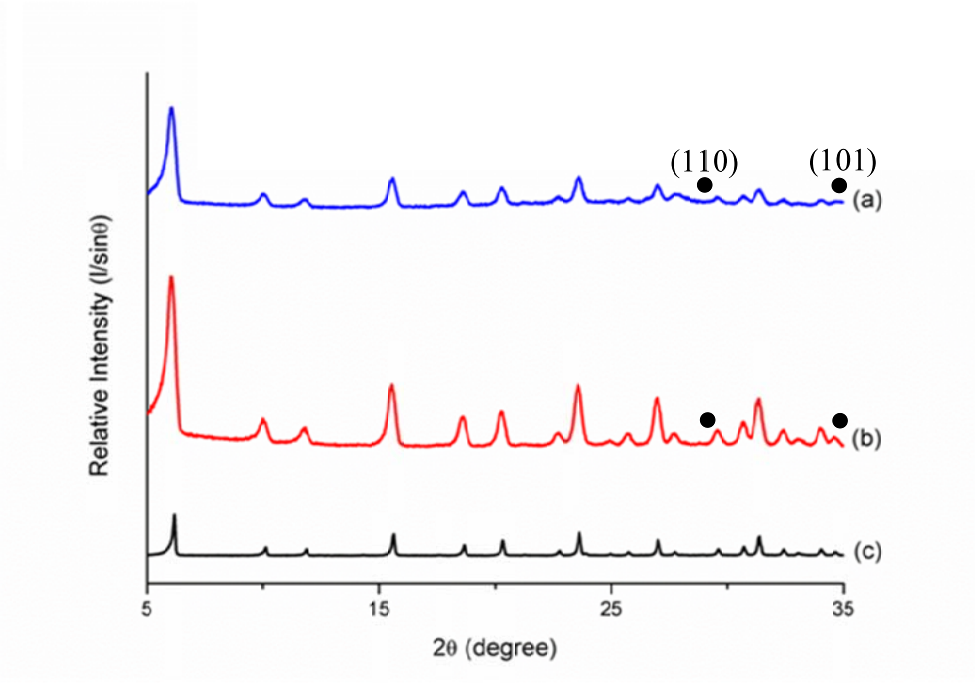

Figure 26. Powder XRD patterns of (a) Reused Ru-Y1 with ruthenium content 3.8 wt.%, (b) Fresh Ru-Y1 with ruthenium content 3.8 wt.%, and (c) host material zeolite Y. ●RuO_2

The survey scan and high resolution 3d and 3p XPS spectra of the Ru-Y1 sample (3.98 wt.% Ru) as prepared and after ten runs of catalytic decomposition of nitrous oxide are displayed in Figures 27, 28, and 29, respectively. The survey scan XPS spectra of fresh and reused Ru-Y1 samples, given in Figure 27, show the presence of ruthenium as the only element in addition to the zeolite framework elements (O, Si, Al, Na) and carbon coming from air during XPS sampling.

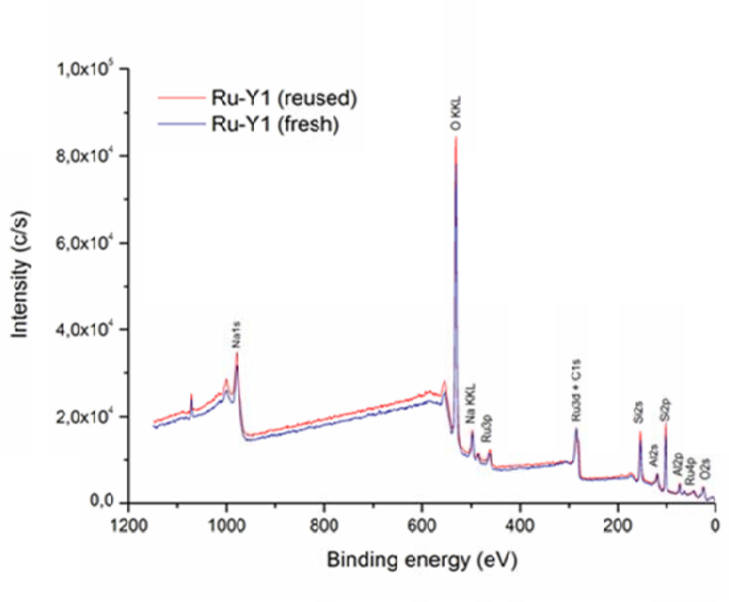

Figure 27. (a) XPS survey scan of fresh Ru-Y1 with ruthenium content 3.8 wt.%, (b) XPS survey scan of reused Ru-Y1 with ruthenium content 3.8 wt.% after 10 catalytic cycles.

The high resolution 3d and 3p spectra of fresh Ru-Y1 sample given in Figure 28 (a) and (b) respectively exhibit three peaks at 284.4 eV ,at 280.8 eV and at 462.6 eV which can be readily assigned to ruthenium oxides $3d_{3/2}$, $3d_{5/2}$ and $3p_{3/2}$ respectively [123,124]. Ruthenium(III) ion, ion-exchanged into zeolite Y, has an environment similar to that of Ru-oxide; Ruthenium(III) ion is in strong electrostatic interaction with at least two or three framework oxygen atoms of zeolite Y. Therefore, Ru-oxide is considered as reference for the comparison of XPS results of the Ru(III)-zeolite Y sample [116,117]. Zeolite confined ruthenium(0) nanoclusters exhibits two peaks at 283 eV and 464 eV for $3d_{5/2}$ and $3p_{3/2}$, respectively [75].

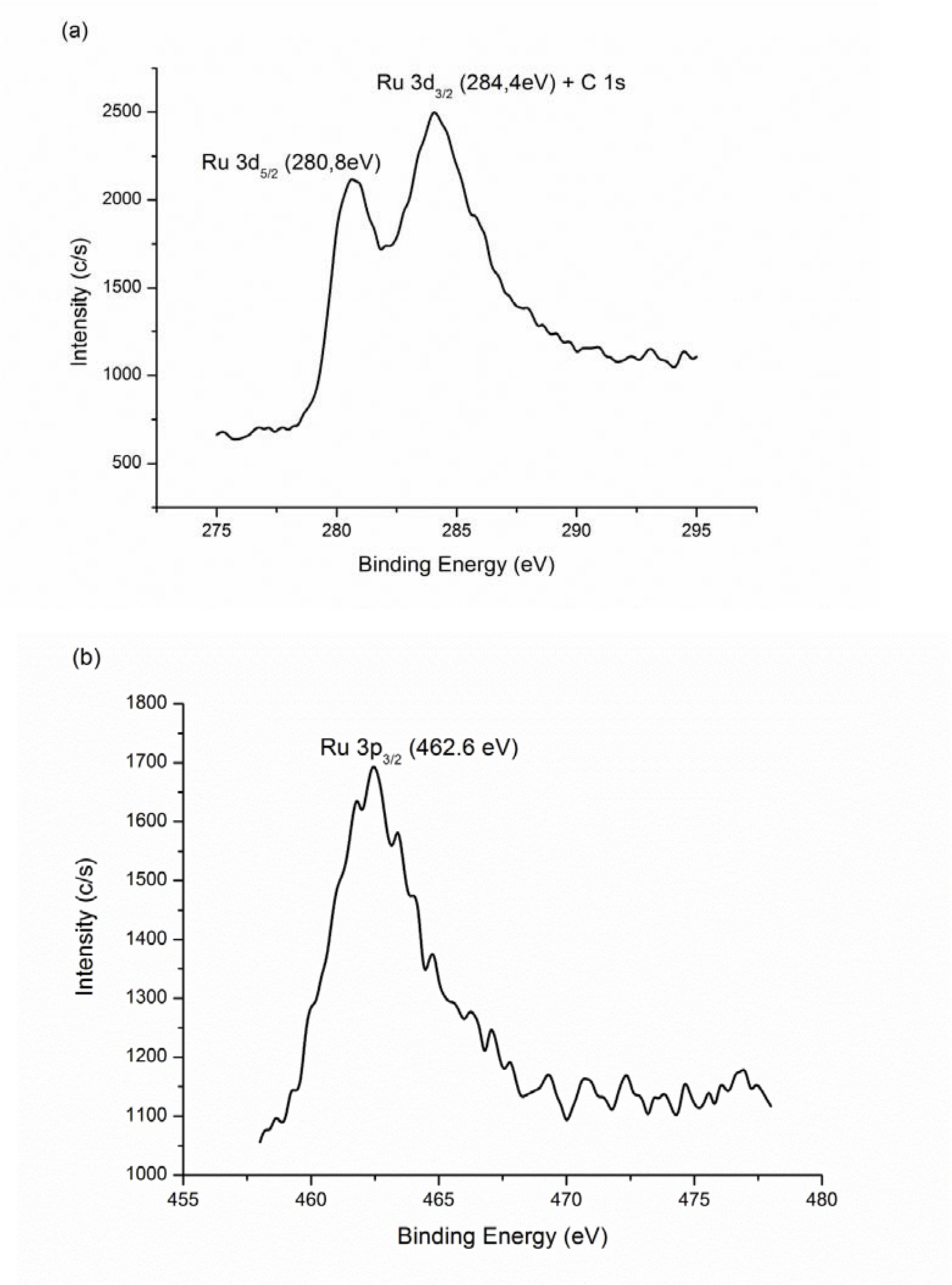

Figure 28. (a) High resolution 3d XPS and (b) High resolution 3p XPS spectrum of fresh Ru-Y1 with ruthenium content 3.8 wt.%

Compared to the fresh sample, a slight negative shift is noticed in the 3d and 3p XPS spectra of the reused catalyst, giving binding energies of 283.4 eV, 279.4 eV, and 461.2 eV for $3d_{3/2}$, $3d_{5/2}$, and $3p_{3/2}$ respectively (Figure 29).

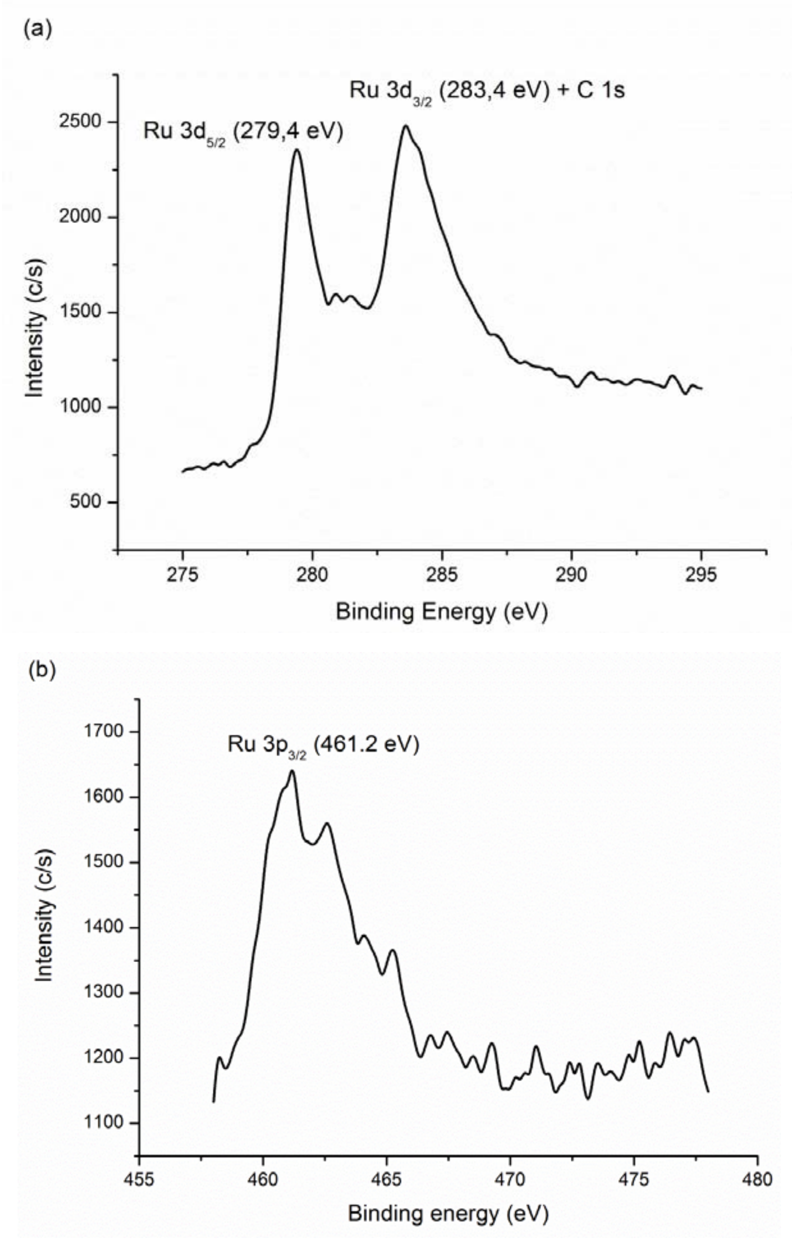

Figure 29. (a) High resolution 3d XPS and (b) High resolution 3p XPS spectrum of reused (after 10 catalytic cycles) Ru-Y1 with ruthenium content 3.8 wt.%

FT-IR spectra were taken for zeolite Y, fresh and reused Ru-Y1(after ten catalytic cycles) samples with ruthenium content 3.8 wt.%. All the samples essentially give the same spectrum indicating that the framework of zeolite did not change during the catalytic reactions. These three samples gave the same typical zeolite spectra given in Figure 30. Also, the detailed FTIR spectrum of fresh Ru-Y1 taken in the range of 4000-450 cm^{-1} with 200 scans was given in Figure 31.The bands due to the presence of zeolite water lie in the range of 1600–3700 cm^{-1}. The FTIR bands connected with the internal Si–O (Si) and Si–O(Al) vibrations in tetrahedral or alumino- and silicooxygen bridges lie in the range of 1200–400 cm^{-1} [125].

Figure 30. (FTIR spectra of zeolite Y, fresh Ru-Y1 and reused Ru-Y1, 4000-650 cm^{-1}, 4 scans)

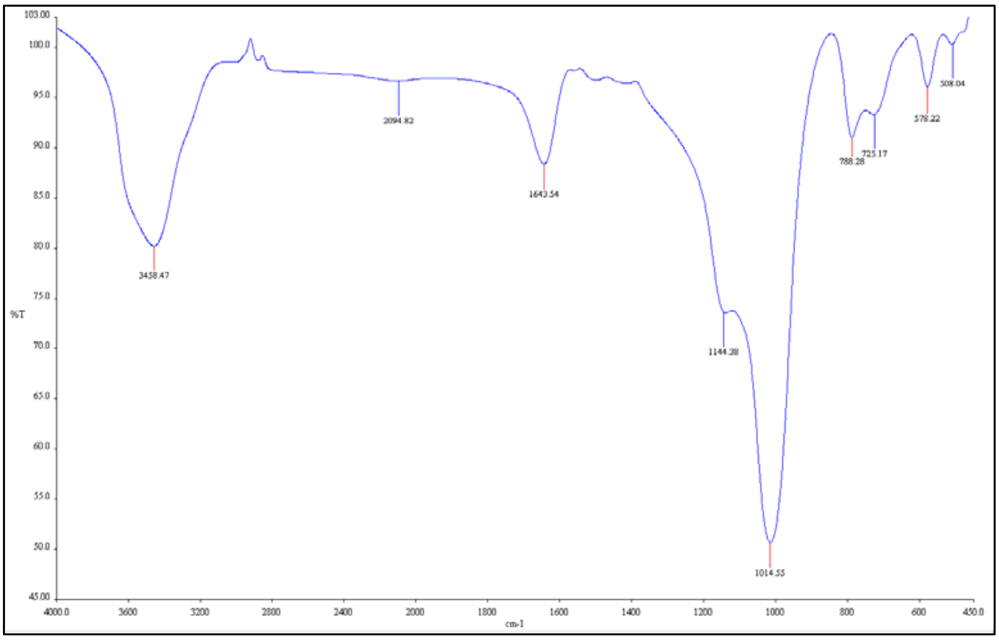

Figure 31. FTIR spectrum of fresh Ru-Y1 taken in the range of 4000-450 cm^{-1} with 200 scans

4.2 Catalytic activity of Ru-Y

The catalytic decomposition of nitrous oxide was carried out in a continuous flow vertical reactor at a flow rate of 100 mL/min of 1000 ppm N_2O in He with a space velocity of GHSV = 19,000 h^{-1} unless otherwise specified. Vertical reactor, placed in a vertical oven and fed by the gas mixture, was set to 200 °C at the beginning of the test and, then, the temperature was increased in 25 °C steps by holding thirty minutes at each temperature until the observation of complete decomposition. Figure 32 shows the plot of concentration of gases versus temperature for catalytic decomposition of nitrous oxide in the presence of Ru-Y1 catalyst with 3.8 wt.% Ru.

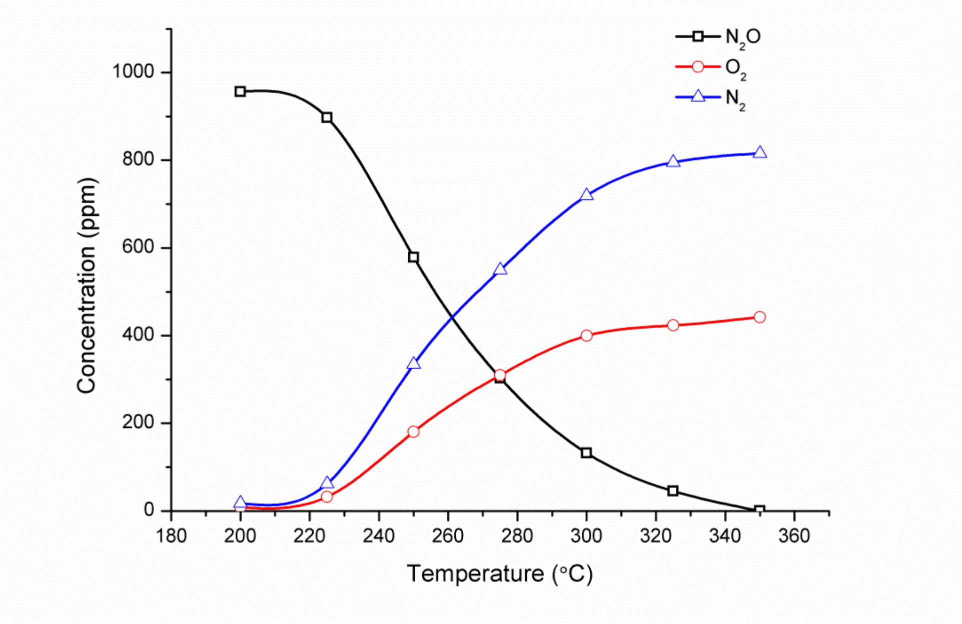

Figure 32. Concentration versus temperature plots monitored during the decomposition of nitrous oxide to nitrogen and oxygen at temperatures in the range 200-350 ºC with 100 mL/min flow of 1000 ppm N_2O in the presence of Ru-Y1 (3.8 wt.%) catalyst.

Nitrous oxide concentration starts to decrease as temperature increases whereas nitrogen and oxygen concentrations increase in a molar ratio of 2:1 as determined by GC. The formation of decomposition products N_2 and O_2 becomes noticeable at temperatures above 225 °C and reaches the maximum level at 350 °C. From these data, conversion was calculated at each temperature by using Eq. (7) in section 3.5. Figure 33 shows the conversion versus temperature graph for the decomposition of nitrous oxide in the presence of Ru-Y1 catalyst.

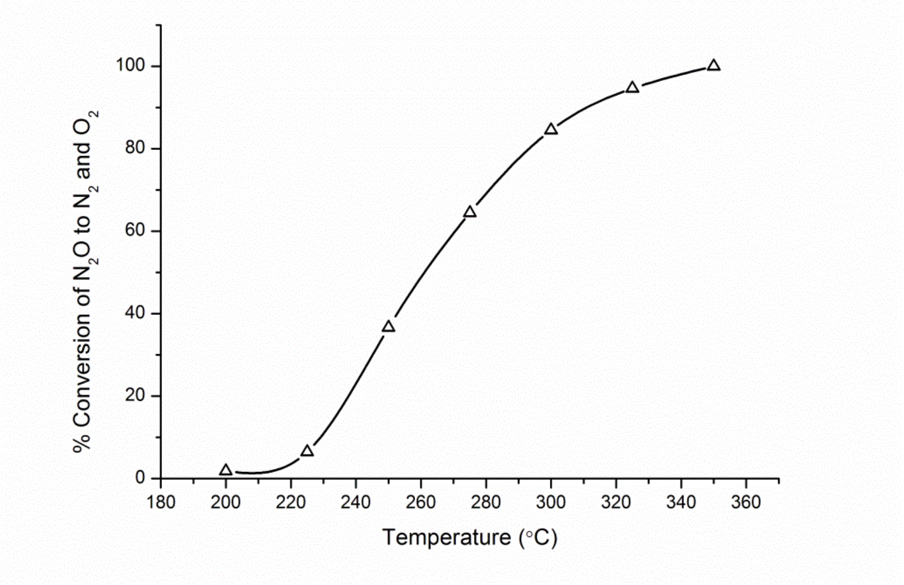

Figure 33. The plot of conversion of nitrous oxide to nitrogen and oxygen versus temperature in the range 200-350 ºC with 100 mL/min flow of 1000 ppm N_2O in the presence of Ru-Y1 (3.8 wt.%) catalyst.

The decomposition starts at 225 °C with a conversion lower than 10% and increases rapidly as the temperature increases and is completed at 350 °C when 100% conversion is achieved. During the catalytic test, the molar ratio of nitrogen to oxygen remains constant at 2:1 indicating that nitrous oxide decomposes only to nitrogen and oxygen, in other words, no side product is observable.

In order to study the effect of metal loading of zeolite on the catalytic activity, experiments were performed starting with 100 mg of Ru-Y sample with different ruthenium content under the same conditions as before. Figure 34 shows the plots of conversion versus temperature for the catalytic decomposition of nitrous oxide depending on the ruthenium loading of zeolite Y. The Ru-Y1 catalyst with the maximum loading of 3.98 wt.% exhibits expectedly the highest conversion at all temperatures. As the ruthenium content of catalyst decreases the conversion of nitrous oxide to oxygen and nitrogen decreases at all temperatures. In other words, the temperature of complete conversion shifts slightly to higher values from 350 ºC for Ru-Y1 (3.98 wt.%) catalyst to 425 ºC for Ru-Y5 (0.36 wt.%) catalyst. It is noteworthy that conversion values obtained by using Ru-Y1 are almost the double of those obtained by using the second highest loading catalyst Ru-Y2 (2.03 wt.%). Such a result is not unexpected as the amount of ruthenium in the 100 mg catalyst increases with the increasing loading. Therefore, another set of experiments were performed by keeping the amount of ruthenium constant, but still using Ru-Y catalysts with different ruthenium content.

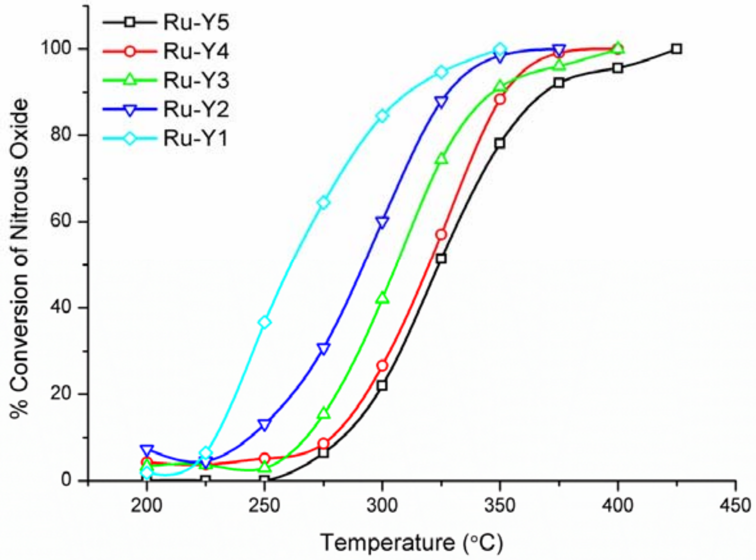

Figure 34. Conversion versus temperature plots for the decomposition of nitrous oxide to nitrogen and oxygen performed starting with 100 mg catalyst of Ru-Y1 (3.8 wt.%) , Ru-Y2 (2.03 wt.%) , Ru-Y3 (1.00 wt.%), Ru-Y4 (0.65 wt.%), and Ru-Y5 (0.36 wt.%) at a flow rate of 100 mL/min flow of 1000 ppm N_2O in the range of 200-425 ºC.

In order to keep the amount of ruthenium in the catalyst constant at 1.6 ± 0.1 mg in the reactor, the enough amount of Ru-Y catalyst with varying ruthenium loading was placed into the reactor. However, no experiment could be performed using the lowest loading Ru-Y5 catalyst (0.36 wt.%) since the amount of the catalyst material required exceeded the capacity of the small scale reactor to operate under the same flow rate. The results of the experiments performed by using the other four Ru-Y catalysts but keeping the amount of ruthenium constant otherwise under the same experimental conditions as before were illustrated by the conversion versus time plots for the decomposition of nitrous oxide to nitrogen and oxygen in Figure 35. The inspection of the plots given in Figure 35 indicates that the highest conversion at any temperature is obtained by using the Ru-Y2 catalyst (2.03 wt.%), not by using the highest loading Ru-Y1 catalyst (3.98 wt.%). This case can be explained by the short contact time of nitrous oxide with ruthenium(III) as the amount of catalyst in the reactor is small for the zeolite sample Ru-Y1 with highest ruthenium loading.

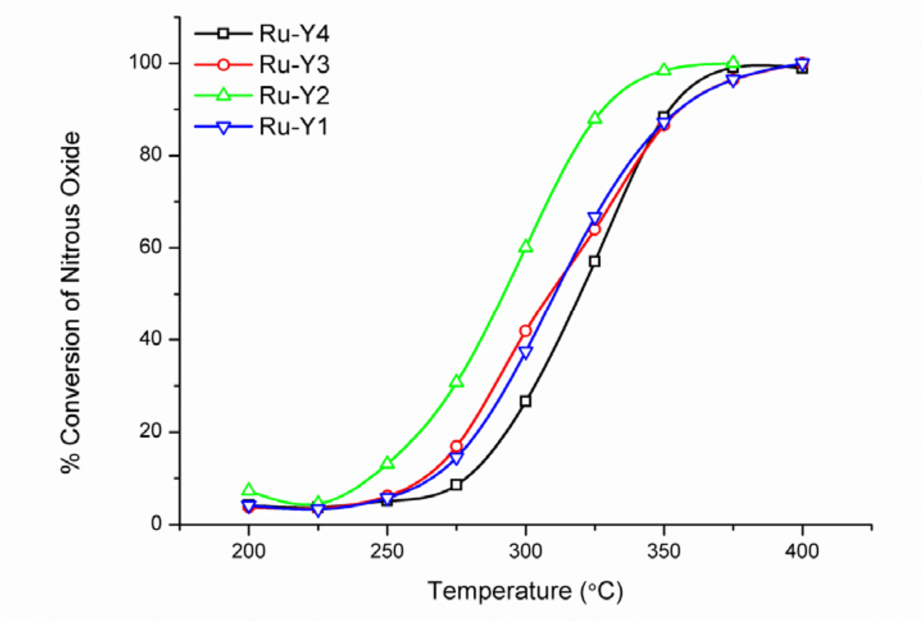

Figure 35. Conversion versus temperature plots for the decomposition of nitrous oxide to nitrogen and oxygen performed starting with 1.6 ± 0.1 mg Ru using various amount of Ru-Y1 (3.8 wt.%) Ru-Y2 (2.03 wt.%), Ru-Y3 (1.00 wt.%) and RuY4 (0.65 wt.%) catalyst at 100 mL/min flow of 1000 ppm N_2O at temperature in the range 200-400 ºC.

4.3 Effect of flow rate on the catalytic activity of Ru-Y

Catalytic decomposition of nitrous oxide to nitrogen and oxygen was performed at various flow rates in the range 50-500 mL/min at constant temperature of 350 ºC starting with 100 mg of Ru-Y1 catalyst (3.98 wt.%). The change in concentration of the reactant nitrous oxide as well as the products nitrogen and oxygen was monitored by gas chromatography. Figure 36 shows the plot of concentration of the reactant and product gases versus the flow rate. It is noteworthy that as flow rate increases the concentrations of nitrogen and oxygen are unaltered and the molar ratio of nitrogen to oxygen also remains constant at 2.0, whereas nitrous oxide concentration in the exhaust gases increases slightly. That the concentrations of nitrogen and oxygen remain unaltered indicates that the decomposition rate of nitrous oxide doesn't depend on the flow rate in the range 50-500 mL/min. Therefore, the concentration of unreacted nitrous oxide in the exhaust gases increases as the flow rate increases. Consequently, the conversion of nitrous oxide to nitrogen and oxygen is not complete at high flow rates, as some nitrous oxide molecules can pass through the reactor without getting contact to the catalyst surface. Since the concentration of nitrous oxide in the exhaust gases significantly increases with the increasing flow rate above 150 mL/min, this flow rate of 150 mL/min can be considered as the upper limit for achieving at least 95% conversion of nitrous oxide to nitrogen and oxygen at 350 ºC in this reactor system with 100 mg of Ru-Y1 catalyst. In order to increase the flow rate of nitrous oxide – helium mixture, without affecting the conversion of nitrous oxide, an enlargement of the reactor system would be required.

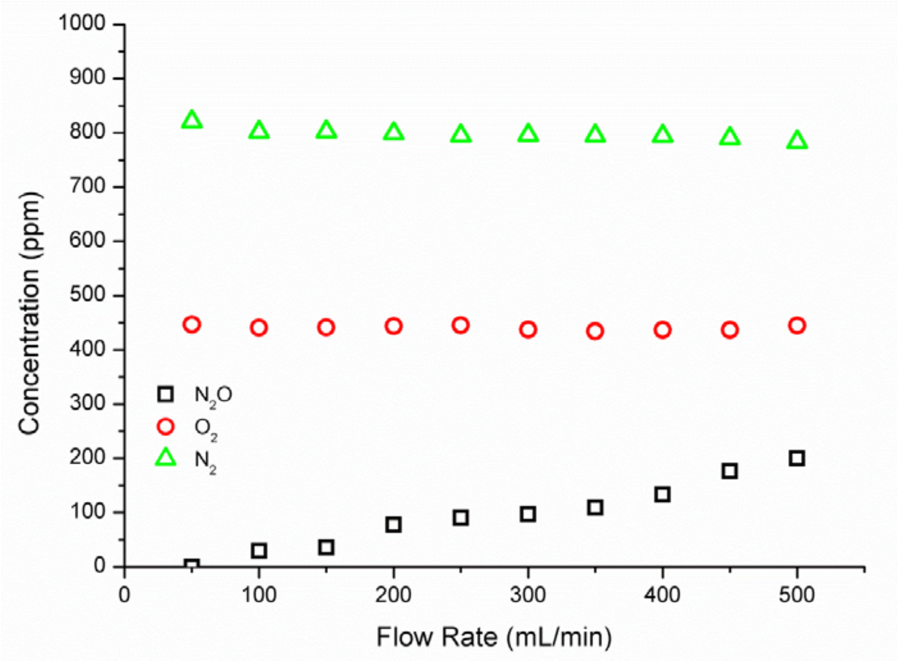

Figure 36. Plot of concentration versus flow rate of 1000 ppm N_2O for the catalyst Ru-Y1 (3.8 wt.%) at 350 ºC

4.4 Reusability of the Ru-Y Catalyst

Ru-Y catalysts were prepared in the form of powder and stored under ambient conditions until the use in catalytic decomposition of nitrous oxide. The reusability of catalyst was tested in a subsequent run of nitrous oxide decomposition performed by using the catalyst recovered after the previous run. Catalytic activity of Ru-Y1 (3.98 wt.%) was recorded as the conversion of nitrous oxide to nitrogen and oxygen at 350 ºC. Figure 37 shows the variation in conversion with the number of catalytic runs. Until the ninth run after 30 days the change in catalytic activity is negligible as the catalyst provides 97 % conversion at 350 ºC in the ninth run. In the tenth run after 5 months, the catalyst can still provide 87 % conversion of nitrous oxide to nitrogen and oxygen at 350 ºC. All the catalytic runs were performed with the same sample of Ru-Y1 without application of preheating to high temperature above 500 ºC or any additional pretreatments. Conclusively, ruthenium(III) ion exchanged zeolites are highly active, long-lived, and reusable catalyst in the decomposition of nitrous oxide. Thus, they can be used directly for replicate runs of nitrous oxide decomposition without any pretreatment for a relatively long time up to five months.

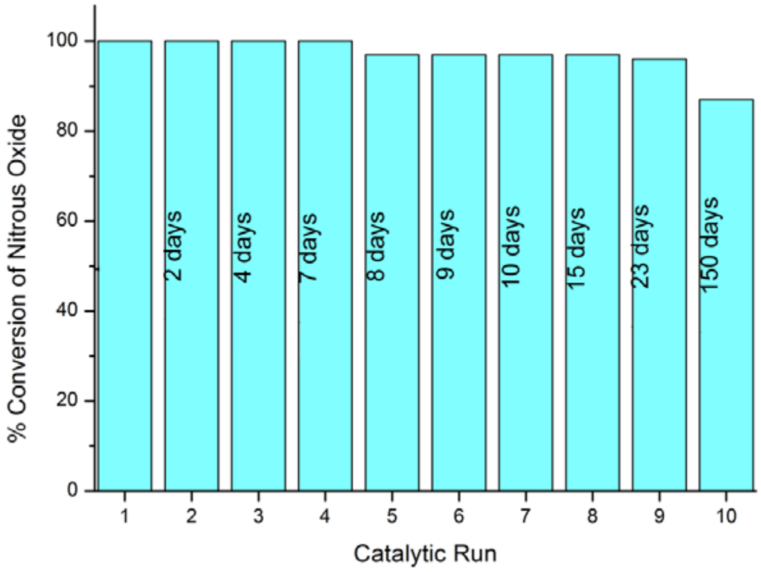

Figure 37. The percentage conversion of nitrous oxide to nitrogen and oxygen in successive catalytic runs each performed at 350 ºC starting with 100 mg Ru-Y1 (3.8 wt.%) catalyst and a flow rate of 100 mL/min of 1000 ppm N_2O.

4.5 Catalytic activity of zeolite confined ruthenium(0) nanoclusters

A control experiment was needed to check whether starting with ruthenium(0), instead of ruthenium(III), still in the zeolite cages would give a different activity in the catalytic decomposition of nitrous oxide to nitrogen and oxygen. For this purpose, zeolite confined ruthenium(0) nanoclusters were prepared from the reduction of ruthenium(III) ions in the highest loading of Ru-Y1 sample (3.98 wt.%) with sodium borohydride and tested in the catalytic decomposition of nitrous oxide in the temperature range 200-400°C under the same conditions as before. Figure 38 shows the plot of conversion versus temperature for the decomposition of nitrous oxide started with 100 mg of zeolite confined ruthenium(0) nanoclusters. The catalytic activity of zeolite confined ruthenium(0) nanoclusters is not as high as that of ruthenium(III) ion exchanged zeolite Y of the same loading. In the test starting with zeolite confined ruthenium(0) nanoclusters, the decomposition of nitrous oxide starts at 250 °C and the complete conversion is achieved at 375 °C while using the Ru-Y1 catalyst provides the complete conversion at 350 °C. During decomposition of nitrous oxide, ruthenium(0) is likely being oxidized forming the same active catalyst as the one in the case of ruthenium(III) ion exchanged zeolite Y. However, some of the ruthenium(0) nanoclusters in the cages of zeolite may migrate toward the external surface prior to oxidation at high temperatures.

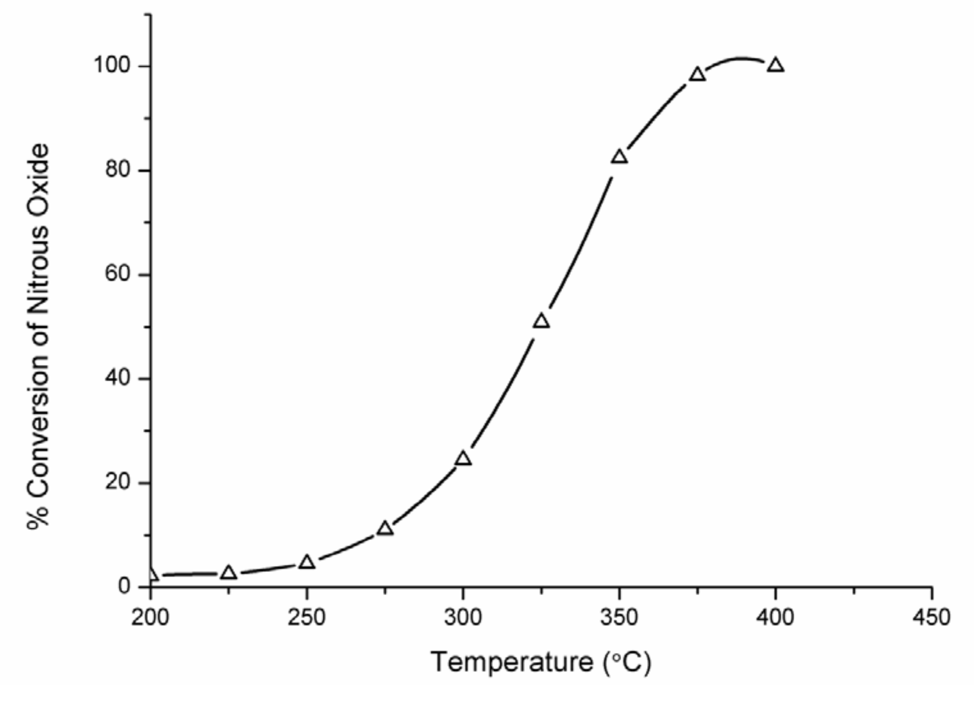

Figure 38. The conversion versus temperature plot for the decomposition of nitrous oxide to nitrogen and oxygen performed starting with 100 mg zeolite confined ruthenium(0) catalyst (3.8 wt.% Ru) and a flow rate of 100 mL/min of 1000 ppm N_2O.

4.6 Comparison of catalytic activity of ruthenium-zeolite Y catalyst with that of other Group-8 metal-zeolite Y.

After having observed such a high catalytic activity of ruthenium(III) ion exchanged into zeolite Y, the most important issue is to find out whether the other two metal(III) ions of the same Group 8 would show similar activity. For this purpose, iron(III) and osmium(III) ion exchanged zeolite Y samples, Fe-Y and Os-Y, respectively, were prepared by using iron(III) chloride or osmium(III) chloride and following the same ion exchange procedure as the one used for ruthenium(III) [121]. The catalytic decomposition of nitrous oxide was performed starting with 100 mg of Fe-Y or Os-Y catalyst with a metal loading of 3 wt.% otherwise under the same conditions as described previously. Note that the catalyst sample was directly placed into vertical reactor without any pretreatment and the catalytic decomposition of nitrous oxide was followed in the temperature range 200-600 °C at a flow rate of 100 mL/min by monitoring the reactant and product gases by gas chromatography. Side products were followed by NOx analyzer. Figure 39 shows the plots of conversion versus temperature for the catalytic decomposition of nitrous oxide starting with Fe-Y, Ru-Y and Os-Y all together for comparison. Obviously, the iron(III) and osmium(III) ion-exchanged zeolite Y do not show catalytic activity as high as the one obtained by using ruthenium(III) ion-exchanged zeolite catalyst.

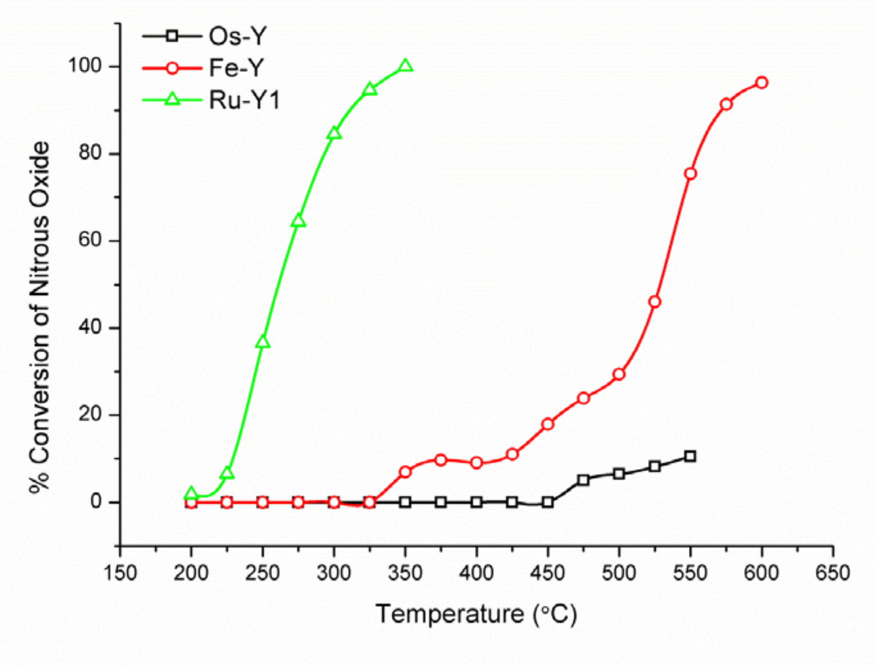

Figure 39. Conversion versus temperature plots for the decomposition of nitrous oxide to nitrogen and oxygen performed starting with 100 mg of Ru-Y1 (3.98 wt.% Ru), Fe-Y (3.02 wt.% Fe) and Os-Y (3 wt.% Os) catalyst and a flow rate of 100 mL/min of 1000 ppm N_2O at temperature in the range of 200-600 °C

Moreover, the catalytic decomposition of nitrous oxide started with Fe-Y catalyst yields nitrogen and oxygen in a molar ratio higher than 2:1 and the conversion doesn't show a smooth change with temperature below 500 °C while it produces the N_2 and O_2 gases in the molar ratio of 2:1 at temperatures above 500 °C and the complete conversion is achieved at 600 °C. On the other hand, Os-Y catalyst doesn't show any catalytic activity in the decomposition of nitrous oxide at temperatures up to 450 °C. Although a conversion less than 10 % is observed at higher temperature, the nitrogen to oxygen molar ratio is about 5:1. During the decomposition at 550 °C, side products were determined by NOx analyzer for 30 minutes and only evolution of NO less than 1 ppm was detected (Figure 40) It is likely that osmium(III) is oxidized forming the volatile OsO_4 which might be either inactive in the decomposition of nitrous oxide or escape from the zeolite cages into gaseous state when heated to high temperatures.

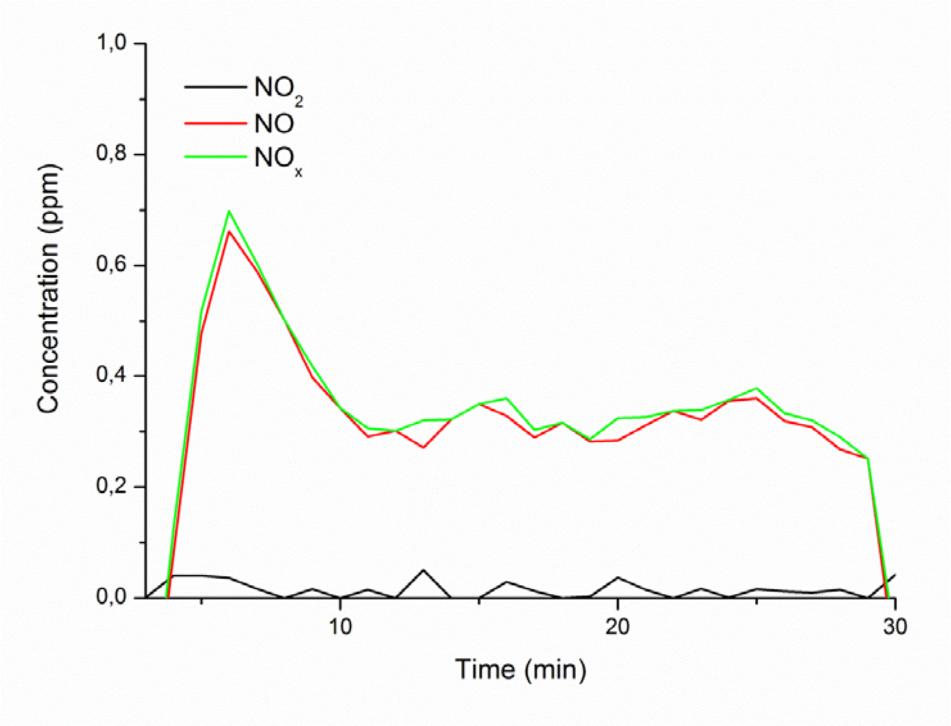

Figure 40. NOx evolution versus time graph monitored by NOx analyzer during the decomposition of nitrous oxide at 550 °C performed starting with 100 mg of Os-Y (3 wt.% Os) and a flow rate of 100 mL/min of 1000 ppm N_2O.

4.7 Preparation and characterization of rhodium(III) exchanged zeolite-Y

Rhodium exchanged zeolite Y (Rh-Y) was prepared by using the ion exchange reaction of Rh^{+3} with the extra framework cations of zeolite Y in six different metal loadings by following exactly the same procedure as described previously for ruthenium exchanged zeolite Y [121]. $RhCl_3$. H_2O was added to a suspension of zeolite Y in water and stirred for three days at room temperature. Sample was filtered and collected in the powder form. Rh-Y samples were prepared as six different rhodium loadings by addition of appropriate amount of rhodium salt at the beginning of the preparation process. Metal contents in zeolite were determined by ICP-OES and given in Table 6.

Table 6. The Rhodium contents in Rh-Y catalysts.

Catalyst	% Rh content
Rh-Y1	2.12 ± 0.02
Rh-Y2	0.64 ± 0.01
Rh-Y3	0.48 ± 0.01
Rh-Y4	0.42 ± 0.04
Rh-Y5	0.30 ± 0.01
Rh-Y6	0.153 ± 0.001

The XRD patterns of fresh and reused rhodium(III) exchanged zeolite Y catalysts having a rhodium content of 0.64 wt.% were compared with the zeolite Y XRD patterns. The comparison of XRD patterns given in Figure 41 shows that the crystal lattice of zeolite Y is not affected by the ion exchange reaction of Rh(III) with the extra framework sodium cations. The lattice also remains unchanged after three catalytic runs. It can be concluded from XRD patterns that there is no sign of any distortion in crystal lattice of zeolite due to exchange and catalytic reactions. (The characteristic peaks of rhodium exists at 40º, 48º, 70º for (111), (200) and (220) reflections respectively [126].)

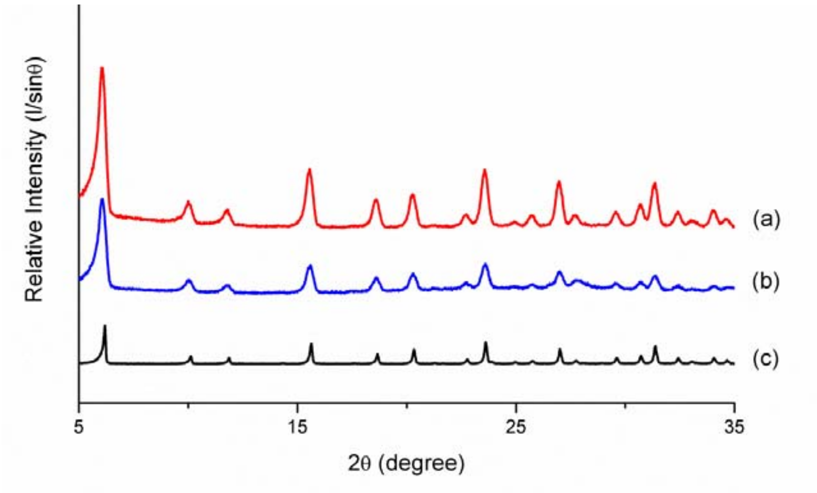

Figure 41. Powder XRD patterns of (a) Reused Rh-Y2 with rhodium content 0.64 wt.%, (b) Fresh Rh-Y1 with ruthenium content 0.64 wt.%, and (c) host material zeolite Y.

The oxidation state of rhodium and the surface composition of zeolitic catalyst materials were investigated by X-ray photoelectron spectroscopy (XPS). The survey scan XPS spectra of fresh and reused samples of Rh-Y2 catalyst with a rhodium content of 0.64 wt.% given in Figure 42 indicate the presence of rhodium in addition to zeolite framework elements (O, Si, Al, Na) plus the C from air during the XPS sampling.

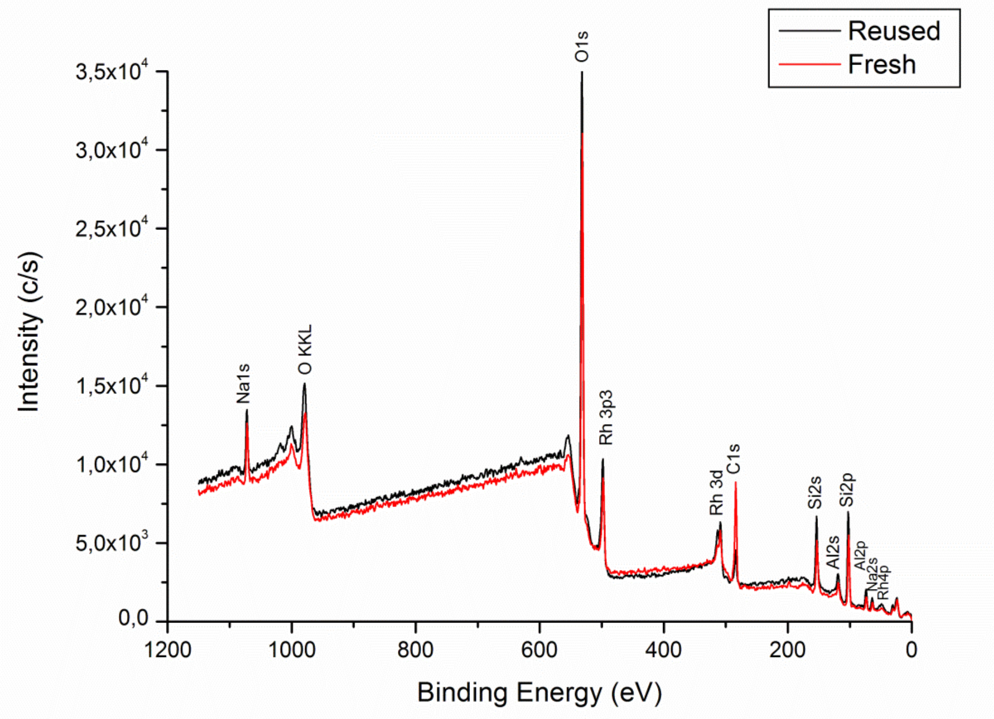

Figure 42. XPS Survey scan of fresh and reused samples of Rh-Y2 with a rhodium content of 0.64 wt.%.

The high resolution 3d and 3p spectra of fresh and reused catalysts were given in Figure 43 and Figure 44, respectively. Both fresh and reused samples exhibit two prominent peaks for $3d_{3/2}$ and $3d_{5/2}$ at 313.3 eV and 309 eV, respectively and a peak at 497,8 eV for 3 $p_{3/2}$. The peak at 309 eV for $3d_{5/2}$ clearly indicates the presence of Rh^{+3} ions surrounded by framework oxygen atoms in the zeolite [127].

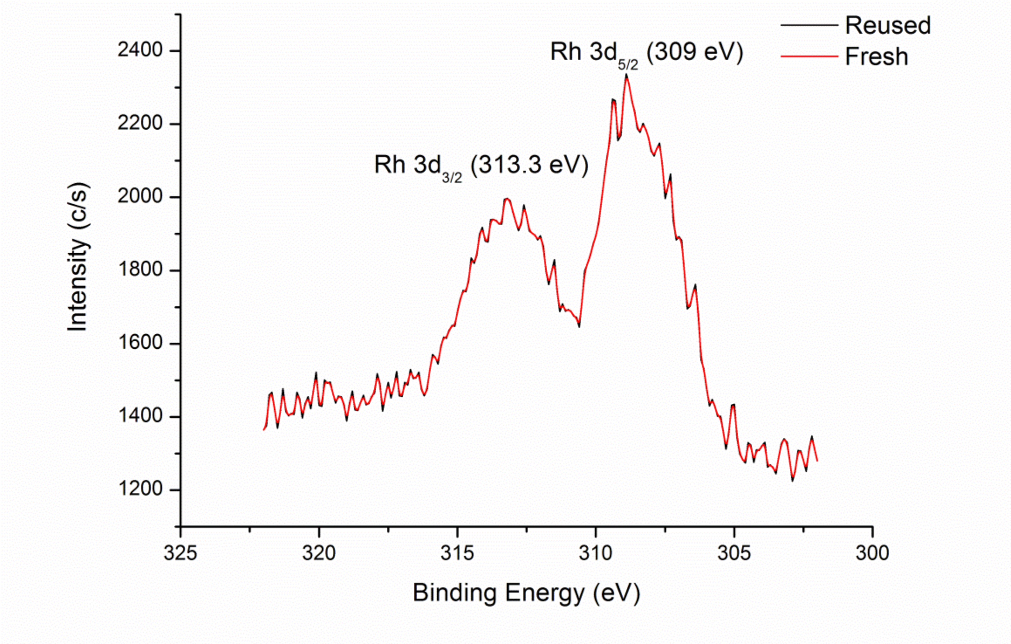

Figure 43. The high resolution 3d spectra of fresh and reused Rh-Y2 sample with a rhodium content of 0.64 wt.%

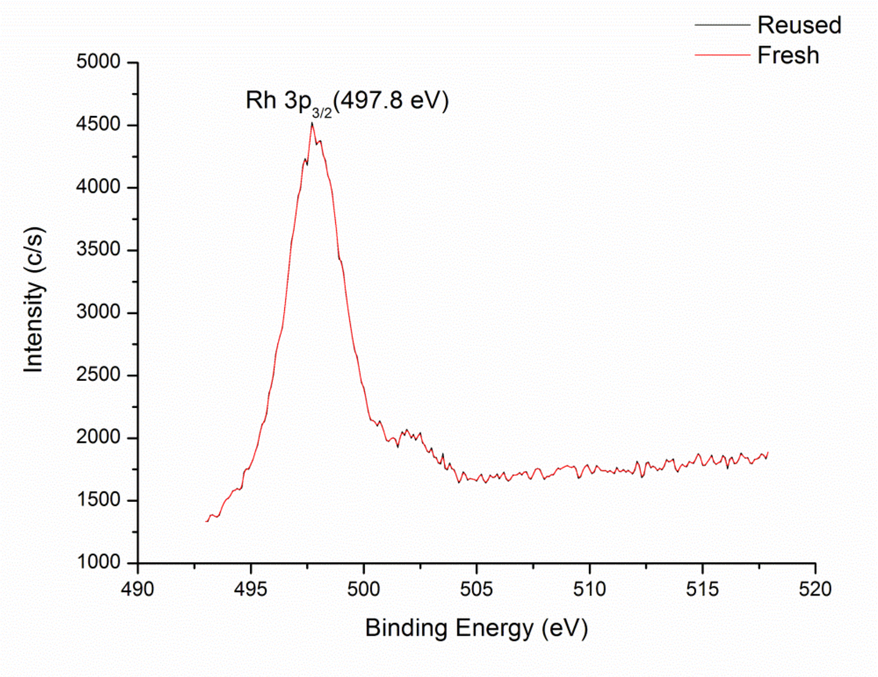

Figure 44. The high resolution 3p spectra of fresh and reused Rh-Y2 sample with a rhodium content of 0.64 wt.%

4.8 Catalytic activity of Rh-Y

Catalytic activity tests of rhodium(III) exchanged zeolite Y samples were carried out in a vertical reactor at a flow rate of 100 mL/min nitrous oxide (1000 ppm in He) as described in Section 4.2. Since no activity was observed at temperatures below 300 °C, the reactions were started at 300 °C and the temperature was increased in 25 °C steps and samples were held thirty minutes at each temperature step. The tests were continued until the observation of complete conversion. At first, the same reaction conditions were used as the ones used in the previous studies for the ruthenium catalysts to obtain comparable results. However, the conversion of nitrous oxide is observed to decrease during waiting periods between 425-450 ºC. Figure 45 shows that the catalytic activity decreases noticeably at 450 ºC for 100 mg Rh-Y2 catalyst under a flow rate of 100 mL/min of 1000 ppm N_2O. This decrease in conversion stops above 450 ºC and complete conversion is obtained at 550 ºC.

Two analyses were performed with reused and fresh samples in order to understand whether the reason of deactivation was a formation of a side product such as NO or NO_2. First data was collected at every thirty seconds for 140 minutes during the heating from 250 °C to 550 °C for fresh Rh-Y6 (0.153 wt.%) and NO, NOx and NO_2 concentrations were monitored by using NOx analyzer. As it can be seen from Figure 46, decomposition of nitrous oxide over Rh-Y6 catalyst did not give a side reaction and no NOx products were detected.

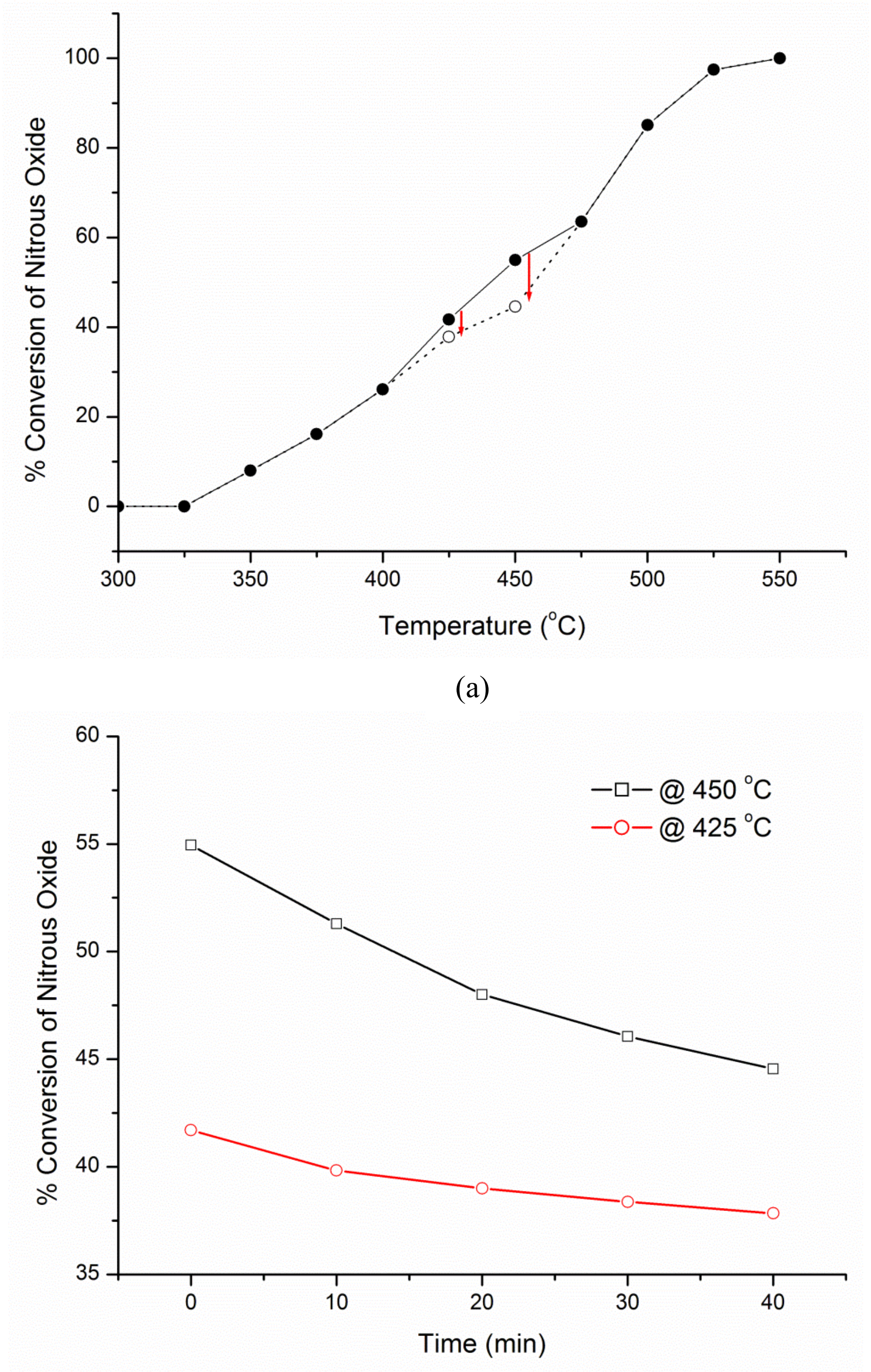

(a)

(b)

Figure 45. (a) The conversion versus temperature plot for the decomposition of nitrous oxide to nitrogen and oxygen performed starting with 100 mg Rh-Y2 catalyst (0.64 wt.% Rh) and a flow rate of 100 mL/min of 1000 ppm N_2O.(b) The conversion versus time plots for the decomposition of nitrous oxide to nitrogen and oxygen at 425 °C and 450 °C for 100 mg Rh-Y2 catalyst (0.64 wt.% Rh). (Flow rate:100 mL/min)

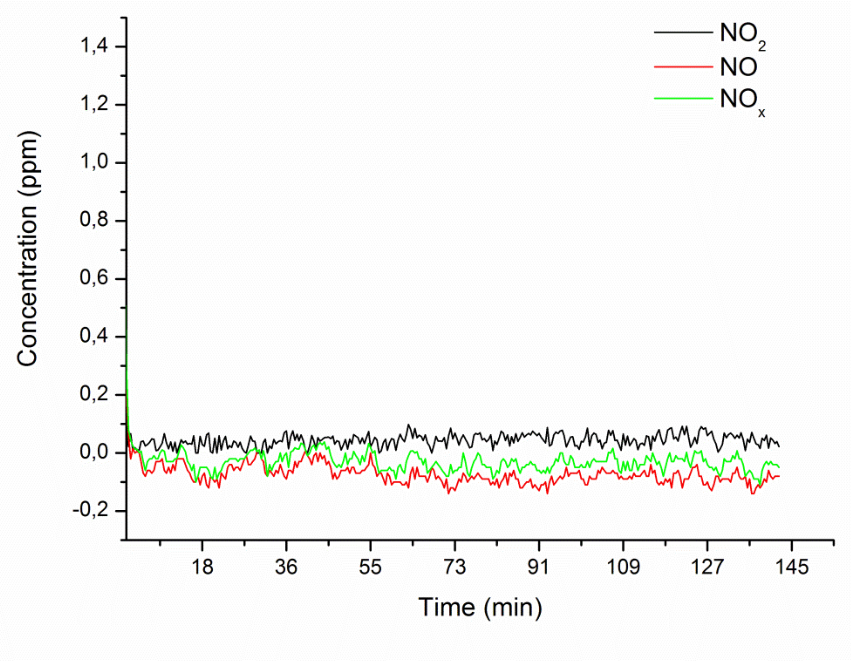

Figure 46. NOx evolution versus time graph monitored by NOx analyzer during the decomposition of nitrous oxide at 550 °C performed starting with 100 mg of Rh-Y6 (0.153 wt.% Rh) and a flow rate of 100 mL/min of 1000 ppm N_2O.

Second experiment was performed with the Rh-Y2 (0.64 wt.% Rh) sample which was used in four catalytic runs before NOx analysis. The sample was heated from 250 °C to 550 °C with a heating rate of 3 °C/min and NO, NO_x and NO_2 concentrations were monitored at every 30 seconds for 210 minutes. The results were shown in Figure 47. There is also no evolution of NOx gases during these experiments with the reused Rh-Y2 (0.64 wt.% Rh).

It is clear that the deactivation of rhodium catalysts is not related to the evolution of NOx gases. The nitrogen to oxygen ratio was determined to be 2:1 by GC measurements, which also supports this conclusion.

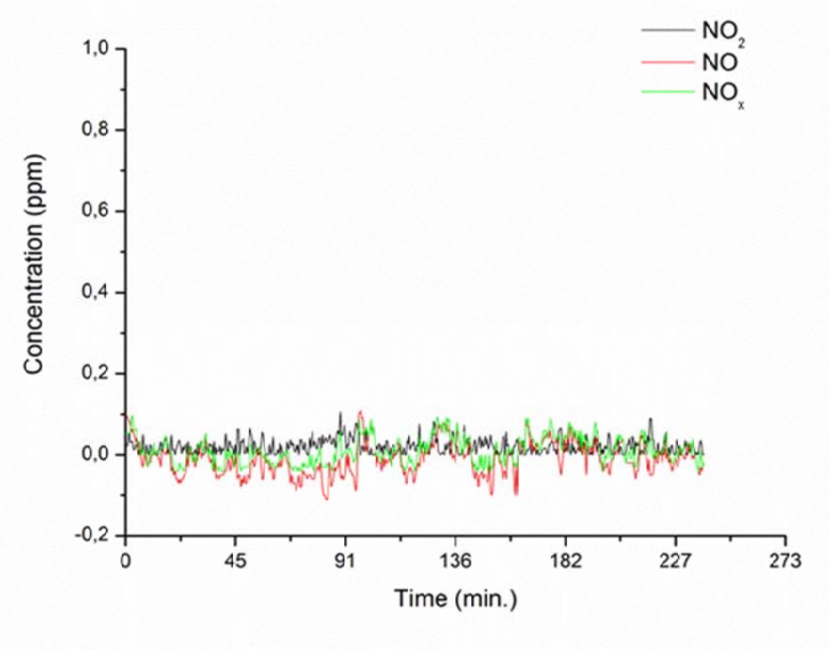

Figure 47. NOx evolution versus time graph monitored by NOx analyzer during the decomposition of nitrous oxide at 550 °C performed starting with 100 mg of Rh-Y2 (0.64 wt.% Rh) and a flow rate of 100 mL/min of 1000 ppm N_2O

Since the deactivation doesn't lead to the formation of any NOx gases, experimental procedure was changed in order to observe regular increase for nitrous oxide conversions in the presence of rhodium exchanged zeolite. The activity of rhodium catalysts was inspected by continuous heating between 250-550 °C at a rate of 3 °C/min and a flow rate of 100 mL/min of 1000 ppm N_2O. The plots of conversion versus temperature for the catalytic decomposition of nitrous oxide depending on the rhodium loading of zeolite Y were shown in Figure 48. Since the loadings of Rh-Y3 and RhY4 samples are close to each other (*Rh-Y3: 0.48 wt.%, Rh-Y4: (0.42 wt.%)* Rh-Y4 was not included to the comparative activity tests and analyses were performed with other five catalysts. Catalysts start to decompose nitrous oxide above 300 °C and the reaction is completed by 550 °C. In addition, all samples were followed for two hours at the temperatures where complete conversions were achieved, and deactivation was not observed for any of Rh-Y samples during this period. Rh-Y1 having the highest rhodium content of 2.12 wt. % shows the highest activity giving a total conversion at 475 °C. Generally, as the rhodium content of catalysts decreases, temperature at which the complete conversion is achieved slightly shifts to the higher values. However, the lowest loading catalyst, Rh-Y6 (0.153 wt.%) did not follow the decreasing trend and showed second highest activity after Rh-Y1 (2.12 wt.%).

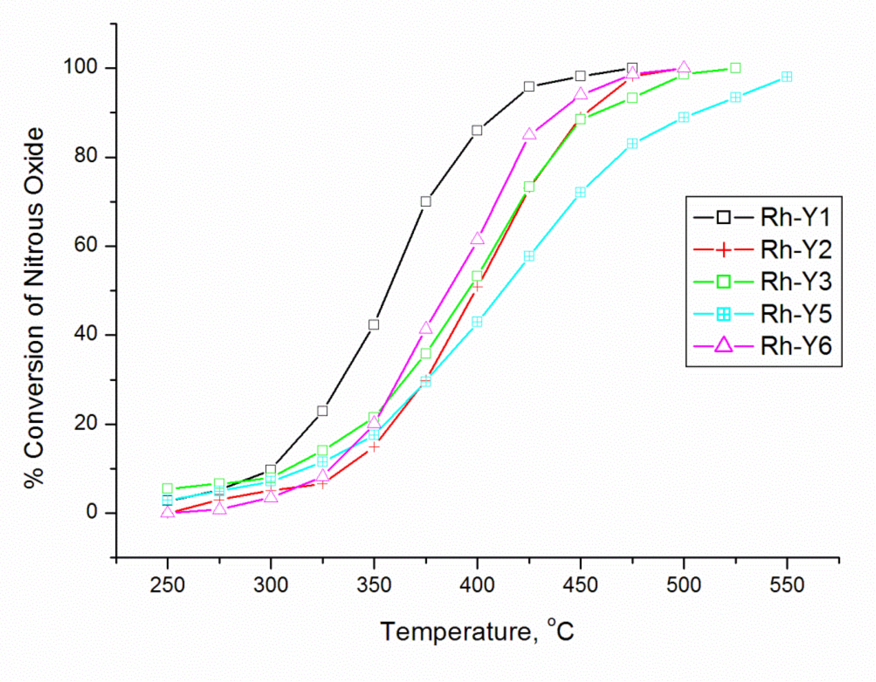

Figure 48. Conversion versus temperature plots for the decomposition of nitrous oxide to nitrogen and oxygen performed starting with 100 mg catalyst of Rh-Y1 (2.12 wt.%) , Rh-Y2 (0.64 wt.%) , Rh-Y3 (0.48 wt.%), Rh-Y5 (0.30 wt.%) and Rh-Y6 (0.153 wt.%) by continuous heating at a flow rate of 100 mL/min of 1000 ppm N_2O in the range of 250-550 ºC.

The high activity of Rh-Y6 (0.153 wt.%) was retested and compared with other catalysts by keeping rhodium content in reactor constant. Decomposition of nitrous oxide to nitrogen and oxygen was studied with three catalysts having the same rhodium amount of 0.15 ± 0.01 mg in the reactor under the same conditions as in the previous studies (1000 ppm N_2O in He at a rate of 100 mL/min). The starting temperature was set to 250 °C and temperature was continuously increased to 550 °C at a heating rate of 3 °C/min. The concentrations of nitrous oxide, nitrogen and oxygen were monitored at every 25 °C. The calculated conversion values were given in Figure 49. Rh-Y1 (2.12 wt.%) could not be studied since the amount of catalyst having 0.15% rhodium needed was too small for the reactor capacity. Rh-Y6 catalyst gave the highest activity among three samples and complete conversion was obtained at 475 °C. Other two samples, Rh-Y3 and Rh-Y5 started to decompose nitrous oxide above 400 °C and could not reach complete conversion even at 575 °C. The lower activity of zeolite sample with high rhodium loading can be attributed to the insufficient contact time of nitrous oxide with the catalyst as the amount of samples in the reactor is relatively small.

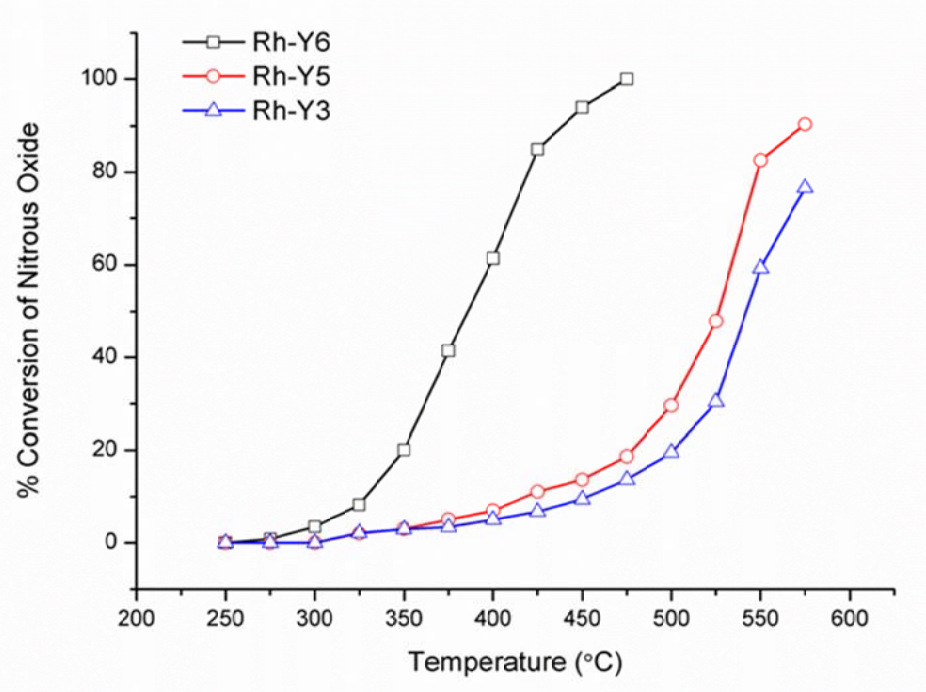

Figure 49. Conversion versus temperature plots for the decomposition of nitrous oxide to nitrogen and oxygen performed starting with 0.15 mg Rh using various amount of Rh-Y3 (0.48 wt.%), Rh-Y5 (0.30 wt.%), Rh-Y6 (0.15 wt.%) catalysts at 100 mL/min flow of 1000 ppm N_2O at temperature in the range 250-550 °C.

After the application of continuous heating procedure to rhodium catalysts, the catalytic decomposition of nitrous oxide were carried out by cooling the catalyst preheated in order to obtain steady decomposition and observe the true activity of rhodium exchanged zeolites in decomposition of nitrous oxide. By this way, more reliable data could be collected since the temperature throughout the catalyst in the reactor gets equilibrated and there will be sufficient time for nitrous oxide to interact with catalyst to provide steady decomposition at the temperature of measurement. In this procedure, temperature was first increased from 300 ºC to 600 ºC with the increments of 25 °C by a heating rate of 3 °C/min and samples were held thirty minutes at each temperature step in the same way as followed before. Then, the procedure was repeated adversely; that is, samples were cooled down to 300 ºC with 25 °C steps by -3 °C/min cooling rate. Figure 50 shows the experimental results obtained by using Ru-Y6 catalyst in three different procedures; continuous heating (procedure-1), stepwise heating by 30 minutes waiting at each 25 °C steps (procedure-2) and stepwise cooling by 30 minutes waiting at each 25 °C steps (procedure-3). It was already mentioned that procedure-1 results in higher activity for decomposition of nitrous oxide when compared to procedure-2. In addition, procedure-3 also resulted in significantly higher activity than procedure-2 by doubling nitrous oxide conversion between 400 ºC and 500 ºC. Recall that the activity of the rhodium exchanged zeolites decreases between 425 ºC and 450 ºC when procedure-2 was applied as seen in Figure 45.

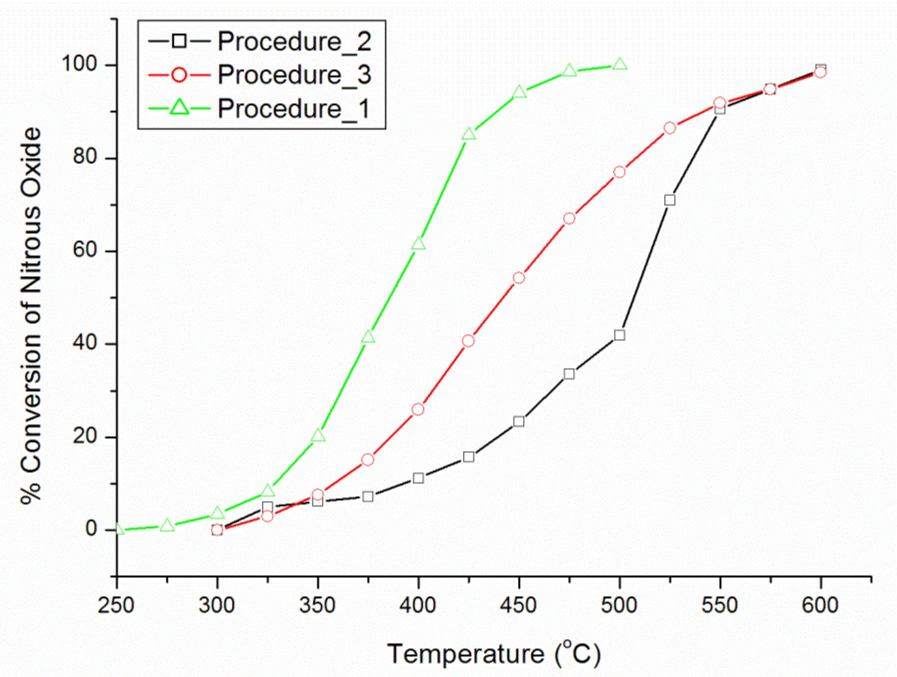

Figure 50. Conversion versus temperature plots for the decomposition of nitrous oxide to nitrogen and oxygen performed with 100 mg Rh-Y6 (0.153 wt.%) 100 mL/min flow of 1000 ppm N_2O by applying; Procedure-1: continuous heating by rate of 3 ºC/min between 250-500 ºC, Procedure-2: 300 ºC to 600 ºC by applying 30 minutes waiting at every 25 ºC step, Procedure-3 cooling from 600 ºC to 300 ºC by applying 30 minutes waiting at every 25 ºC step.

These three procedures were also applied to Rh-Y5 catalyst, and similar results were obtained as shown in Figure 51. In Procedure-1, Rh-Y5 catalyst gives higher conversion values at all temperatures, compared to those obtained in Procedure-2 or Procedure-3. Conclusively, the Procedure-1 provides the highest activity for the rhodium(III)-zeolite Y in the catalytic decomposition of nitrous oxide.

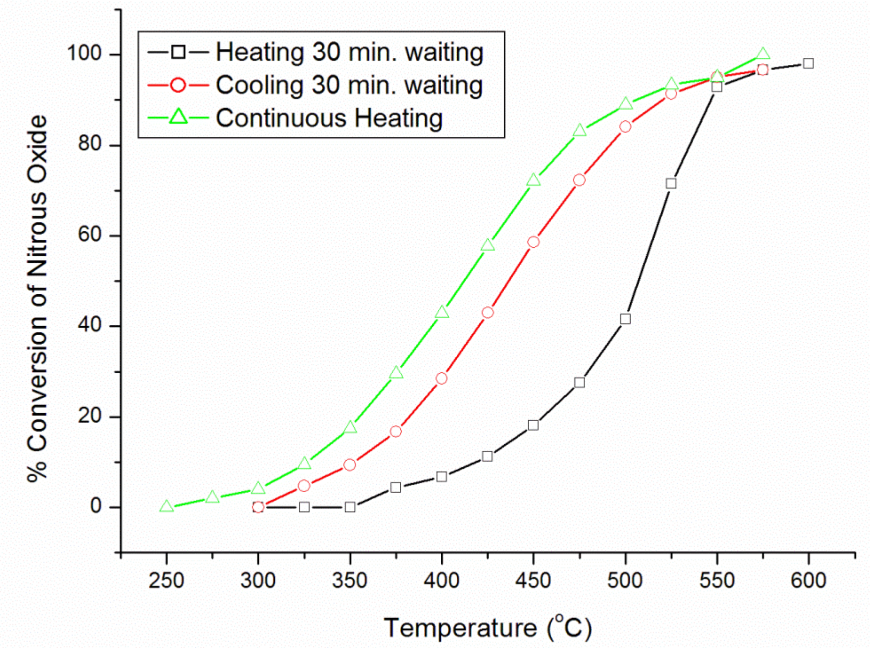

Figure 51. Conversion versus temperature plots for the decomposition of nitrous oxide to nitrogen and oxygen performed with 100 mg Rh-Y5 (0.30 wt.%) 100 mL/min flow of 1000 ppm N_2O by applying; Procedure-1: continuous heating by rate of 3 ºCmin^{-1} between 250-550 ºC, Procedure-2: 300 ºC to 600 ºC by applying 30 minutes waiting at every 25 ºC step, Procedure-3 cooling from 600 ºC to 300 ºC by applying 30 minutes waiting at every 25 ºC step.

In order to understand the reason for activity differences between these three procedures, the mechanism of nitrous oxide decomposition over rhodium catalysts must be considered. It is already known that the decomposition of nitrous oxide occurs in three steps via Langmuir-Hinselwood (LH) or Eley-Rideal (ER) mechanisms [32,33].

$$N_2O \longrightarrow N_2 + O_{ad} \qquad (8)$$

$$2O_{ad} \leftrightarrow O_2 \qquad (9)$$

$$N_2O + O_{ad} \longrightarrow N_2 + O_2 \qquad (10)$$

In case of LH mechanism, nitrous oxide dissociation occurs on the surface of catalyst producing nitrogen gas and an adsorbed oxygen atom. Then, recombination of adsorbed oxygen atoms results in desorption of dioxygen. However, this mechanism needs high temperatures to occur (8-9). On the other hand, ER mechanism postulates that nitrous oxide molecules collide with adsorbed oxygen atoms to form nitrogen and oxygen as products at low temperatures (10) [54].

In addition, a third mechanism has been proposed in literature as hot atom mechanism (HA) where only hot nascent O_{ad} atoms are produced by first step (8) and desorbed via step (9) [128].

However, experiments performed with labeled ^{18}O have shown that the decomposition of nitrous oxide over Rh/USY catalysts follows LH mechanism at low temperatures too [129,130]. Temperature programmed desorption measurements have shown that oxygen atoms desorb from surface of supported catalysts above 873K [119]. Therefore, at low temperatures, adsorbed oxygen atoms need extra energy from surrounding for desorption from the catalyst surface. This additional energy may be supplied by the exothermic decomposition of nitrous oxide ($\Delta H = -81.7$ kJ/mol) where N≡N bond is formed and N-O bond is broken [129]. Consequently, the exothermicity of nitrous oxide decomposition can assist the desorption of oxygen from the catalyst surface. This explains the LH mechanism for desorption of oxygen at low temperatures.

The behavior of the plots given in Figure 50 and Figure 51 can be explained as reaction assisted desorption of oxygen where exothermic decomposition of nitrous oxide provides the energy required for the breakage of the surface-oxygen bond. Probably, continuous heating enhances the mechanism by supplying additional energy for desorption of oxygen adsorbed on the catalyst surface. It is noteworthy that continuous heating provides complete conversion at lower temperature than that obtained by stepwise heating and cooling and after complete conversion, no deactivation is observed even though samples are held at those temperatures for two hours. However, when the samples were held at each 25 ºC step for some time in stepwise heating, as in Figure 45, and the desorption of oxygen gets slower, so the breakage of surface-oxygen bond, and thus, the conversion decreases below 500 ºC. In the case of cooling procedure, the reaction temperature was slowly decreased from 600 ºC to 300 ºC at a rate of -3 ºC/min. Note that cooling is performed in a controlled way by using additional heating. During the cooling down additional heat is supplied which can assist the desorption of oxygen.

The catalytic decomposition of nitrous oxide by cooling measurements was performed by using all of rhodium exchanged catalysts, the results of which are shown in Figure 52 altogether. The experiments were started with 100 mg catalysts having various rhodium contents, and the system was heated first to 600 ºC by following the same stepwise heating program used before. Then, the system was cooled down to 300 ºC stepwise by applying 25 ºC steps and keeping the system at each temperature step for 30 minutes.

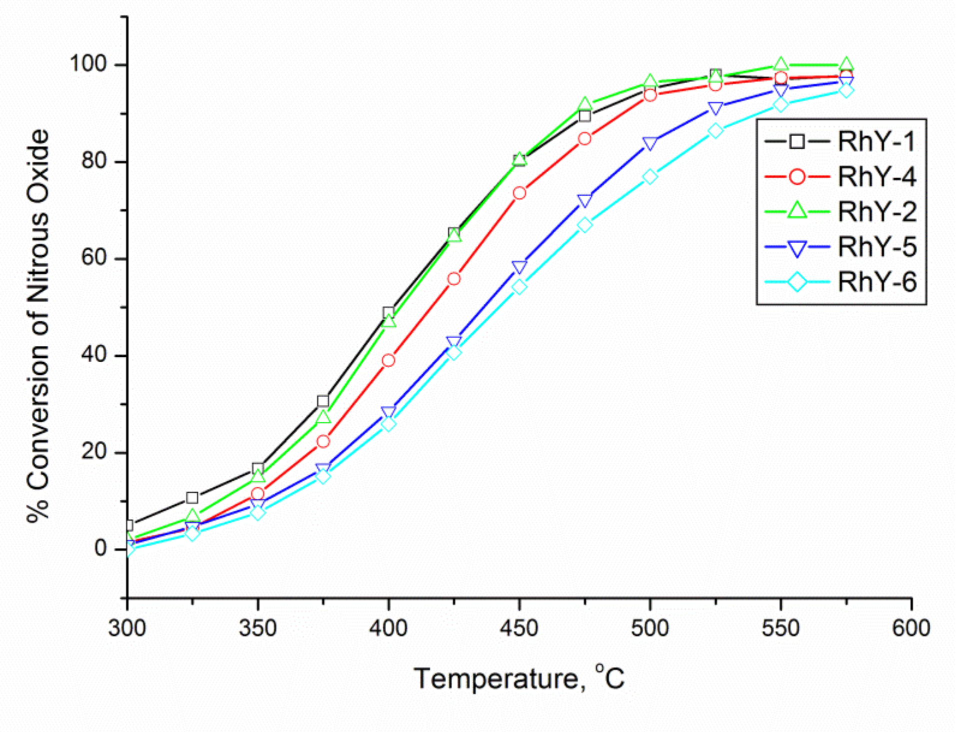

Figure 52. Conversion versus temperature plots for the decomposition of nitrous oxide to nitrogen and oxygen performed starting with 100 mg catalyst of Rh-Y1 (2.12 wt.%) , Rh-Y2 (0.64 wt.%) , Rh-Y4 (0.42 wt.%), Rh-Y5 (0.30 wt.%) and Rh-Y6 (0.153 wt.%) at a flow rate of 100 mL/min flow of 1000 ppm N_2O in the range of 600-300 ºC.

Figure 52 shows that catalytic activity is directly proportional to the metal loading of the zeolite with the exception of Rh-Y2 sample. As the rhodium content of catalyst decreases, the nitrous oxide conversion decreases at all temperatures. Rh-Y1 (2.12 wt.%) and Rh-Y2 (0.64 wt.%), which are two highest loadings among the samples, give the highest activity and provide complete conversion of nitrous oxide to its products at 525 ºC. The conversion plots of these samples are very similar to each other although the rhodium content of Rh-Y1 is three times more than that of Rh-Y2.

In the second set of experiments, performed by cooling, the amount of rhodium was kept constant and their activity was measured by varying the temperature. For this experiment, the amount of sample used was restricted to 100 mg capacity. Rh-Y6 (sample with the lowest rhodium content having 0.153 wt.%) was chosen as a sample for keeping the amount of rhodium constant (0.153 mg). The amount of the other samples was calculated based on this rhodium content. Rh-Y1 (2.12 wt.%) could not be used since the amount of catalyst sample calculated was not sufficient for performing the experiment. Catalytic activity of Rh-Y2 (0.64 wt.%), Rh-Y5 (0.30 wt.%) and Rh-Y6 (0.153 wt.%) was studied under the same conditions as mentioned in Figure 53.

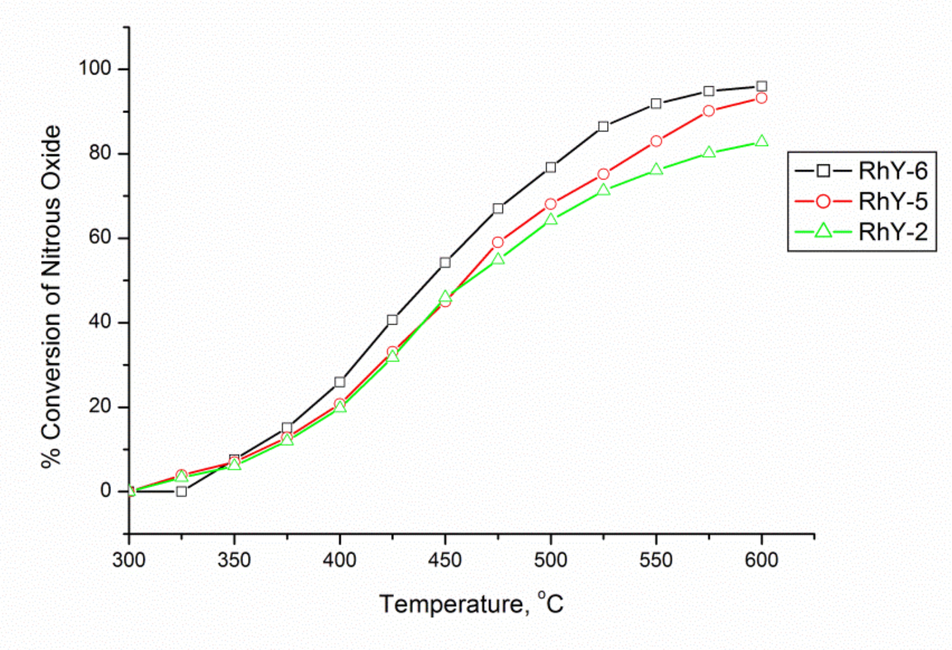

Figure 53. Conversion versus temperature plots for the decomposition of nitrous oxide to nitrogen and oxygen performed starting with 0.15 mg Rh using various amount of Rh-Y2 (0.64 wt.%), Rh-Y5 (0.30 wt.%), Rh-Y6 (0.153 wt.%) catalysts at 100 mL/min flow of 1000 ppm N_2O at temperature in the range 600-300 ºC.

A close inspection of the plots in Figure 53 shows that Rh-Y6 catalyst (0.153 wt.%) exhibits higher conversion at all temperature than those of Rh-Y5 (0.30 wt.%) and Rh-Y2 (0.64 wt.%). It is noteworthy that Rh-Y2 catalyst with the highest Rh loading gives only 80% conversion at 600 ºC. This observation can be ascribed to the short contact time of nitrous oxide with the catalyst as the amount of Rh-Y2 sample used in this experiment is relatively small (24 mg).

The decrease in conversion observed in using Rh-Y2 catalyst during the stepwise heating was retested by decreasing the flow rate of N_2O from 100 mL/min to 50 mL/min in order to see whether the flow rate of 100 mL/min was slow enough for catalyst to get in contact with nitrous oxide completely. Figure 54 shows that, at all temperatures, the conversion increases when flow rate is reduced from 100 mL/min to 50 mL/min. This result also supports the explanation stating that short contact time of substrate with the catalyst causes a decrease in the conversion of nitrous oxide.

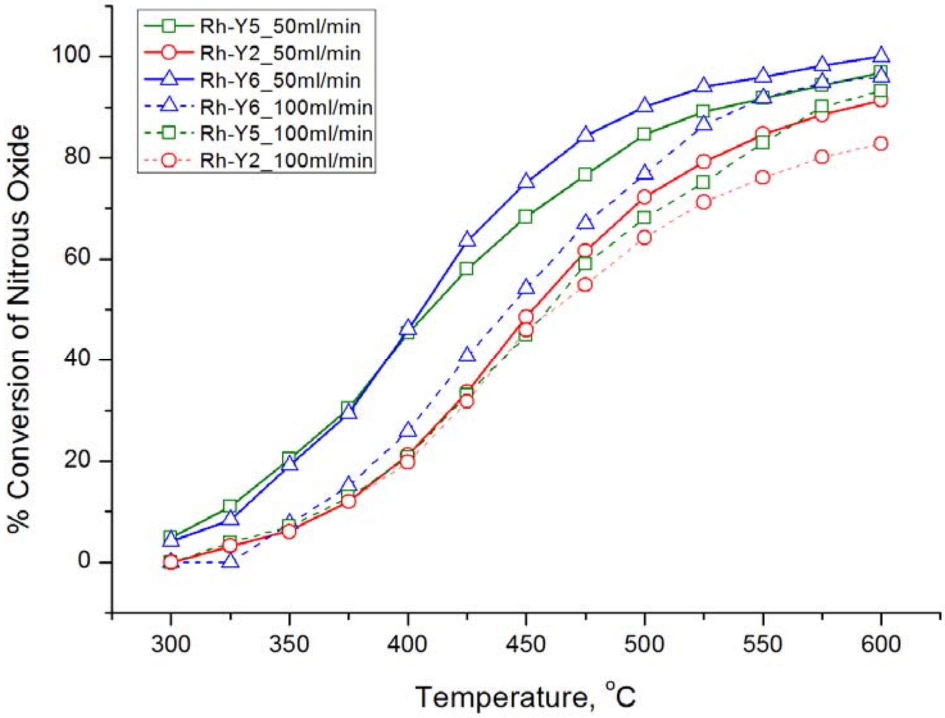

Figure 54. Conversion versus temperature plots for the decomposition of nitrous oxide to nitrogen and oxygen performed starting with 0.15 mg Rh using various amount of Rh-Y2 (0.64 wt.%), Rh-Y5 (0.30 wt.%), Rh-Y6 (0.153 wt.%) catalysts at 50 mL/min and 100 mL/min flow of 1000 ppm N_2O at temperature in the range 600-300 ºC.

4.9 Preparation and characterization of iridium(III) ion-exchanged zeolite-Y

Iridium(III) exchanged zeolites were prepared following the same ion exchange procedure as previously described [121]. The metal loadings of catalysts were determined in ICP-MS and given in Table 7.

Table 7. Metal loadings of Ir-Y catalysts determined by ICP-MS

Catalyst	Ir content (mg/kg)	Ir Content (%)
Ir-Y1	675 ± 7	0.0675 ± 0.0007
Ir -Y2	580 ± 9	0.0580 ± 0.0009
Ir -Y3	324 ± 5	0.0324 ± 0.0009
Ir -Y4	322 ± 4	0.0322 ± 0.0004
Ir -Y5	268 ± 1	0.0268 ± 0.0001
Ir -Y6	253 ± 4	0.0253 ± 0.0004

As can be seen from Table 7, metal contents of catalysts are very low. Therefore, the metal loadings are also given in mg/kg units to simplify the expressions of iridium contents. The low iridium contents in the catalysts may be the result of an insufficient ion exchange of Ir(III) ions with Na^+ cations of zeolite Y. The insufficient ion exchange may also lead to the uncertainty in activity measurements.

The XRD patterns of fresh and reused iridium(III) exchanged zeolite Y catalysts having iridium content of 322 ± 4 mg/kg were compared with zeolite Y XRD patterns. Figure 55 exhibits that the crystal lattice of zeolite Y remains unchanged after ion exchange of Ir(III) with zeolite Y. Also, there is no sign of distortion in the lattice after three catalytic runs. As it is indicated before, concentration of iridium in the catalysts is less than 0.1% and thus, it is hard to see iridium phase in XRD patterns. Therefore, XPS analyses were performed in order to see the surface composition and oxidation state of iridium. However, survey scan could not show the existence of iridium. The high resolution 4f XPS spectrum exhibited the presence of iridium, however the satellite peaks belonging $4f_{7/2}$ and $4f_{5/2}$ shells of iridium could not well defined during the analysis due the low metal content (< 0.1wt.%).

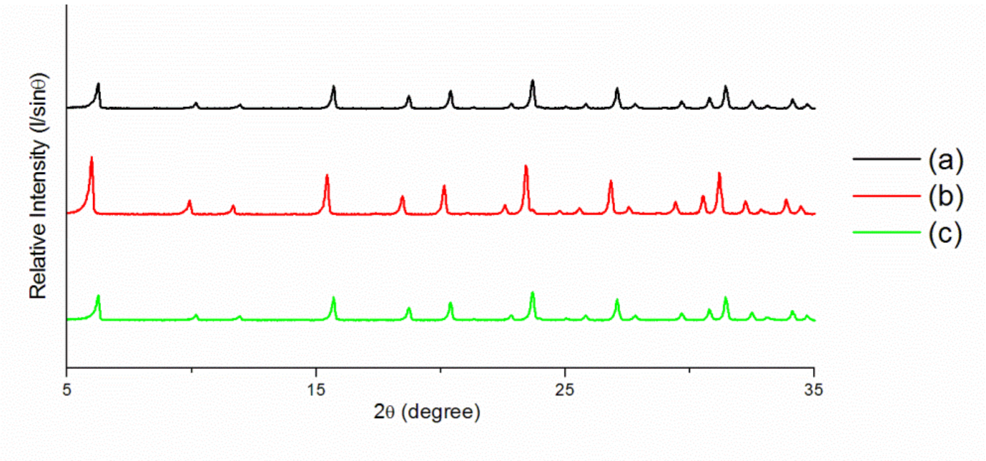

Figure 55. Powder XRD patterns of (a) host material zeolite Y (b) Fresh Ir-Y4 with iridium content of 322 ± 4 mg/kg (b) Reused Ir-Y4 with iridium content of 322 ± 4 mg/kg

4.10 Catalytic activity of Ir-Y

The activity tests of iridium(III) exchanged zeolites in the decomposition of nitrous oxide to nitrogen and oxygen were carried out by using the vertical flow reactor at a flow rate of 100 mL/min nitrous oxide (1000 ppm in He) with a sample weight of 100 mg. During the course of this work, it is found that the conversion of nitrous oxide in the presence of iridium(III) exchanged zeolite Y severely depends on preheating application. For example, when the test with Ir-Y3 sample was started at 350 ºC without preheating to 500 ºC, the conversion of nitrous oxide drastically decreases from 90 % to 10 % indicating the deactivation of catalyst. However, a steady state with a conversion of 60% can be obtained when the sample is previously heated to 500 ºC and cooled down. Figure 56 shows the plots of conversion versus temperature for the experiments performed by using Ir-Y3 sample with and without preheating.

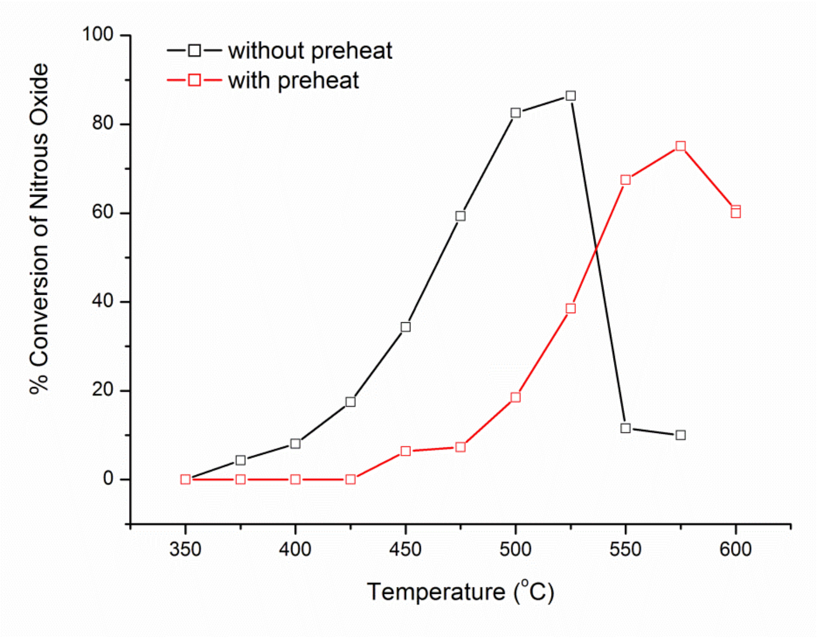

Figure 56. Conversion versus temperature plots for the decomposition of nitrous oxide to nitrogen and oxygen performed starting with 100 mg catalyst of Ir-Y3 (324 mg/kg Ir) with or without preheating to 500 ºC (100 mL/min flow of 1000 ppm N_2O in the range of 350-600 ºC.)

In the first case, samples were preheated to 500 ºC and held at 500 ºC for one hour and then cooled down to 350 ºC. The test was started at 350 ºC by heating the sample and the concentrations of reactant and product gases were followed via GC. Six iridium catalysts were used to study the catalytic activity and the results are given in

Figure 57. Only Ir-Y2 and Ir-Y4 samples having an iridium content of 580 mg/kg and 322 mg/kg, respectively, show complete conversion of nitrous oxide to nitrogen and oxygen at temperatures above 525 ºC. All the other samples are deactivated above 450 ºC. A similar deactivation of iridium catalysts has been previously observed by Ohnishi et.al for iridium catalysts supported by alumina [60]. They have shown that oxygen formed by nitrous oxide decomposition causes a decrease in activity of the catalyst. Ohnishi et al. have also shown in 2006 that loading of the iridium species destroyed the activity of the supports such as Co_3O_4 and NiO [131].

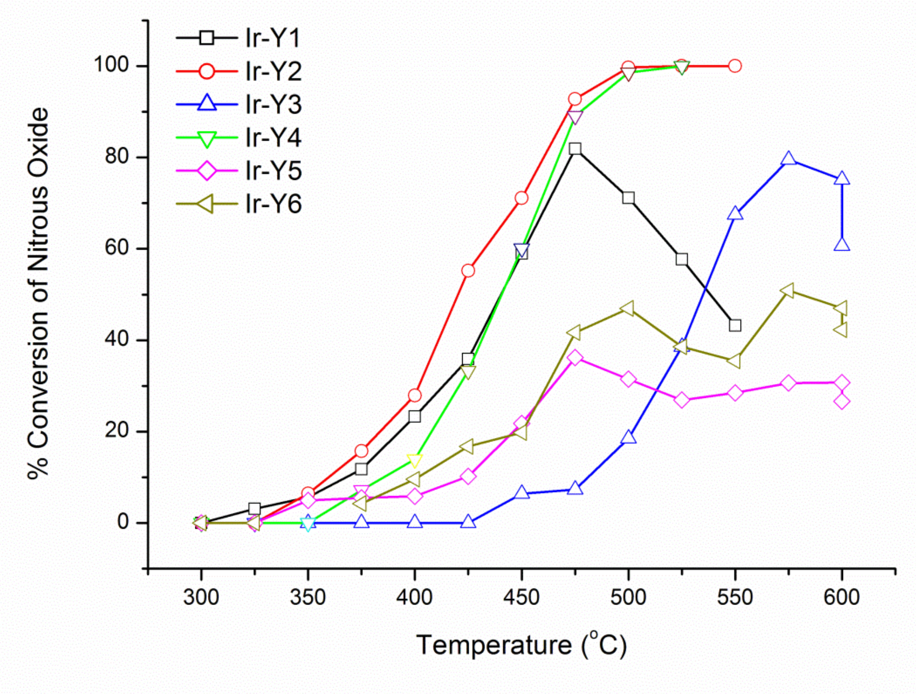

Figure 57. Conversion versus temperature plots for the decomposition of nitrous oxide to nitrogen and oxygen performed starting with 100 mg catalyst of Ir-Y1 (675 mg/kg Ir), Ir -Y2 (580 mg/kg Ir), Ir -Y3 (324 mg/kg Ir), Ir –Y4 (322 mg/kg Ir), Ir -Y5 (322 mg/kg Ir)and Ir -Y6 (268 mg/kg Ir)at a flow rate of 100 mL/min flow of 1000 ppm N_2O in the range of 300-600 ºC.

All iridium zeolite Y samples exhibit the ratio of nitrogen to oxygen as 2:1 indicating side reactions did not occur throughout the experiments. This observation was also verified by NOx analysis. The test was carried out for 150 minutes in the range of 350 -550 ºC. For the first 70 minutes test sample was heated to 550 ºC and hold at that temperature for 70 minutes more. There is no significant NOx formation during decomposition reaction of nitrous oxide.

4.11 Comparison of catalytic activity of rhodium-zeolite Y catalyst with that of other Group-9 metal-zeolite Y.

Activities of rhodium(III), iridium(III) and cobalt(II) exchanged zeolites were compared to each other in order to find out the best catalytic activity among Group 9 metal zeolite catalysts. Rhodium(III) and iridium(III) exchanged zeolites were investigated in details in previous sections. Therefore, the samples showing highest catalytic activity were selected and compared with that of cobalt(II) exchanged zeolite Y which was prepared by following the same ion exchange procedure as the one used for the first two catalysts and having loading of 5 wt.% Co. Figure 58 exhibits the catalytic activities of these three catalysts collected by following Procedure-1 (using continuous heating).

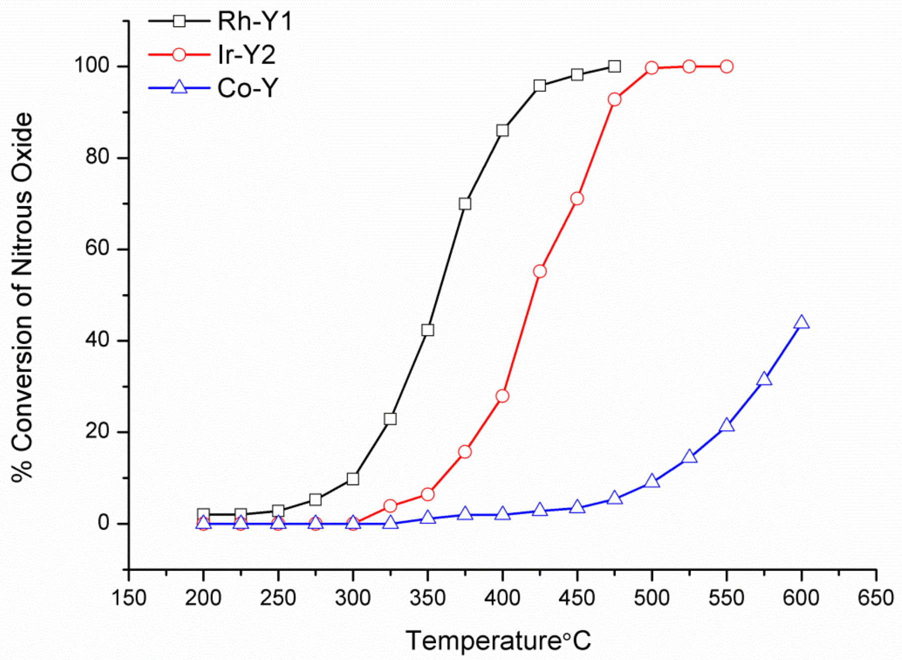

Figure 58. Conversion versus temperature plots for the decomposition of nitrous oxide to nitrogen and oxygen performed starting with 100 mg sample of Rh-Y1 (2.12 wt.% Rh), Ir-Y2 (580 mg/kg wt.% Ir) and Co-Y (5 wt.% Co) catalyst and a flow rate of 100 mL/min of 1000 ppm N_2O at temperature in the range of 200-600 °C.

Rhodium(III) exchanged zeolite shows the highest catalytic activity by starting decomposition of nitrous oxide over 300 ºC and giving complete conversion at 475 ºC. Conversion of nitrous oxide over iridium(III) exchanged zeolite starts at 325 ºC and total conversion is obtained at 500 ºC. Although the temperatures at which the complete conversion was obtained are close to each other, at lower temperature rhodium(III) exchanged zeolite provides higher conversion than that obtained by using iridium(III) exchanged zeolite as seen in Table 8.

Table 8. Conversion values of Rh-Y1 (2.12 %wt.Rh, Ir-Y2 (580 mg/kg Ir) and Co-Y (5 %wt. Co) catalysts for decomposition reaction of nitrous oxide at a flow rate of 100 mL/min N_2O (1000 ppm in He) between 300 ºC and 550 ºC

Catalyst	Temperature, ºC										
	300	**325**	**350**	**375**	**400**	**425**	**450**	**475**	**500**	**525**	**550**
Rh-Y1	9	23	42	69	86	95	98	100	-	-	-
Ir- Y2	0	4	6	16	28	55	71	93	99	100	-
Co-Y	0	0	1	2	2	3	3	5	9	15	21

Note that, the experiments of Rh-Y catalysts were carried out without any pretreatment whereas Ir-Y catalysts were preheated to 500 ºC and cooled down to 300 ºC before starting the measurement. Compared to the rhodium and iridium exchanged zeolite catalyst, cobalt(II) ion exchanged zeolite shows much lower activity in the temperature range 300-600 ºC.

4.12 The difference in activity of metals depending on the location of ions within the zeolite cages

As it is mentioned before in section 1.3, activity of catalysts depends on both metal and zeolite characteristics and combination of appropriate metal ions with host material results highly active catalysts. Locations of metal ions in zeolite cages have high impact in catalyst activity since these locations determine chemical properties of catalyst and interactions of metal ions with substrates. Studies carried out with Group 8 and 9 metal ion exchanged zeolite Y in decomposition of nitrous oxide shows that Ru(III) ion exchanged zeolite Y comes forward by its high activity among other catalysts. The high activity of Ru-Y can also be explained by locations of Ru^{+3} cations in the cages of zeolite Y.

Cation sites in the zeolite can be determined by either computational studies or instrumental analysis such as Far-IR and NMR spectroscopies. Locations of extra framework Na^+ cations in zeolite Y were previously identified by far-IR spectroscopy [132] and also verified by ^{23}Na-NMR spectroscopy [133]. In far-IR region, extra framework cation vibrations were determined in both α and β- cages of zeolite Y between 200-50 cm^{-1} [132]. The presence of Ru^{+3} cations were also identified in α and β- cages of zeolite Y after exchange reaction with Na^+ cations by far-IR spectroscopy. Vibrations of Ru^{+3} cations shifted to the lower frequency region between 80-50 cm^{-1} since Ru^{+3} is trivalent and heavier than extra framework Na^+ [74].

Supercages (α-cages) of zeolite Y enable more sufficient interaction of substrate with metal cations than β- cages as can be seen from the framework structure of FAU (Section 1.4, Figure 5). The high activity of Ru-Y catalysts can be explained by dispersion ratio of cations in the cages. Most probably, majority of Ru^{+3} cations present in the more accessible supercages (α – cages) of zeolite Y, thus nitrous oxide can contact with active metallic sites of zeolite easily and readily.

This situation can be generalized for both Ru(III) ion exchanged zeolite Y having various metal contents and the other metal ion exchanged catalysts. As metal cations in zeolite Y are located in β- cages, which are less accessible when compared to supercages, the activity of catalysts will decrease.

CHAPTER 5

CONCLUSION

In summary, this study on preparation of Group 8 and Group 9 ion exchanged zeolite Y catalysts for decomposition of nitrous oxide has led to following conclusions and insights:

- The Group 8 and 9 metal(III) ion-exchanged zeolite catalysts can easily be prepared from the ion exchange of metal(III) ions with the extra framework Na^+ cations of zeolite Y.

- The characterization of metal(III) ion–exchanged zeolites was performed by ICP-OES, XRD and XPS techniques. XRD results show that the ion exchange procedure did not cause any alteration in the framework lattice of zeolite. Also, the oxidation state of metal and surface composition were studied by XPS spectra indicating the presence of transition metal in addition to the framework elements of zeolite (O, Si, Al, Na) and C from air during the XPS sampling.

- Of the Group 8 metals, ruthenium(III) ion-exchanged zeolite catalyst shows high activity in decomposition of nitrous oxide at temperatures below 425 °C. Ru-Y1, the highest ruthenium loading catalyst (3.98 wt.%), provides the highest conversion at all temperatures and gives complete conversion at 350 °C.

- During catalytic decomposition of nitrous oxide catalyzed by ruthenium exchanged zeolite Y, the molar ratio of nitrogen to oxygen remains constant as 2:1 indicating that nitrous oxide decomposes only nitrogen and oxygen. No NOx formation is observed at any stage of decomposition.

- In catalytic tests performed with constant catalyst amounts (100 mg), as ruthenium loading of catalysts increases the conversion of nitrous oxide increases at all temperatures and complete conversion is observed at slightly lower temperature down to 350 °C.

- In catalytic tests performed by keeping the ruthenium amount in the catalysts constant as 1.6 ± 0.1 mg, the zeolite catalyst with the highest ruthenium content (Ru-Y1) does not provide the highest catalytic activity, which is attributed to the short contact time of nitrous oxide with ruthenium(III) since the amount of catalyst in the reactor is small relative to the reactive volume.

- The flow rate of 150 mL/min appears to be the upper limit for performing the catalytic decomposition of nitrous oxide in a tubular reactor having a diameter of ¼ to achieve conversion higher than 95%. An enlargement in the reactor is necessary to apply higher flow rates without affecting the conversion of nitrous oxide.

- The reusability tests performed with Ru-Y1 shows that catalyst provides 97% conversion after 30 days in the ninth run 87% conversion of nitrous oxide after 5 months in the tenth run at 350 °C. Ruthenium(III) ion-exchanged zeolite is highly active, long-lived and reusable catalyst in decomposition of nitrous oxide. The results of Ru-Y catalysts are compared with those of other ruthenium catalysts and given in Table 9.

Table 9. The comparison of Ru-Y catalyst results with those of other ruthenium catalysts in the literature.

Zeolite Type	**Preparation Method**	**Pretreatment**	**Complete Conversion Temperature**	**Durability & Reusability**	**Ref.**
ZSM5	Impregnation	500ºC-1h	350°C	No information	[61]
Al_2O_3	Impregnation	500ºC-1h	>350°C	No information	
ZSM-5	Ion-exchange	-	320°C	No information	[62,63]
HNaUSY	Ion-exchange	-	320°C	Not stable	
Al_2O_3	Impregnation	500ºC-4h	425°C	No information	[134]
Al_2O_3	Impregnation	400ºC-1h	400°C	No information	[135]
γ-Al_2O_3	In situ reduction of ethylene glycol method	600 ºC	500°C	Partial deactivation (activation decrease to 85 %) after 4 hours	[136]
Zeolite Y	**Ion-exchange**	**-**	**350°C**	**No deactivation for 1 month (9 runs)**	**[137]**

- High activity of Ru-Y catalysts for the catalytic decomposition of nitrous oxide to nitrogen and oxygen at low temperatures is advantageous for large scale tests.

- Ruthenium(0) nanoclusters, prepared from the reduction of ruthenium(III) ions in the highest loading zeolite sample (3.98 wt.% Ru),are also active catalyst in the decomposition of nitrous oxide, though lower than that obtained by using ruthenium(III) ion exchanged zeolite. The lower catalytic activity of ruthenium(0) nanoclusters than that of ruthenium(III) ion exchanged zeolite might be due to the migration of ruthenium(0) nanoclusters in the cages of zeolite toward the external surface prior to oxidation at high temperature.

- The activity order of Group 8 metal(III) ion exchanged zeolite catalysts in the decomposition of nitrous oxide is ruthenium(III) > iron(III) > osmium(III). Despite the high activity of ruthenium(III) ion–exchanged zeolite catalysts, iron(III) and osmium(III) ion exchanged zeolites do not show significant activity in decomposition of nitrous oxide. Iron(III) exchanged zeoliteY provides complete conversion of nitrous oxide at 600 °C whereas osmium(III) exchanged zeolite Y gave only 15% conversion at 550 °C. Additionally, the decomposition of nitrous oxide catalyzed by iron(III) or osmium(III) ion-exchanged zeolite causes the formation of side products as detected by NOx analyzer.

- Of the Group 9 metals, rhodium(III) exchanged zeolite Y shows activity in decomposition of nitrous oxide between 300 °C and 550 °C depending on the conditions. Some deactivation of the catalyst is observed when the system is held at constant temperature between 400 °C and 500 °C in stepwise heating program, though without formation of NOx.

- When rhodium(III) ion-exchanged zeolite catalyst is used in continuous heating procedure, the decomposition of nitrous oxide starts at 300 °C and the reaction is completed at temperature below 550 °C. When the complete conversion is achieved no deactivation is observed upon further heating or cooling down.

- Rhodium(III) ion-exchanged zeolite Y with a metal loading of 2.12 wt.% Rh shows the highest activity providing complete conversion of nitrous oxide at 475 °C when 100 mg catalyst used. When the amount of rhodium in the catalyst is kept constant at 0.15 ± 0.01 mg, the rhodium(III) ion-exchanged zeolite Y with metal loading 0.153 wt.% Rh gives the highest activity providing complete conversion of nitrous oxide at 475 °C while the others with higher metal loading do not provide complete conversion even at temperatures up to 575 °C. This low activity may be due to the insufficient contact time of nitrous oxide with catalysts as the amount of samples with high metal loading in the reactor is relatively small.

- When the decomposition of nitrous oxide is followed during the stepwise cooling of the sample heated first stepwise to 600 °C, the rhodium(III) ion-exchanged zeolite with metal loading of 0.30 and 0.15 wt.% Rh provide significantly higher activity between 400 ºC and 500 ºC compared to the results obtained during heating.

- The difference in catalytic activity measured during the stepwise heating up or cooling down is explained by considering the reaction mechanism proposed for the catalytic decomposition of nitrous oxide: The energy required for the desorption of oxygen atoms adsorbed on the catalyst surface is provided by the exothermic nitrous oxide decomposition. In the controlled heating or cooling the additional heating can supply the energy required for the desorption of oxygen from the catalyst surface. However, when sample is held at constant temperature during the stepwise heating, the breakage of surface-oxygen bonds gets slower and, thus, the conversion of nitrous oxide decreases. When the rhodium content catalyst is kept constant, the rhodium(III) ion-exchanged zeolite with lowest metal loading of 0.15 wt.% Rh shows the highest catalytic activity in decomposition of nitrous oxide performed by cooling down the sample preheated to 600 ºC. That the higher loaded zeolite samples give lower catalytic activity than the lower loaded ones can be explained by the short contact time of substrate with the catalyst as the amount of sample is too small relative to the reactor size. Similarly, decreasing the flow rate from 100 mL/min to 50 mL/min leads to an increase in the contact time of substrate with the catalyst and thus, an increase in the conversion of nitrous oxide.

- The activity order of the Group 9 metals ion-exchanged to zeolite Y in decomposition of nitrous oxide: rhodium(III) > iridium(III) >> cobalt(II). Rhodium(III) ion-exchanged zeolite Y shows higher conversion of nitrous oxide at all temperatures when compared to iridium(III) ion-exchanged zeolite Y. Cobalt(II) ion-exchanged zeolite Y can provide conversion less than 40 % conversion at 600 ºC.

- The activity of Group 8 and Group 9 metal ion exchanged zeolite Y catalysts are compared with each other regarding the conversion of nitrous oxide and the temperature of complete decomposition in Figure 59.

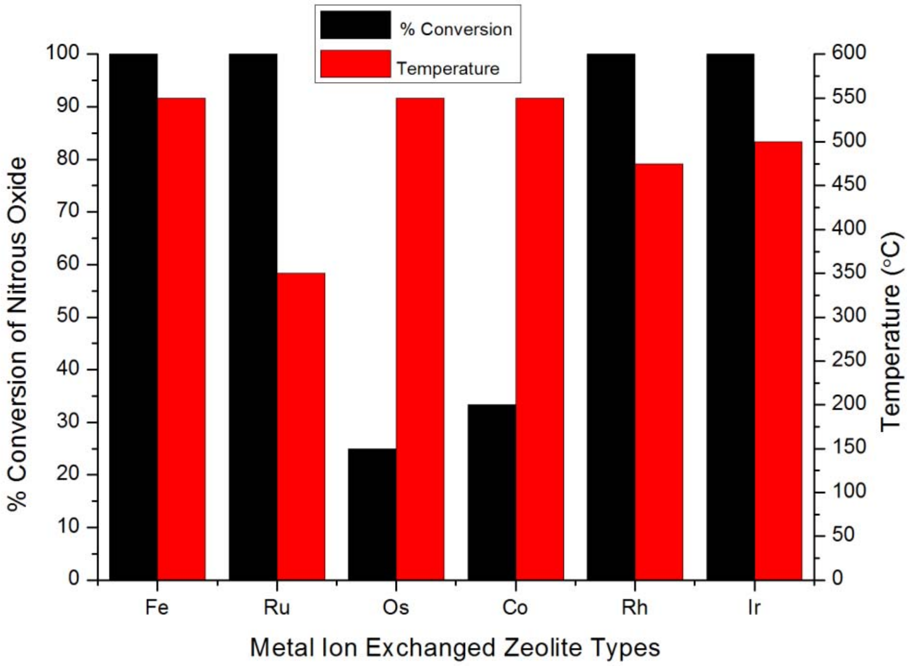

Figure 59. Comparison of group 8 and group 9 metal ion exchanged zeolites according to their conversion ratios and the temperature values where the highest conversions were achieved.

In this study; the activity of group 8 and 9 metal ion exchanged zeolite catalysts was studied for nitrous oxide decomposition in order to compensate the hot gas requirement of all-up round test set-up. Results of activity experiments showed that ruthenium(III) ion-exchanged zeolite Y is a good candidate with its high activity at low temperature, reusability and long life time. Rhodium(III) ion-exchanged zeolite Y is also a promising catalyst for nitrous oxide decomposition since it was able to decompose nitrous oxide totally at 475 ºC.

REFERENCES

[1] Suksankraisorn K., Patumsawad S., Vallikul P., Fungtammasan B., Accary A., Energy Convers. Manage. 2004, 45, 947–962.

[2] Robertson G.P., Paul E.A., Harwood R.R., Science 2000, 289, 1922–1925.

[3] Crutzen P.J., Mosier A.R., Smith K.A., Winiwarter W., Atmospheric Chemistry and Physics, 2008, 8, 389-395.

[4] Wojtowicz M. A., Pels J. R., Moulijn J. A., Fuel. Proc. Technol. 1993, 34, 1.

[5] Choe J. S., Cook P. J., Petrocelli F. P., ANSPG Conference, Destin-FL-USA, (1993)1-13.

[6] Albritton D.L., Derwent R.G., Isaksen I.S.A, Lal M., Wuebbles D.J., Climate Change Radiative Forcing of Climate Change, Intergovernmental Panel on Climate Change, Chapter 5, Chambridge University Press, 1994.

[7] Olivier J.G.J., Bouwman A.F., Van der Hoek K.W., Berdowski J.J.M, Global Air Emission Inventories for Anthropogenic Sources of NOx, NH3 and N2O in 1990, 1st International Nitrogen Conference, Elsevier Sci. Ltd, Netherlands, 1998, 135–148.

[8] IPCC, Climate Change 2007 Synthesis Report, Valencia, Spain, 2007, 1–52.

[9] Xing H., Wang E., Smith C. J., Rolston D., Geoderma Q.Yu., 2011, 167-168, 328-339.

[10] Suddick E.C., Six J., Science of Total Environment, 2013, 465, 298-307.

[11] Hassouna M., Robin P., Cherpiot A., Edovard N., Medas B., Biosystems Engineering, 2013, 114, 318-326.

[12] Zakirov V., Sweeting M., Acta Astronamica, 2001, 48: 5-12, 353-362.

[13] Lawrence T. J., PhD Thesis: Research into Resistojet Rockets for Small Satellite Applications, University of Surrey, 1998

[14] Whitehead J. C., Hydrogen Peroxide Propulsion For Smaller Satellite, 1st Hydrogen Peroxide Propulsion Workshop, 1998.

[15] McCormick J.C., Hydrogen Peroxide Rocket Manual, FMC Corporation. Buffalo, NewYork, 1965, I-2, III-6, VII-33.

[16] Sellers J. J., Ph D Thesis: Investigation into Low-Cost Propulsion Systems for Small Satellites, University of Surrey, 1996

[17] Sutton G. P., Rocket Propulsion Elements ,6th Edition, John Wiley and Sons. Inc.,1992, 18

[18] Humble R.W., Henry G. N., Larson W. J., Space Propulsion Analysis and Design, Space Technology Series, McGraw-Hill, 1995, 87, 156-160

[19] The Space Review, www.spacereview.com/article/2315/2, last visited May 2014.

[20] Thicksten Z., Macklin F., Campbell J., Handling Considerations of Nitrous Oxide in Hybrid Rocket Motor Testing, 44th AIAA/ASME/SAE/ASEE Joint Propulsion Conference & Exhibit, Hartford, CT, 2008.

[21] Nitrous Oxide/Alcohol Bipropellant Rocket Motor, http://aeroconsystems.com/cart/hybrid-motors/rattworks-tribrid-nitrous/alcohol-bipropellant-rocket-motor/ , last visited May 2014

[22] Zakirov V.A., PhD Thesis: Investigation into Nitrous Oxide Propulsion Option for Small Satellite Applications, University of Surrey, 2001, 19

[23] Wilson M., MSc. Thesis: Catalytic Decomposition of Nitrous Oxide Monopropellant for Hybrid Motor Ignition, Utah State University, 2013, 3.

[24] Fink L., Propulsion and Energy Hybrid Rockets, Aerospace America, 1998, 64

[25] Zakirov V. A., Lawrence T. J., Sellers J. J., Sweeting M. N., Nitrous oxide as a Rocket Propellant for Small Satellites, 5th International Symposium on Small Satellite Systems and Services, France, 2000

[26] Lide D.R., CRC Handbook of Chemistry and Physics, 76th Edition, CRC Press Inc., 1995

[27] Sarışın M.N., PhD thesis : Dissertation of Master of Science on Design of a Connected Pipe Test Facility for Ramjet Applications, METU, 2005

[28] Truitt R. W., Fundamentals of Aerodynamic Heating, The Ronald Press Company, New York, 1960

[29] Joseph H., Joseph K. , Gas Tables, John Wiley & Sons, 1948

[30] George S.K., Speed of Sound in Standard Air, The Journal of the Acoustical Society of America, 1986, 79:5, 1359-1366.

[31] Atkins P.W., Jones L. L., Chemistry: Molecules, Matter, and Change, 3rd Edition, W.H. Freeman and Company, New York, 1997.

[32] Guisnet M., Gilson J. P., Zeolites for Cleaner Technologies, Imperial College Press, 2002.

[33] Hussain M., Fino D., Russo N., J. Hazard. Materials, 2012, 211-212, 255-265.

[34] Kaptejin F., Mirasol J.R., Molijn J. A., Appl. Catal: B 1996, 9, 25-64.

[35] Hinshelwood C. N., Prichard C.R., Proc. R. Soc: A, 1925, 108, 211.

[36] Huttig G.F., Novak-Schruber W., Kittel H., Z. Phys. Chem., 1934, 171, 83.

[37] Huttig G.F., Tschakct H. E., Kittel H., Z. Anorg. Chem., 1935, 223, 241.

[38] Panov G.I., Sobolev V.I., Khatitonov A.S., J. Mol. Catal. 1990, 61, 85.

[39] Leglise J., Petunchi J. O., Hall W.K., J. Catal. 1984, 86, 392.

[40] Akbar S., Joyner R.W., J. Chem. Soc. Faraday Trans. 1981, 1: 77, 803.

[41] Dandl H., Emig G., In proceedings of Environmental Catalysis, 1st World Conference, Italy, 1995, 615-618

[42] Valyon J., Millmanu W.S., Hall W.K., Catal. Lett. 1994, 24, 215.

[43] Sobolev V. I., Panov G.I., Kharitonov A. S., Romannikov V. N., Volodin A. M., Ione K. G., J. Catal. 1993, 139, 435.

[44] Fu C. M., Korchak V.N., Hall W.K., J. Catal. 1981, 68, 166.

[45] Aparicio L.M., Ulla M.A., Milman W.S., Dumesic J. A., J. Catal. 1988, 110, 330.

[46] Oi J., Obuchi A., Bamwenda G.R., Ogata A., Yagita H ., Kushiyama S., Mizuno K., Appl. Catal:B. 1997, 12, 277-286.

[47] Wang J., Xıa H., Ju X., Fan F., Feng Z., Li C., Chinese J. Catal. 2013, 34 876-888.

[48] Liu N., Zhang R., Chen B., Li Y., Li Y., J.Catal. 2012, 294, 99-112.

[49] Da Crus R. S., Mascarenhas A.J.S., Andrade H.M.C., Appl. Catal. B: Environmental, 1998, 18, 223-231.

[50] Correa C.M., Villa A.L., Zapata M., Catal. Lett. 1996, 38, 27.

[51] Campa M.C., De Rossi S., Ferraris G., Indovina V., Appl. Catal. B: 1996, 8, 315.

[52] Armor J.N., Stud. Surf. Sci. Catal. 1995, 92, 51.

[53] Zhang X., Shen Q., He C., Ma C., Cheng J., Liu Z., Hao Z., Catal. Sci. Technol. 2012, 2, 1249-1258.

[54] Yuzaki K., Yarimizu T., Aoyagi K., Ito S., Kunimori K., Catal. Today, 1998, 45, 129-134.

[55] Yuzaki K., Yarimizu T., Aoyagi K., Ito S., Kunimori K., Catal. Letters, 1997, 47, 173-175.

[56] Centi G., Galli A., Montanari B., Perathoner S., Vaccari A., Catal. Today 1997, 35, 113-120.

[57] Haber J., Nattich M., Machej T., Appl. Catal. B: 2008, 77, 278-283.

[58] Hussain M., Akhter P., Fino D., Russo N., Chem. Eng. J. 2013, 1, 164-174.

[59] Shen Q., Li L., Hao Z., Xu Z. P., Appl. Catal. B: 2008, 84, 734-741.

[60] Ohnishi C., Iwamoto S., Inoue M., Chem. Eng. Science, 2008, 63, 5076-5082.

[61] Li Y-J., Armor J. N., Appl. Catal. B: 1992,1, L21-29

[62] Chang Y., Mc Carty J. G., Wachsman E.D., Appl. Catal. B: 1996, 6, 21-23

[63] Chang Y., Mc Carty J. G., Wachsman E.D., Appl. Catal. B:1994, 4, 283-299.

[64] Carl J. P., Larse S.C., J. Catal. 2000, 196, 352-361.

[65] Labhsetwar N., Dhakad M., Biniwale R., Mitsuhashi T., Haneda H., Reddy P.S.S., Bakardjieva S., Subrt J., Kumar S., Kumar V., Saiprasad P., Rayalu S., Catal. Today, 2009, 141, 205–210.

[66] Doraiswamy L.K., Üner D., Chemical Reaction Engineering Beyond the Fundementals, CRC Press, 2013

[67] Kaduk J. A., Faber J., The Rigaku J. 1995, 2, 14-34.

[68] Sun Y., Sun T., Seff K., Chem. Rev. 1994, 94, 857.

[69] Ryoo R., June C., Pak C., Guk-Kim J., Yong-Lee J., J. Am. Chem. Soc. 1992, 114, 76.

[70] Guczi L., Kiricsi I., Appl. Catal. A: Chem. 1999, 186, 375.

[71] Guczi L., Beck A., Horvath D., Top. Catal. 2002, 19, 157.

[72] Ríos R. C. A., Oviedo V. J. A., Henao M. J. A., Catal. Today, 2012, 190, 61-67.

[73] Kulprathipanja S., Zeolites in Industrial Seperation and Catalysis, Wiley-VCH, Weinheim, 2010.

[74] Zahmakıran M., PhD. Thesis: The Preparation And Characterization Zeolite Framework Stabilized Ruthenium (0) Nanoclusters, A Suberp Catalysts For The Hydrolysis Of Sodium Borohydride And The Hydrogenation Of Aromatics Under Mild Conditions, METU, 2010.

[75] Zahmakıran M., Özkar S., Langmuir, 2008, 24, 7065-7067.

[76] Gates B.C., Catalytic Chemistry, John Wiley and Sons, Canada, 1992.

[77] Shriver D.F., Atkins P. W., Langford C. H., Inorganic Chemistry, 2nd Edition, Oxford University Press, New York, 1994.

[78] Anthonsen T., Reactions Catalyzed By Enzymes In Applied Biocatalysis, Harwood Academic Publishers, United Kingdom, 1999.

[79] Smith J. V., Origin And Structure Of Zeolites In Zeolite Chemistry And Catalysis, JAREd., Am. Chem. Soc. Monogr. 1976, 171, 1.

[80] Cronsted A. F., Akad. Handl, Stockholm, 1756, 18, 120.

[81] Deville C., Comptes Rendus Acad. Sci. 1862, 54, 324.

[82] Friedel G., Bull. Soc. Fr. Mineral. Cristallogr. 1896,19, 363-390.

[83] Wiegel O., Steinhoff E., Z. Kristallogr. 1925, 61, 125-154.

[84] Bhatia S., Zeolite catalysis: Principles and Applications, CRC Press, 1990

[85] Baerlocher C.H., Meier W.M., Olson D.H., Atlas of Zeolite Framework Types, 5th Revised Edition, Elsevier, Amsterdam, 2001.

[86] Walspurger S., Sommer J., Reactions in Zeolites, Molecular Encapsulation; Organic Reactions in Constraint Systems, Wiley, UK, 2010.

[87] Barrer R. M., Hydrothermal Chemistry of Zeolites, Academic Press, New York, 1982.

[88] Auerbach M. S., Carrado A. K., Dutta P. K., Handbook of Zeolite Science and Technology, Marcel Dekker Inc, New York, 2003.

[89] Yoshikawa M., Wagner P., Lovallo M., Tsuji K., Takewaki T., Chen C.Y, Beck L., Jones C., Tsapatsis M., Zones S.I., Davis M., J. Phys. Chem. B: 1998, 102, 7139-7147.

[90] Wessels T., Baerlocher C., Mccuster L. B., Creyghton E.J., J. Am. Chem. Soc. 1999, 121, 6242-6247.

[91] McCusker L.B., Baerlocher C., Jahn E., Blow M., Zeolites, 1991, 11, 308-313.

[92] Estermann M., McCusker L.B., Baerlocher C., Merrouche A., Kessler H., Nature, 1991, 352, 320-323.

[93] McCusker L. B., Baerlocher C., Grosse-Kunstleve R., Brenner S., Wessels T., Chimia, 2001, 55, 497-504.

[94] McLeary E.E., Jansen J.C., Kaptajein F., Micropor. Mesopor. Mater. 2006, 90, 198–220.

[95] Snurr R.Q., Karger J., J. Phy Chem. B: 1997, 101, 6469-6473.

[96] Corbin D.R., Abrams L., Jones G.A., Smith M.L., Dybowski C.R., Hriljac J.A., Parise J.B., J. Chem.Soc. Chem. Commun. 1993, 1027-1029

[97] Engelhardt G., Vankoningsveld H., Zeolites, 1990, 10, 650-656.

[98] Koningsveld H.V., Jansen J.C., Micropor. Mater. 1996, 6, 159-167.

[99] Koningsveld H.V., Jansen J.C., Bekkum H. V., Acta Crystallogr. Sec B Str. Sci. 1996, 52, 140-144.

[100] Nair S., Tsapatsis M., J. Phys. Chem. B : 2000, 104, 8982-8988.

[101] Meier W. M., Olsen D.H., Atlas of Zeolite Structure Type, International Zeolite Association, Zurich, 1978.

[102] Bekkum H., Flanigen E.M., Jansen J. C., Introduction to Zeolite Science and Practice, Amsterdam; Elsevier, Vol 58, 1991

[103] Corma A., Chem. Rev. 1995, 95, 559-614.

[104] Flanigen E. M., Grose R. W., Adv. Chem. Ser. 1971, 101, 76-101.

[105] Wilson S. T., Lok B. M., Messina C. A., Cannan T. R., Flanigen E. M., J. Am. Chem. Soc., 1982, 104, 1146-1147.

[106] Millini R., Perego G., Bellussi G., Top. Catal. 1999, 9, 13-34.

[107] Newsam J.M., Vaughan D.E.W., Strohmaier K.J., J. Phys. Chem. 1995, 99 9924-9932.

[108] McCuster L. B., Grosse R. W., Baerlocher C., Yoshikawa M., Davis M.E., Micropor. Mater. 1996, 6, 295-309.

[109] O'Keeffe M., Yaghi O.M., Chem. Eur. J. 1999, 5, 2796-2801.

[110] Lin Y., Finke R.G., J. Mol. Catal. A: Chem. 1996, 29, 114.

[111] R. Pool, Science, 1990, 248, 1186.

[112] Corain B., Schmid G., Toshima N., Metal Nanoclusters in Catalysis and Materials Science, Elsevier, Amsterdam , Netherlands, 2008

[113] Gaffet E., Tachikart M., El Kedim O., Matter. Charact. 1996, 36, 185.

[114] Richards R. M., Surface and Nanomolecular Catalysis, Taylor and Francis, Boca Raton, 2006

[115] Fu X., Wang Y., Wu Y., Gui L., Langmuir, 2002, 18, 4619.

[116] Tano T., Esumi K., Meguro K., J. Colloid Interface Sci., 1989, 133, 530.

[117] Duteil A., Queau R., Chaudret B., Mazel R., Bradley J. S., Chem. Mater., 1993, 5, 341.

[118] Klabunde K. J., Habdas J., Kardenas G., Chem. Mater., 1989, 1, 481.

[119] Reetz M. T., Helbig W., J. Am. Chem. Soc. 1994, 116, 7401.

[120] Seydock M., Biosensors and Bioelectronics, 2005, 20, 2454–2469.

[121] Breck D. W., Zeolite Molecular Sieves, Wiley, New York, 1984, p 549

[122] (a) Tang H., Li J., J. Fuel Chem Technol, 2011, 39 (8), 615-620 (b) Rynkowski J.M., Paryjczak T., Lenik M., Appl. Catal. A: General, 1995, 126, 257-271

[123] Sunol J.J., Bonneau M.E., Roue´ L., Guay D., Schulz R., Appl.Surf. Sci. 2000, 158, 252 (Figure 6D)

[124] Bianchi C.L, Ragaini V., Materials and Physics, 1991, 29, 297-306.

[125] Hassan H., Hameed B. H., Desalination, 2011, 276, 45-52.

[126] Ojeda M., Rojas S., Boutonnet M., Pérez-Alonso F. J., Garcia F. J., Fierro G., Appl. Catal. A: General, 2004, 274, 33–41

[127] Siri G.J., Guerrero-Ruiz A., Rodriguez Ramos I., Terreros P., J.L.G. Fierro, Appl. Catal. A: 1993, 107, 59-71.

[128] Caratzoulas S., Jackson B., Persson M., J. Chem. Phys. 1997, 107, 6420.

[129] Uetsuka H. Aoyagi K; Tanaka S, Yuzaki K, Ito S, Kameoka S, Kunimori K, Catal Letters, 2000, 66, 87-90.

[130] Yuzaki K., Tanaka S., Ito S., Uetsuka H., Kameoka S., J. Of. Catal., 200 (2001) 203-208

[131] Ohnishi C., Asano K., Iwamoto S., Chikama K., Inoue M., Studies in Surf. Sci. And Catal. 2006, 162, 737-744.

[132] Baker M.D., Godber J., Ozin G.A., J. Am. Chem. Soc., 1985, 107, 3033

[133] Jelinek R., Özkar S., Ozin G.A., J. Am. Chem. Soc, 1992, 114,4907

[134] Zeng H.C, Pang X.Y., Appl. Catal. B: 1997, 13, 113-122

[135] Reddy S., Pasha N., Rao C.,Lingaiah N., Suryanarayana I., Prasad P. S.,Catal. Commun., 2007, 8, 1406-1410

[136] Komvokis V., Marti M.,Delimitis A., Vasalos I. A., Triantofyllidis K.S., Appl. Catal. B:, 2011, 103, 62-71

[137] Curdaneli Edinç P., Ozkar S., Microporous and Mesoporous Materials, 2014,196, 51-58

CURRICULUM VITAE

PERSONAL INFORMATION

Surname, Name: Edinç Cürdaneli, Pelin
Nationality: Turkish (TC)
Date and Place of Birth: 1979, Ankara
Marital Status: Married
Phone: +903125909228
Fax: +903125909148

EDUCATION

Degree	Institution	Year of Graduation
M.S.	Chemistry Dept., METU	2005
B.S.	Chemistry Dept., METU	2002
High School	Yıldırım Beyazıt, Ankara	1997

PROFESSIONAL EXPERIENCE

Year	Place	Enrollment
2003-Current	SAGE, TÜBİTAK	Chief Research Engineer

PUBLICATIONS

1. Ozkar S., Önal A., Edinç P., *Synthesis, characterization, and electronegativity of tetracarbonyl(6-ferrocenyl-2,2’-bipyridine)tungsten(0)*, Journal of Organometallic Chemistry, 2007, 692 (10), 1983-1989

2. Pitcher M. W., Edinç P., Majesti M., Metin Ö., Şen F.,Aslan Y., Türksoylu Ö., Yiğitsoy B., *Recent Advances in the Synthesis and Applications of Inorganic Polymer*, Phosphorous, Sulphur and Silicon and Related Elements, 2007, 182 (12), 2861-2880

3. Edinç P., Ozkar S., *Ruthenium(III) ion-exchanged zeolite Y as highly active and reusable catalyst in decomposition of nitrous oxide to sole nitrogen and oxygen* , Microporous and Mesoporous Materials, 2014,196, 51-58